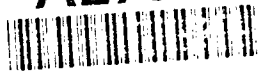


AD-A279 631



MONITORING BIOREMEDIATION OF VOLATILE ORGANIC COMPOUNDS
(VOCs) USING FOURIER TRANSFORM INFRARED (FT-IR)
SPECTROMETRY

by

VANCE P. VISSER

B.S., Trevecca Nazarene College, 1984

DTIC
ELECTE
MAY 24 1994
S F D

A THESIS

submitted in partial fulfillment of the
requirements for the degree

MASTER OF SCIENCE

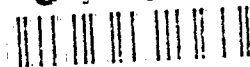
This document has been approved
for public release and sale; its
distribution is unlimited.

Department of Chemistry
College of Arts and Sciences

KANSAS STATE UNIVERSITY
Manhattan, Kansas

1994

94-15421



Approved by:

Major Professor

Robert M. Hamaker

ROBERT M. HAMMAKER

20030228025

94 5 28 23

MONITORING BIOREMEDIATION OF VOLATILE ORGANIC COMPOUNDS
(VOCs) USING FOURIER TRANSFORM INFRARED (FT-IR)
SPECTROMETRY

by

VANCE P. VISSER

B.S., Trevecca Nazarene College, 1984

A THESIS

submitted in partial fulfillment of the
requirements for the degree

MASTER OF SCIENCE

Department of Chemistry
College of Arts and Sciences

KANSAS STATE UNIVERSITY
Manhattan, Kansas

1994

Approved by:

Major Professor

Robert M. Hammaker

ROBERT M. HAMMAKER

Accession For	
NTIS	CRA&I
DTIC	TAB
Unannounced	
Justification	
By	
Distribution	
Availability Code	
Dist	Avail and/or Special
A-1	

ABSTRACT

Bioremediation has repeatedly been demonstrated to be an innovative and effective technology for a wide variety of chemically contaminated environments. Although, once predominantly used in wastewater treatment, bioremediation technology is now being applied to soils, ground and surface water, and sludges. The contaminants include chemicals such as crude oil, petroleum hydrocarbons, fuels, and solvents. Regardless of the type of contaminant, the success of any bioremediation approach includes these essential elements: site characterization, initial bioassessment testing, detailed laboratory testing, hydrologic modeling, installation and start-up, process monitoring and operation, final sampling and closure, reporting and management¹. A major expense in bioremediation can be associated with monitoring the degradation of contaminants. This cost may be reduced by applying readily available, simple analytical methods and instrumentation to the monitoring of the bioremediation process. Our research involves the monitoring of the bioremediation of ground water contaminated by low levels of volatile organic compounds (VOCs) by adapted alfalfa plants and their associated rhizosphere bacteria. We are involved in the monitoring of the atmosphere above the plants during the remediation process. We are focusing on applying Fourier transform infrared (FT-IR) spectrometry to the atmospheric monitoring of these VOCs during plant bioremediation. Initially, a commercially available FT-IR spectrometer was used to monitor the atmosphere above plants growing in the presence of dissolved organic contaminants such as toluene².

Recent work extends the use of open path FT-IR spectrometry in the study of the remediation of chlorinated compounds, specifically 1,1,1-trichloroethane (TCA) and trichloroethylene (TCE) in the atmosphere, ground water and plant tissue.

REFERENCES

1. King, R. Barry, Long, G.M., Sheldon, J.K., Practical Environmental Bioremediation, Boca Raton, Florida: Lewis Publishers, 1992, p. 13.
2. Davis, L.C., Chaffin, C., Muralidharan, N., Visser, V.P., Fateley, W.G., Erickson, L.E., and Hammaker, R.M., "Monitoring the Beneficial Effects of Plants in Bioremediation of Volatile Organic Compounds". In: L.E. Erickson, D. Tillison, S.C. Grant and J.P. McDonald (eds.), Proceedings of the 8th Annual Conference on Hazardous Waste Research. Engineering Extension Service, Kansas State University, Manhattan, KS. 1993. p. 236-249.

DEDICATION

FOR SHERRI DAWN, THE WIND BENEATH MY WINGS, AND OUR
THREE CHILDREN; ASHLEY, BRITTNEY, AND MATTHEW. THE
FOUR OF YOU ARE MY INCESSANT SOURCES OF LOVE, JOY,
STRENGTH AND ENCOURAGEMENT.

FOR JOHN AND ALICE VISSER, MY GRANDPARENTS, WHOSE
LIVES WILL ALWAYS BE WORTHY OF EMULATION, FROM
BEGINNING TO END AND THROUGHOUT ETERNITY.

FOR FALLEN COMPADES, LEST WE FORGET THE SACRIFICES
MADE BY THOSE WHO WERE SO COMMITTED TO THEIR OATH
THAT THEY GAVE THEIR LIVES IN DEFENSE OF THE
CONSTITUTION OF THE UNITED STATES OF AMERICA AGAINST
ALL ENEMIES, FOREIGN AND DOMESTIC, ENSURING OUR
FREEDOM FOR LIFE, LIBERTY AND THE PURSUIT OF HAPPINESS.

NO MISSION TOO DIFFICULT,
NO SACRIFICE TOO GREAT,
DUTY FIRST!

TABLE OF CONTENTS

	PAGE
Abstract	
Dedication	i
Table of Contents	ii
List of Figures	iii
List of Tables	vii
Acknowledgements	viii
Chapter One, Introduction to Thesis	1
Chapter Two, Introduction to Bioremediation	4
Chapter Three, Fourier Transform Infrared (FT-IR) Spectroscopy	15
Chapter Four, Open Path FT-IR Monitoring of Bioremediation	23
Chapter Five, Calibration and Quantification Procedures	42
Chapter Six, Practical Applications of FT-IR Monitoring of Bioremediation	101
Chapter Seven, Conclusion	127
Additional References	129

LIST OF FIGURES

FIGURE	PAGE
1 Photograph of Plant Treatment System	25
2 Schematic Diagram of Plant Treatment System	26
3 Photograph of Spectrometer Set Up	28
4 Schematic Diagram of Spectrometer Set Up	29
5 Methane Spectrum Example	31
6 Phenol Spectrum Example	32
7 Toluene Spectrum Example	33
8 Carbon Dioxide Spectrum Example	34
9 Toluene Spectrum Example	36
10 Phenol Spectrum Example	37
11 Graph of Relative Δ in CO ₂ Concentration	40
12 Four Calibration Spectra of Trichloroethylene	45
13 Four Point Calibration Curve for TCE	46
14 Calibration Spreadsheet for Trichloroethylene	48
15 Calibration Spectrum of Carbon Dioxide	52
16 Four Point Calibration Curve for CO ₂	53
17 Calibration Spreadsheet for Carbon Dioxide	54
18 Calibration Spectrum of Chloroform	55
19 Four Point Calibration Curve for Chloroform	56

FIGURE	PAGE
20 Calibration Spreadsheet for Chloroform	57
21 Calibration Spectrum of 1,1-Dichloroethane	58
22 Four Point Calibration Curve for 1,1-Dichloroethane	59
23 Calibration Spreadsheet for 1,1-Dichloroethane	60
24 Calibration Spectrum of 1,2-Dichloroethane	61
25 Four Point Calibration Curve for 1,2-Dichloroethane	62
26 Calibration Spreadsheet for 1,2-Dichloroethane	63
27 Calibration Spectrum of 1,1-Dichloroethylene	64
28 Four Point Calibration for 1,1-Dichloroethylene	65
29 Calibration Spreadsheet for 1,1-Dichloroethylene	66
30 Calibration Spectrum of cis-1,2-Dichloroethylene	67
31 Four Point Calibration Curve for cis-1,2-Dichloroethylene	68
32 Calibration Spreadsheet for cis-1,2-Dichloroethylene	69
33 Calibration Spectrum of trans-1,2-Dichloroethylene	70
34 Four Point Calibration Curve for trans-1,2-Dichloroethylene	71
35 Calibration Spreadsheet for trans-1,2-Dichloroethylene	72
36 Calibration Spectrum of Methane	73
37 Four Point Calibration Curve for Methane	74
38 Calibration Spreadsheet for Methane	75
39 Calibration Spectrum of Phenol	76
40 Four Point Calibration Curve for Phenol	77

FIGURE	PAGE
41 Calibration Spreadsheet for Phenol	78
42 Calibration Spectrum of Toluene	79
43 Four Point Calibration Curve for Toluene	80
44 Calibration Spreadsheet for Toluene	81
45 Calibration Spectrum of 1,1,1-Trichloroethane	82
46 Four Point Calibration Curve for 1,1,1-Trichloroethane	83
47 Calibration Spreadsheet for 1,1,1-Trichloroethane	84
48 Calibration Spectrum of 1,1,2-Trichloroethane	85
49 Four Point Calibration Curve for 1,1,2-Trichloroethane	86
50 Calibration Spreadsheet for 1,1,2-Trichloroethane	87
51 Calibration Spectrum of Vinyl Chloride	88
52 Four Point Calibration Curve for Vinyl Chloride	89
53 Calibration Spreadsheet for Vinyl Chloride	90
54 Nonlinear Calibration Curve of Carbon Dioxide	92
55 Nonlinear Calibration Curve of Carbon Dioxide	93
56 Diagram of 50 cm Cell	94
57 Calibration Spectrum of Carbon Dioxide	97
58 Four Point Calibration Curve for Carbon Dioxide	98
59 Calibration Spreadsheet for Carbon Dioxide	99
60 Graph of Change in Relative Carbon Dioxide Concentration With Plants	103

FIGURE	PAGE
61 Graph of Change in Relative Carbon Dioxide Concentration Without Plants	104
62 Spectrum Containing TCA and TCE With Overlaid Calibration Spectra	106
63 Spectrum of Hexane (2964 cm^{-1})	108
64 Hexane Spectra Shows Absorbance Decrease Over Time	109
65 TCA and TCE Spectra with Plants	111
66 TCA and TCE Spectra with Plants Cut	112
67 Graph of TCA Accumulation Over Time	113
68 Graph of TCE Accumulation Over Time	114
69 Spectrum of Plant Sample Head Space Gas	117
70 Spectra of Groundwater Samples (TCA and TCE)	119
71 Spectra of Groundwater Samples (Methane)	120
72 Graph of TCA Concentration in Groundwater Samples	121
73 Graph of TCE Concentration in Groundwater Samples	122
74 Graph of Methane Concentration in Groundwater Samples	123

LIST OF TABLES

TABLE	PAGE
1 Spectrometer Specifications	20
2 Experimental Data for Example Calculation	47
3 Calibrations Using 50 cm Cell	49
4 Calibrations Using 5 cm Cell	50
5 Index of Calibration Information Figure Numbers	51
6 Data Used for Graphs in Figures 65 and 66	115
7 TCA, TCE, and Methane Concentration (PPM) Present in Groundwater Sample	124
8 Limits of Detection (LOD) .5 m and 2.44 m Pathlengths	125

ACKNOWLEDGEMENTS

A wealth of gratitude and appreciation needs to be extended to a host of individuals and agencies which were instrumental in my completion of graduate school here at Kansas State University. I will attempt to address this issue briefly. Everyone should know and understand that absence of specific thanks here in this document is in no way, a reflection of any lack of gratitude or appreciation, but rather an effort to keep it short and sweet.

I must begin by thanking the three men that comprise my graduate committee, Dr. Robert M. Hammaker, Dr. Lawrence C. Davis and Dr. William G. Fateley. I have learned many things in the last two years and have enjoyed working with each of you.

Dr. Hammaker, I appreciate you allowing me to join your research group and I hope that one day I am able to demonstrate the same meticulous and organized professionalism you bring to your duties every day. The graduate students in the KSU Chemistry Department are fortunate to have you looking out for them.

Dr. Davis, I am grateful to you for involving me in your bioremediation research. I hope that somehow the puzzle pieces we found together will somehow help you unlock the mysteries of the biodegradation pathways associated with these volatile organic compounds.

Dr. Fateley, thank you seems like an inadequate expression for me to make use of. Always remember, you have my word. I am certain that I would not be able to find the right terms so I will use some words that have come to be very special to me.

"THERE ARE MANY TRAILS IN THIS LIFE, BUT THE ONE THAT MATTERS MOST, FEW MEN ARE ABLE TO WALK..... EVEN COMANCHE MEN. IT IS THE TRAIL OF A TRUE HUMAN BEING. I KNOW THAT YOU ARE ON THAT TRAIL. IT IS A GOOD THING FOR ME TO SEE. IT IS GOOD FOR MY HEART."

from: Dances With Wolves, by Michael Blake.

I also must say thanks to the rest of the Fateley/Hammaker gang and wish you all the best in the future.

D.O.M. ASSOCIATES, INC. MANHATTAN, KANSAS. For equipment and other resources.

U.S. ARMY. For the support and the opportunity to attend graduate school.

U.S. ENVIRONMENTAL PROTECTION AGENCY REGION VII.

This research was partially supported by the U.S. EPA under assistance agreements R815709 and R-319653 to the Great Plains-Rocky Mountain Hazardous Substance Research Center for regions 7 and 8 under project 90-13 and an EPA grant (CR81-7790-01-1) to Dr Fateley and Hammaker. It has not been submitted to the EPA for peer and administrative review and, therefore, may not necessarily reflect views of the agency and no official endorsement should be inferred. The U.S. Department of Energy, Office of Restoration and Waste Management, Office of Technology Development and the Center for Hazardous Substance Research also provided partial funding.

CHAPTER ONE

INTRODUCTION TO THESIS

In the last few decades, our society's scientists have worked diligently to ensure we have a safe and clean environment. Environmental issues are at the forefront in almost all facets of life and a concerted effort is being put forth to minimize the harm pollution and hazardous waste has brought to our environment. One of the major environmental concerns that confronts us is the clean up of areas that are actively discharging volatile organic compounds (VOCs) from contaminated soil and/or ground water into the atmosphere. Some of the presently practiced remediation strategies (excavation, removal and incineration) are very expensive and fail to mineralize or eliminate all residual contamination and waste. In an attempt to develop a complete process to economically overcome environmental contamination issues, extensive research has been done to understand the natural course of bioremediation.

Fourier transform infrared (FT-IR) spectrometry is a versatile, mobile analytical system which can easily be transported to locations where active remediation efforts are underway. FT-IR is an excellent tool for monitoring bioremediation of volatile organic compounds because it provides a means for rapid analysis of small amounts of material in a variety of environments. During the course of our study, FT-IR has been successfully applied to the determination of contaminant levels in the gas phase, ground water and plant tissue. The information presented in this thesis will summarize our experimental design and methodology.

The format for this document will be an overview of bioremediation and Fourier transform infrared (FT-IR) spectrometry, followed by the presentation of acquired experimental results. The experimental information presented will describe how FT-IR spectrometry was used in monitoring the bioremediation of volatile organic compounds (VOCs) such as 1,1,1-trichloroethane (TCA) and trichloroethylene (TCE). Additionally, an outline of calibration procedures, calibration spectra and Beer's law calibration curves for compounds studied is included. The thesis will conclude with a summary of our results and a brief discussion of potential research efforts for investigation in the future. Finally, a list of additional references found in current, scientific literature is presented to assist anyone interested in further investigation of bioremediation.

CHAPTER TWO

INTRODUCTION TO BIOREMEDIATION

As we struggle to preserve our natural resources and clean up the widespread pollution of our earth, bioremediation technology should be of great interest to a unlimited audience. This audience would include chemists, biochemists, microbiologists, geochemists, chemical engineers, environmentalists and anyone else concerned with the potential commercial applications of the chemical processes of microorganisms. A large number of man-made organic compounds have made their way into our environment as a consequence of the activities of industry and agriculture. These compounds have varying degrees of persistence and present a legitimate concern for society. It is out of this concern for our environment that bioremediation technologies have enjoyed such rapid development and application.

Billions of dollars are spent annually to remove toxic compounds that have been released into the environment. The Great Plains-Rocky Mountain Hazardous Substance Research Center, headquartered at Kansas State University, is searching for cost-effective technologies to clean up these compounds and prevent contamination. At the focal point of the center's efforts is research designed to enhance nature's remediation capabilities and many research projects funded through the center involve bioremediation. The emphasis on bioremediation is driven by its economic advantages. Quite frankly, it is considerably cheaper than present remediation alternatives and, as pointed out by Dr. Larry Erickson in a recent interview, bioremediation technological applications will save billions of dollars¹.

Bioremediation, the practice of reclamation or cleanup of contaminated sites through employment of microorganisms for degradation and destruction of pollutants², is one of the most innovative and effective technologies used in treatment of contaminated environments today. Bioremediation uses natural biological processes to clean up the chemical contamination caused by man's activities. As contaminants are introduced into the environment, naturally occurring microbes immediately begin to acclimate themselves and to biodegrade this new food source.

Bioremediation is not a brand new idea. It has been used for many years in wastewater treatment. The Romans, for example, built intricate sewer networks as early as 600 B.C. for collecting wastewater which subsequently underwent biological treatment³. Microorganisms did the work of biodegrading organic waste and the Romans found that a sort of self-purification took place over time. This purification occurred through the anaerobic microbial digestion of the organic material and present day sewage systems still operate in a very similar fashion. Today, bioremediation is routinely applied to soils, sludges, ground water, process water, and surface waters contaminated with chemicals such as crude oil, petroleum hydrocarbons, fuels, and industrial solvents.

Recent environmental legislation and federal regulatory stipulations have mandated strict guidelines for addressing hazardous materials in the environment. The National Environmental Policy Act (1969), Water Pollution

Control Act (1972), and Safe Drinking Water Act (1974) initially provided a means for rectifying abuse of our environment's natural resources, particularly land and water. It was not until 1976, that the Resource Conservation and Recovery Act (RCRA) and the Toxic Substances Control Act (TSCA) truly provided comprehensive and restrictive regulations to govern soil and water resources. With the implementation of RCRA and the passage of Superfund, greater emphasis became placed on prevention and remediation actions in hazardous waste management. Waste minimization, hazardous materials control and site remediation have all evolved from the necessity to care for our environment.

The management of hazardous waste and safe disposal practices are primary national concerns. Effective handling of newly generated waste and the increasing demand for remediation of contaminated sites further substantiate the need for a greater understanding of bioremediation and its utility to society as we strive to preserve and clean up our environment.

The federal time limit for pollution liability is clearly defined as being "from cradle to grave". There is no statute of limitations for pollution liability and a waste generator remains responsible and liable as long as waste exists. This continued liability is one of the main reasons bioremediation has emerged as an attractive alternative treatment for hazardous organic wastes. Simply stated, the major benefits of bioremediation technology include attractive economics, undisturbed environment with in situ application, destroyed

contaminants, and eliminated liability⁴.

The atmosphere and most surface waters undergo a sort of self-remediation through dispersion and natural healing once the source of pollution is removed. This is not the case for ground waters, surface and subsurface soils where contamination remains a viable threat until an effective remediation technique is employed. Historically, contaminated soils and sludges were either burned, buried, or chemically treated on site. These alternatives are often very costly and regulatory compliance is difficult. Incineration is both costly and becoming increasingly difficult to complete. These methods basically move or transfer the contamination from one form to another and leave the waste generator with continuing liability. The search began for a convenient method that would allow the total destruction of undesirable contaminants in soil and ground water and that replicated the natural healing process demonstrated in the atmosphere and surface waters.

It was well known to petroleum refiners, that left unattended, sludge and other oily wastes, slowly disappeared over the course of time when dumped out on the back forty acres. This procedure, widely used throughout the petroleum industry for hydrocarbon wastes, became known as land farming. Industrial and university researchers investigating the natural degradation of hydrocarbons in the environment found that certain microbes obtain their food and energy requirements from hydrocarbon materials. Some of the common soil bacteria were among these hydrocarbon degrading microbes. A

tremendous amount of research has been performed to discover the mechanisms by which microbes degrade and metabolize hazardous organic chemicals. Bioremediation has proven successful for remediation treatment of crude petroleum, lube oils, organics, alcohols, fuels, some solvents, and oxygen and nitrogen substituted compounds⁵. All soils and ground waters contain many kinds of fungi, protozoans, and bacteria. Of these indigenous microbes, it is the fungi and bacteria that account for the degradation of practically all the hydrocarbon contamination entering the natural environment. The challenge is to entice a beneficial mode of metabolism that will degrade the target contaminants. It is this systematic enhancement of this natural biological degradation by bacteria that comprises the art and science of environmental bioremediation.

All living things must have food, oxygen, water and a suitable environment in which to live and multiply. Food for microbes must provide a carbon source for the synthesis of essential biochemical and cellular components. The carbon source may consist of organic carbon of many varieties, inorganic carbonate or CO₂. Microorganisms which utilize only organic carbon substrates are heterotrophic and comprise the majority of bacteria. Those microbes which can utilize inorganic carbon are lithotrophic and can metabolize and grow in environments containing little or no organic carbon. The bacteria of use in bioremediation are the hydrocarbon degrading heterotrophs and those which can use inorganic carbon and salts.

Microbes are quite sensitive to abrupt changes in their environment. For example, when a hydrocarbon contaminant is introduced into its environment, the microbial population will acclimate to the foreign substance. Some microbes may undergo enzymatic changes in order to deal with this new compound. These enzymatic alterations occur for two reasons, either the microbes attempt to transform the hydrocarbon or the microbes attempt to degrade or mineralize the hydrocarbon for energy and growth⁶. The longer a hydrocarbon has been in contact with a microbial population, the better acclimated it will be. Sites which have been contaminated for extended periods of time, have a better likelihood of having indigenous acclimated contamination degrading microbial populations.

Now that we are familiar with how microbes generally respond to their chemical and physical environments, a more clear grasp of the mechanics of bioremediation is necessary. Without an understanding of the mechanisms of bioremediation, it would be impossible to successfully use this technology.

There are three metabolic pathways by which microbial degradation may occur. These biodegradation processes are aerobic, anaerobic and fermentative. In aerobic respiration, molecular oxygen (O_2) is the final electron acceptor. Aerobic respiration is the most efficient of the three pathways and is the mechanism of choice as long as O_2 is present⁷. During anaerobic respiration, strict and facultative anaerobes are able to flourish in the absence of molecular oxygen. Facultative anaerobes use NO_3 as the final

electron acceptor in lieu of O_2 . The strict anaerobes become active by utilizing sulfate, carbonate, and specific organic compounds as energy sources. These are the sulfate reducing and methanogenic bacteria. Although a myriad of fermentation reactions occur among fermenting bacteria generating a number of acidic and alcoholic compounds, carbon dioxide, methane and hydrogen, fermentation is of little practical use in environmental bioremediation⁸.

Our research of the remediation of groundwater and soil contaminated by volatile organic compounds (VOCs) was designed to study the beneficial effects of plants in the remediation process. Shimp et al.⁹ explained that the use of plants in remediation of soil and groundwater contaminated with organic materials is quite appealing because plants utilize solar energy, vegetation is aesthetically pleasing, harvested plant samples can be tested as indicators of level of remediation, plants help contain contamination by removing water from the soil, rhizosphere microbial communities are able to biodegrade an assortment of organic contaminants, and many plants have a means for transporting oxygen to the rhizosphere. Our research focusses on the bioremediation activity in this area known as the rhizosphere.

The rhizosphere or root zone is the area surrounding the root of a plant. The loss of organic material (rhizodeposition) from the roots of plants as they grow enriches the rhizosphere and stimulates microbial growth. This organic material which is deposited by the plant roots can be classified into four different groups. The four groups, classified by their mode of arrival,

include; exudates, secretions, lysates, and gases¹⁰. The exudates are water soluble compounds, such as sugars, which leak out of the root without the involvement of metabolic energy. Secretions are enzymes or carbohydrates which depend upon metabolic processes for their release. Lysates are released when cells autolyze. Carbon dioxide is an example of a gas which may be rhizodeposited. The important point to note about the rhizosphere is that this enriched area supports larger microbial populations than the soil that encompasses the rhizosphere and makes up the balance of the soil mass.

As shown by Anderson et al.¹¹, evidence in current literature certainly demonstrates that plant roots working together with their associated microbial communities offer a important treatment strategy for in situ biological remediation of chemically contaminated soils. Vegetation has been shown to enhance microbial degradation rates of organic chemical residues in soils and may provide a less expensive alternative technology for soil remediation. Together, the vegetation and microbial colonies associated with the rhizosphere, may eliminate legal liability for hazardous wastes in soils and ground waters through mineralization of hazardous compounds in the rhizosphere in lieu of technologies involving excavation, relocation and/or tons of contaminated soil.

Although there are a number of techniques available to remediate contaminated soil and groundwater, we will focus our attention on in situ treatment. In situ treatment employs microorganisms for on-site

remediation of soil and ground water contaminants in place in the environment. The potential advantages of bioremediation compared to other in situ methods (e.g. desorption, vapor recovery, and containment), include destruction rather than transfer of contaminant, minimal exposure of workers, long-term public health protection, and possible reduction of the remediation process timeline¹².

In recent years, expanded interest in biodegradation of industrial wastes has increased research efforts in remedial treatment of contaminated soil and ground water. One such frequently studied, industrial waste chemical often found in contaminated ground water is trichloroethylene (TCE)¹³. This interest, coupled with the extensive, potential environmental applications for bioremediation, is also the inspiration for our research efforts. Later in this document we will highlight the results of our research involving the monitoring of bioremediation of volatile organic compounds (VOCs) such as toluene, phenol, 1,1,1-trichloroethane (TCA) and trichloroethylene (TCE) utilizing Fourier transform infrared (FT-IR) spectrometry.

REFERENCES:

1. Diebel, Ken, "Plants Studied in Research for Removing Toxic Wastes", The Collegian, Manhattan, Kansas, 12 October 1993, p. 8 (1993).
2. King, R. Barry, Long, Gilbert M., Sheldon, John K., Practical Environmental Bioremediation, Lewis Publishers, Boca Raton, Florida, p. 138, (1992).

3. King, Long, Sheldon, p. 1.
4. King, Long, Sheldon, P. 4.
5. King, Long, Sheldon, p. 9.
6. King, Long, Sheldon, p. 36.
7. King, Long, Sheldon, p. 42.
8. King, Long, Sheldon, p. 45.
9. Shimp, J.F., Tracy, J.C., Davis, L.C., Lee, E., Huang, W., Erickson, L.E., and Schnoor, J.L., "Beneficial Effects of Plants in the Remediation of Soil and Groundwater Contaminated with Organic Materials", *Critical Reviews In Environmental Science and Technology*, 23 (1): 41-77 (1993), CRC Press, Inc. (1993).
10. Whipps, J.M., "Carbon Economy" in The Rhizosphere, Wiley, New York, p.60, (1990).
11. Anderson, Todd A., Guthrie, Elizabeth, and Walton, Barbara T., "Bioremediation", *Environmental Science and Technology*, vol 27, no 13, pp. 2630-2636, (1993).
12. Water Science and Technology Board, Commission on Engineering and Technical Systems, National Research Council, In Situ Bioremediation, When Does It Work?, National Academy Press, Washington, D.C., pp. 43-49, (1993).
13. McClellan, Kristen L., Buras, Netty and Bales, Roger, "Biodegradation of Trichloroethylene by Bacteria Indigenous to a Contaminated Site", *Journal of Environmental Science Health*, A24 (6), pp. 561-570, (1989).

CHAPTER THREE

FOURIER TRANSFORM INFRARED (FT-IR)
SPECTROMETRY

Fourier transform infrared (FT-IR) spectrometry can trace its developmental roots back to Dr. Albert A. Michelson and his invention of the interferometer in 1880, which proved to be of such value to science that Michelson received a Noble Prize for his efforts¹. Since that time, a number of developments have led to FT-IR as we know it today. Instead of providing a comprehensive, historical review of FT-IR, a brief summary of the developmental highlights will be addressed. For further investigation of the historical background of Fourier transform spectroscopy one may read Bell's text² referenced above. In addition, a complete, detailed analysis of Fourier transform infrared spectrometry is presented by Griffiths and de Haseth³.

The advantages of utilizing Fourier transform spectrometers arise from two concepts, the Fellgett and Jacquinot advantages. Any discussion of this technique would be remiss if it failed to mention these two concepts. An interferometer gathers information differently than a grating type spectrometer. The interferometer collects information over the entire range of a spectrum during each time element of a scan, and a grating type spectrometer acquires information only from a narrow region which lies in the exit slit of the instrument. Briefly: the Fellgett advantage can be stated as, an interferometer receives information about the entire spectral range during an entire scan, while a grating instrument only receives information in a narrow band at a given time⁴. The Fellgett or multiplexing advantage essentially made the acquisition of spectral data with dispersive instrumentation nearly obsolete⁵. In

addition to the Fellgett advantage, Fourier transform instruments also enjoy another advantage over dispersive type instruments known as the Jacquinot advantage. The Jacquinot advantage is the absence of beam restricting elements like slits that are present in grating type instrumentation⁶. In FT instrumentation, resolution is not determined by the beam size, but rather, by the travel of the movable mirror and the data collected during a respective stroke of the mirror. This provides FT spectroscopy major optical advantages, which account for an incredible reduction in the data acquisition time for each spectrum obtained with similar resolution on a scanning instrument⁷.

There have been two additional technological advances that propelled the wider application of FT as an analytical technique, the evolution of computers and the manufacture of small gas lasers⁸. Small gas lasers, such as helium-neon lasers, are used to monitor the moving mirror of the interferometer, permitting interferograms to be digitized at precisely equal intervals, which generates an internal standard for all measurements⁹. With advances in computer technology and programming, it is now possible to compute spectra right after an interferogram has been measured. Enhanced data processing capabilities of modern personal computers enable us to rapidly acquire spectra and conduct analysis in a laboratory, or more significantly for our purposes, in a field environment. These advantages and improvements helped establish FT-IR spectrometry as a powerful instrumental technique that can analyze a multitude of samples.

The versatile nature of FT-IR spectrometry has resulted in a wide array of applications that are able to exploit its advantages. One such practical application for FT-IR spectrometry which has been extensively pursued by our research group here at Kansas State University is in the atmospheric monitoring arena. Growing national and international concern for our environment, particularly air quality, resulted in the development of open-path FT-IR spectrometry as a method for atmospheric monitoring of pollutants. The use of FT-IR for atmospheric monitoring is an application which has become an important tool for employment in environmental analysis. The balance of this chapter will discuss the background of and practical suitability of open-path FT-IR spectrometry in atmospheric monitoring.

Inaugural work by members of this research group to evaluate the utility of a mobile FT-IR system for practical purposes such as the determination of the presence of volatile organic compounds (VOCs) contamination in the atmosphere began in 1987. The wide number of sites contaminated by volatile organic compounds is an issue which will continue to hamper our environment and this problem certainly makes an attractive argument for a reliable, on-site analytical method. Open-path Fourier transform (FT-IR) spectrometry proved itself to be a viable technique for conducting such analyses. Preliminary qualitative and quantitative results of this work were published by Spartz et al¹⁰ and the analytical methodology outlined by Spartz is fundamentally still employed today.

The instrumentation used for this initial work was a Bomem DA02 FT-IR spectrometer, equipped with a germanium on potassium bromide (Ge/KBr) beam splitter and a broad band mercury cadmium telluride (MCT) detector, 5000 to 500 cm^{-1} , which is operated at liquid cooled nitrogen temperatures¹¹. Despite its size, this instrument proved to be quite a valuable tool and demonstrated great promise for FT-IR use in atmospheric monitoring of volatile organic compounds. Since that time, research and development of open-path FT-IR for atmospheric monitoring has continued in our research group.

In the spring of 1992, the Fateley/Hammaker research group received a new, lightweight MIDAC FT-IR spectrometer which provided us the ability to operate in a variety of environments. Later, two additional MIDAC instruments were acquired affording us even greater mobility and versatility in the practical analytical use of FT-IR. The collective result of the acquisition of this instrumentation and the group's continued examination of FT-IR have been the advent of a number of practical applications for FT-IR use including atmospheric monitoring of industrial facilities, hazardous waste facilities, wastewater treatment facilities, active soil remediation sites and plant bioremediation of contaminated soil and ground water¹².

A MIDAC FT-IR spectrometer was used for monitoring the plant bioremediation of volatile organic compounds using FT-IR. This particular instrument is a rugged, compact and easily transported FT-IR spectrometer.

The spectrometer requires a computer to store, transform, display and manipulate data collected by the spectrometer. The operating software is Spectra Calc™ which is menu driven and generally user friendly. The general specifications of the instrument are outlined in the table below¹³:

TABLE 1: SPECTROMETER SPECIFICATIONS

RESOLUTION	STEP SELECTABLE, FROM 32 TO 2, 1 OR 0.5 cm^{-1}
SPECTRAL RANGE	350 TO 7800 cm^{-1}
ACCURACY	> 0.01 cm^{-1}
SCAN RATE	0.125 cm/sec
INFRARED BEAM	f# 3.5, 0.5 cm dia at sample
SOURCE	1350K, AIR COOLED, SILICON CARBIDE
BENCH SIZE	29W x 9D x 5.8H (inches)
BENCH WEIGHT	30 POUNDS
POWER	110/220V AC, 50/60 Hz, 50W or 12V DC

More information about the MIDAC spectrometer is outlined in the operator's

manual. For a general overview of the components of Fourier transform instruments, one may consult an instrumental analysis text such as the one by Skoog and Leary¹⁴.

REFERENCES:

1. Bell, Robert John, Introductory Fourier Transform Spectroscopy, Academic Press, Inc., New York, p. 17, (1972).
2. Bell, pp. 1-382.
3. Griffiths, Peter R. and de Haseth, James A., Fourier Transform Infrared Spectrometry, John Wiley & Sons, New York, (1986).
4. Bell, p. 2.
5. Diem, Max, Introduction to Modern Vibrational Spectroscopy, John Wiley & Sons, New York, p. 162, (1993).
6. Diem, p. 162.
7. Diem, p. 162.
8. Griffiths, p. vi.
9. Griffiths, p. vi.
10. Spartz, M.L., Witkowski, M.R., Fateley, J.H., Jarvis, J.M., White, J.S., Paukstelis, J.V., Hammaker, R.M., Fateley, W.G., Carter, R.E., Thomas, M., Lane, D.D., Marotz, G.A., Fairless, B.J., Holloway, T., Hudson, J.L., and Gurka, D.F., "Evaluation of a Mobile FT-IR System for Rapid VOC Determination", American Environmental Laboratory, November 1989, pp. 15-

30, (1989).

11. Spartz, p. 16.

12. Witkowski, M.R., Chaffin, C.T., Havens, B.R., Hoffman, R.M.,
Makepeace, V., Marshall, T.L., Poholarz, J.M., Russell, N.K., Tucker, M.D.,
Visser, V.P., Hammaker, R.M. and Fateley, W.G., "Can You See Carbon
Tetrachloride?", The Pittsburgh Conference 1994 Abstracts (896),
February 27 - March 4, 1994.

13. Midac Corporation, M Series FTIR Spectrometer Operator's Manual,
Costa Mesa, California, revision X-2, 5 October 1992, p. 1-4, (1992).

14. Skoog, Douglas A. and Leary, James J., Principles of Instrumental
Analysis, fourth edition, Saunders College Publishing, pp. 266-270, (1992).

CHAPTER FOUR

OPEN PATH FT-IR MONITORING OF BIOREMEDIATION

THE CURTAIN RAISES

In order to study the beneficial effects of plants on bioremediation, it was necessary to design a plant treatment system which would allow direct measurement of the transfer of contaminants in question out of the aqueous phase (soil and ground water). Dr. Davis, Department of Biochemistry, Kansas State University, was responsible for the design, development and construction of the plant treatment system used in these experiments. Although, a rigorous description of the plant treatment system was previously presented¹, a review of its design and construction is appropriate. A photograph of the plant treatment system is in figure 1. A schematic diagram of the plant chamber is provided in figure 2.

The plant growth chamber consists of two identical halves, each having a channel 10 cm wide, 35 cm deep, and 1.8 m long. The sections were folded in a U shape for convenience. The chamber was filled with Kansas river sand and silt from a local landfill where transport of organic contaminants presents an environmental concern. The soil was packed in and four sampling wells were emplaced. These sampling wells provide a means for extracting samples of groundwater. The water, containing contaminants under study, enters and exits the chamber at the same end. To monitor volatilization or transpiration of volatiles a gas tight, 26 cm high enclosure was constructed to cover the entire chamber. Fluorescent lights 40 cm above the ground surface provide illumination for plant growth. The volume of the entire above ground plant treatment system is approximately 150 liters.

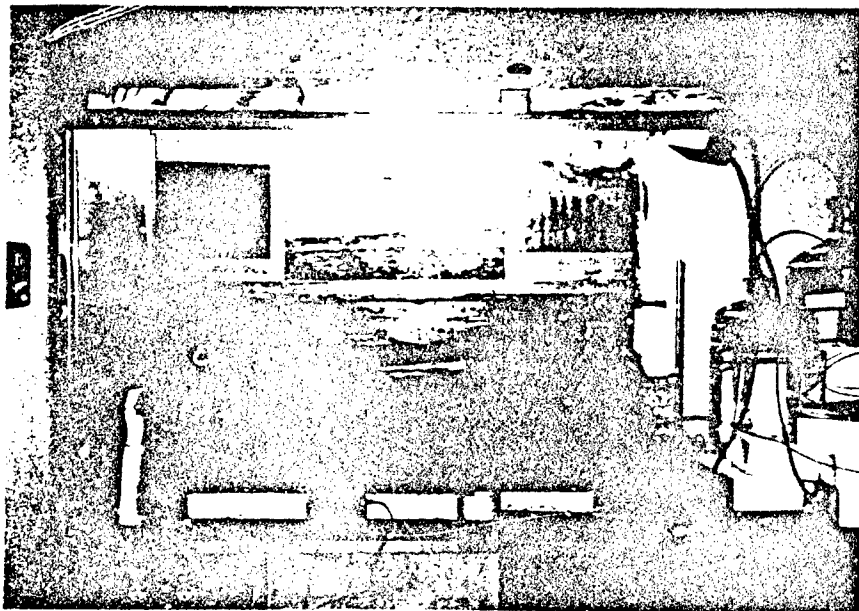


FIGURE 1. PHOTOGRAPH OF PLANT TREATMENT SYSTEM.

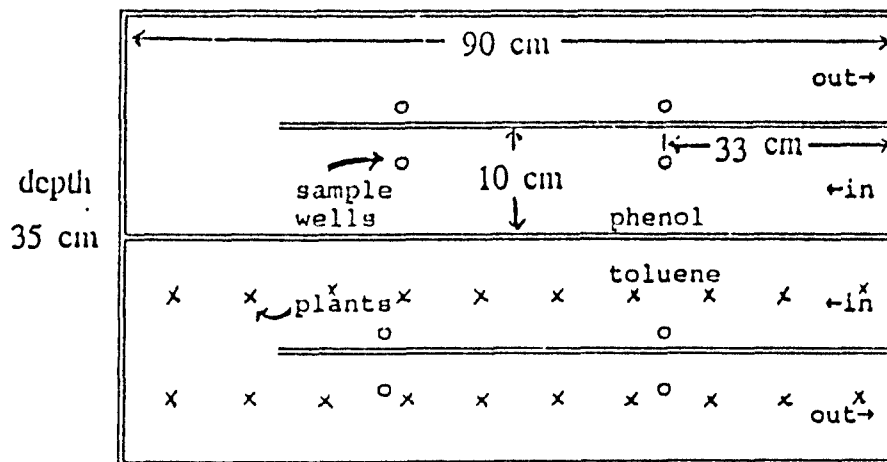


FIGURE 2. SCHEMATIC DIAGRAM OF PLANT TREATMENT
SYSTEM.

Pairs of alfalfa seedlings were planted at 10 cm intervals. The alfalfa plants grew for 6 months to establish a mature stand of plants and to enhance the populations of organisms able to degrade the organic contaminants² prior to the commencement of our study. The ground water is maintained at a depth of 10 cm from the bottom and the compounds of interest are introduced into the water source in the desired concentration.

The spectrometer set up is shown in the photo in figure 3. A schematic diagram of the instrumental set up is in figure 4. The spectrometer is mounted on a plate attached to a quick set tripod. Light from the silicon carbide glower, which serves as the source, is reflected into the chamber through a potassium bromide (KBr) window. The light is then reflected from a mirror set at 45 degrees into a mirror located the end of the chamber, back into the angled mirror and through another KBr window before passing into the spectrometer. The internal pathlength is 2.44 meters. The detector used throughout this work is a broad band, liquid nitrogen cooled MCT (mercury cadmium telluride).

Initial work involved toluene and phenol. FT-IR monitoring of the chamber was used to provide a lot of information simultaneously. Once the chamber was completely sealed off we began our work of acquiring spectral data. By design, we set out to monitor the accumulation (relative concentration) of toluene and phenol in the chamber over time, track the leak rate of the system by observing the decrease in the relative concentration of a

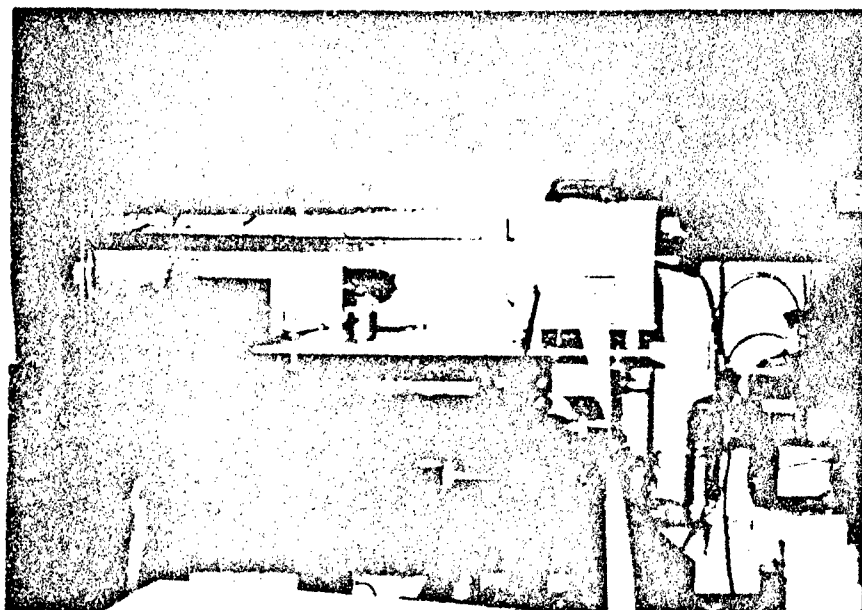


FIGURE 3. PHOTOGRAPH OF SPECTROMETER SET UP.

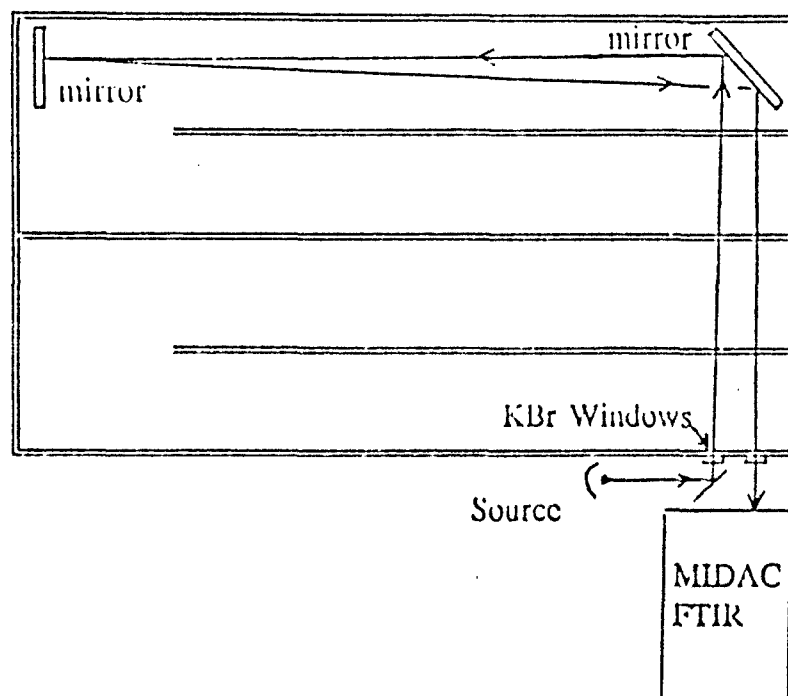


FIGURE 4. SCHEMATIC DIAGRAM OF SPECTROMETER SET UP.

known amount of methane introduced into the system by injection, and measure fluctuations in the relative CO₂ concentration in the chamber as a mechanism to estimate respiration rate.

Using the equipment set up shown in figures 3 and 4, we began our monitoring studies of the plant chamber. The region of the electromagnetic spectrum used in this study is between 400 and 4000 cm⁻¹ (mid infrared). The data collection parameters utilized for all of the experiments reported in this thesis are 1 cm⁻¹ resolution and 255 coadditions per spectrum. Typically, the average signal to noise ratio was 3000 to 1 (1/peak to peak) in the region 1400 to 600 cm⁻¹.

In our first experiment, we acquired a background or reference spectra and then sealed the chamber. Once the chamber was sealed, we injected 5 ml methane into the chamber to establish a leak rate and began collecting 10 spectra at 20 minute intervals for two hours. Representative spectral regions used to monitor the methane and observe relative changes in concentration of phenol, toluene and carbon dioxide are shown in figure 5 (methane spectrum), figure 6 (phenol spectrum), figure 7 (toluene spectrum) and figure 8 (carbon dioxide spectrum). By monitoring the relative change in concentration of the injected methane using the peak at 3017 cm⁻¹ we established a leak with a plot of Δ in concentration over time. After examination of the collected spectra, we were able to detect a slight change in the relative concentration of toluene using the peak at 729 cm⁻¹. In this experiment, we were unable to observe the

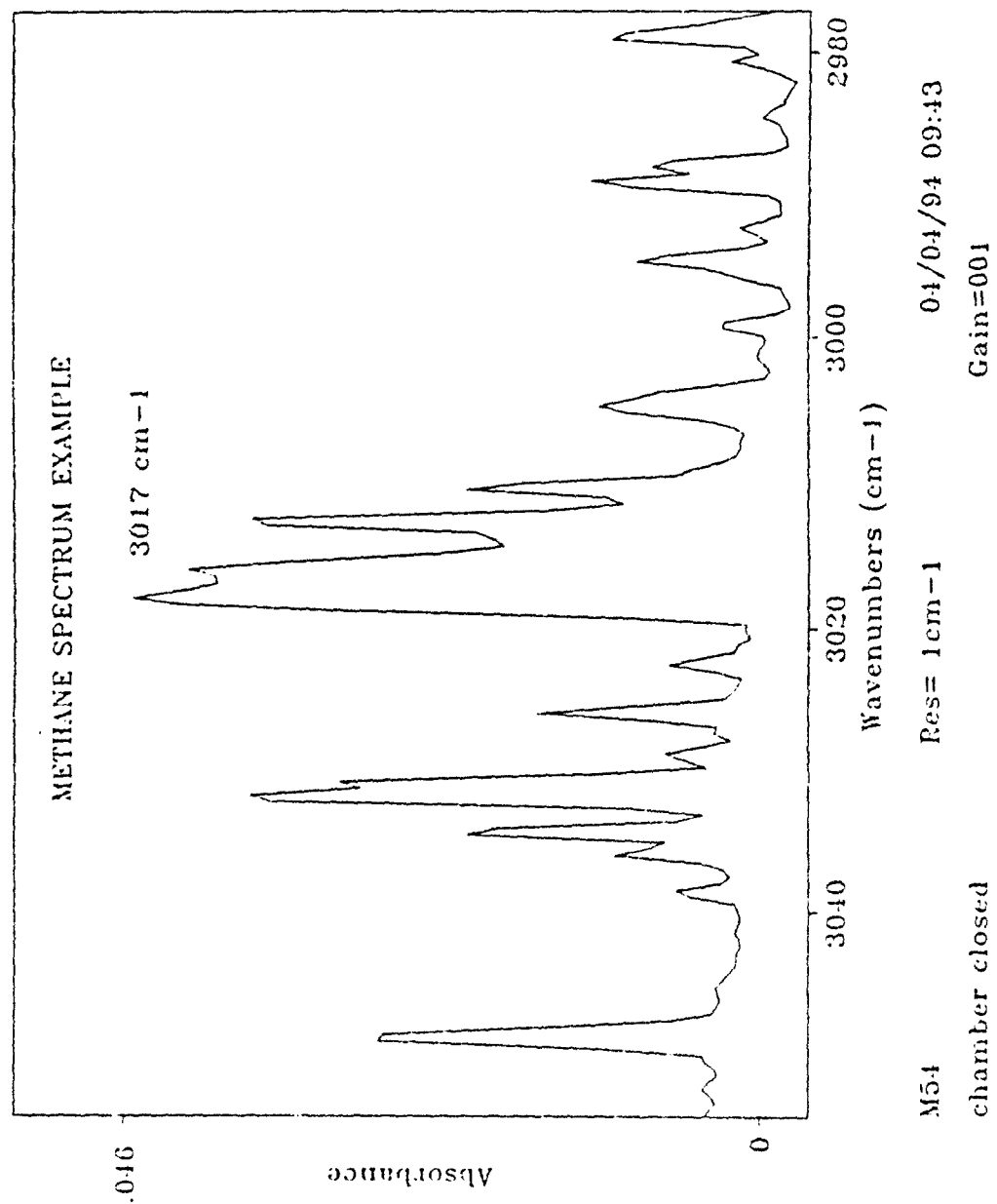


FIGURE 5. METHANE SPECTRUM EXAMPLE.

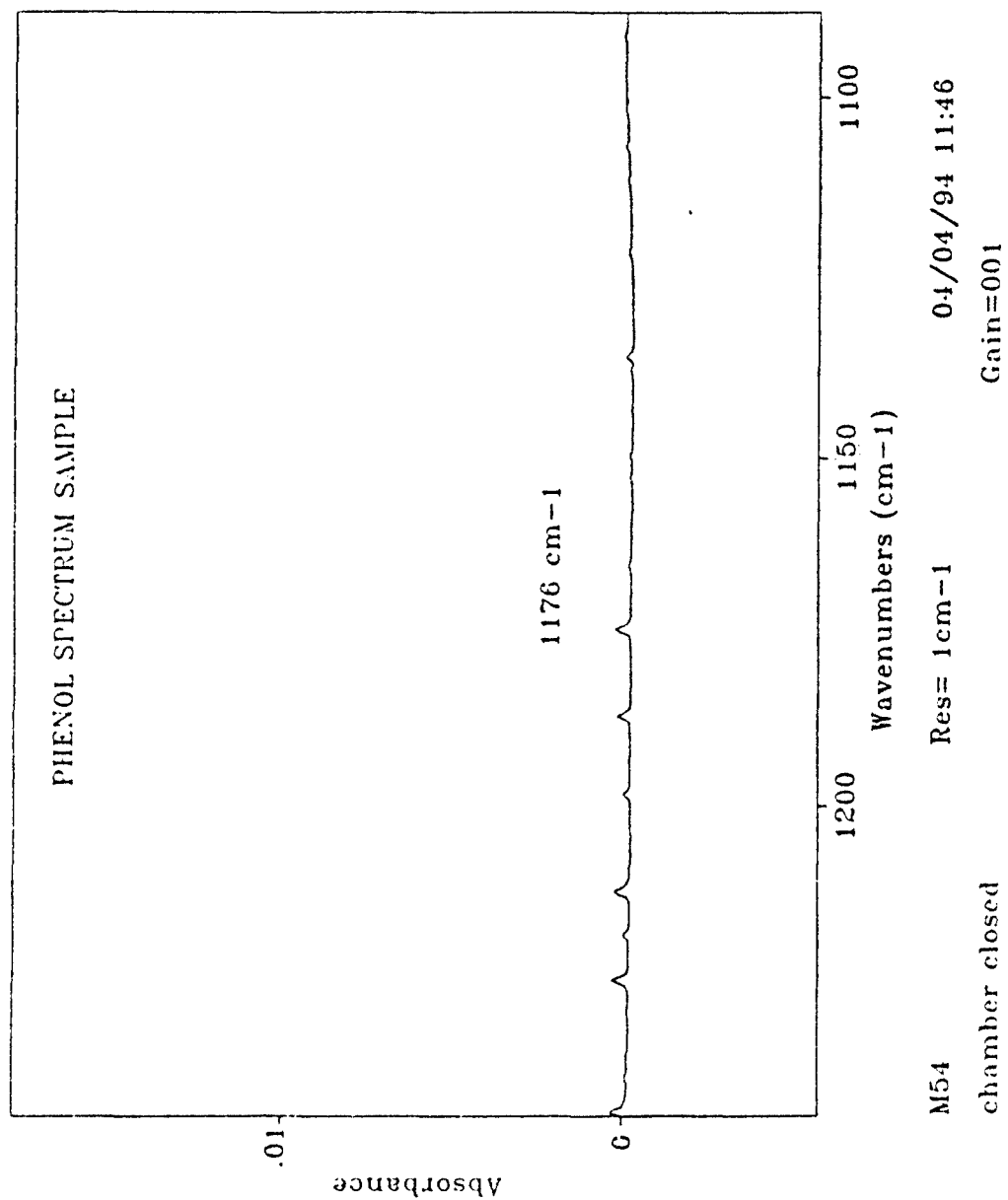


FIGURE 6. PHENOL SPECTRUM EXAMPLE.

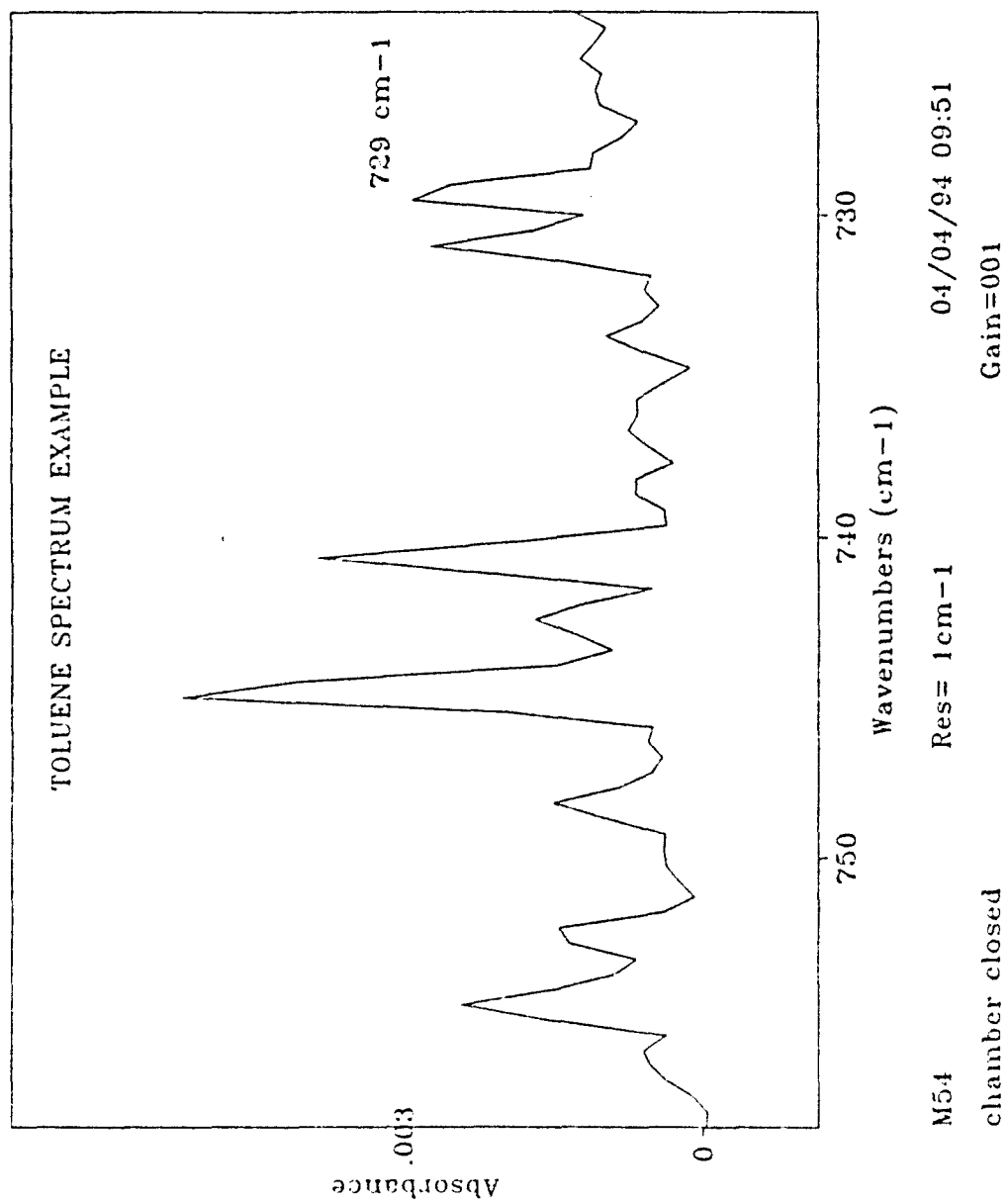


FIGURE 7. TOLUENE SPECTRUM EXAMPLE.

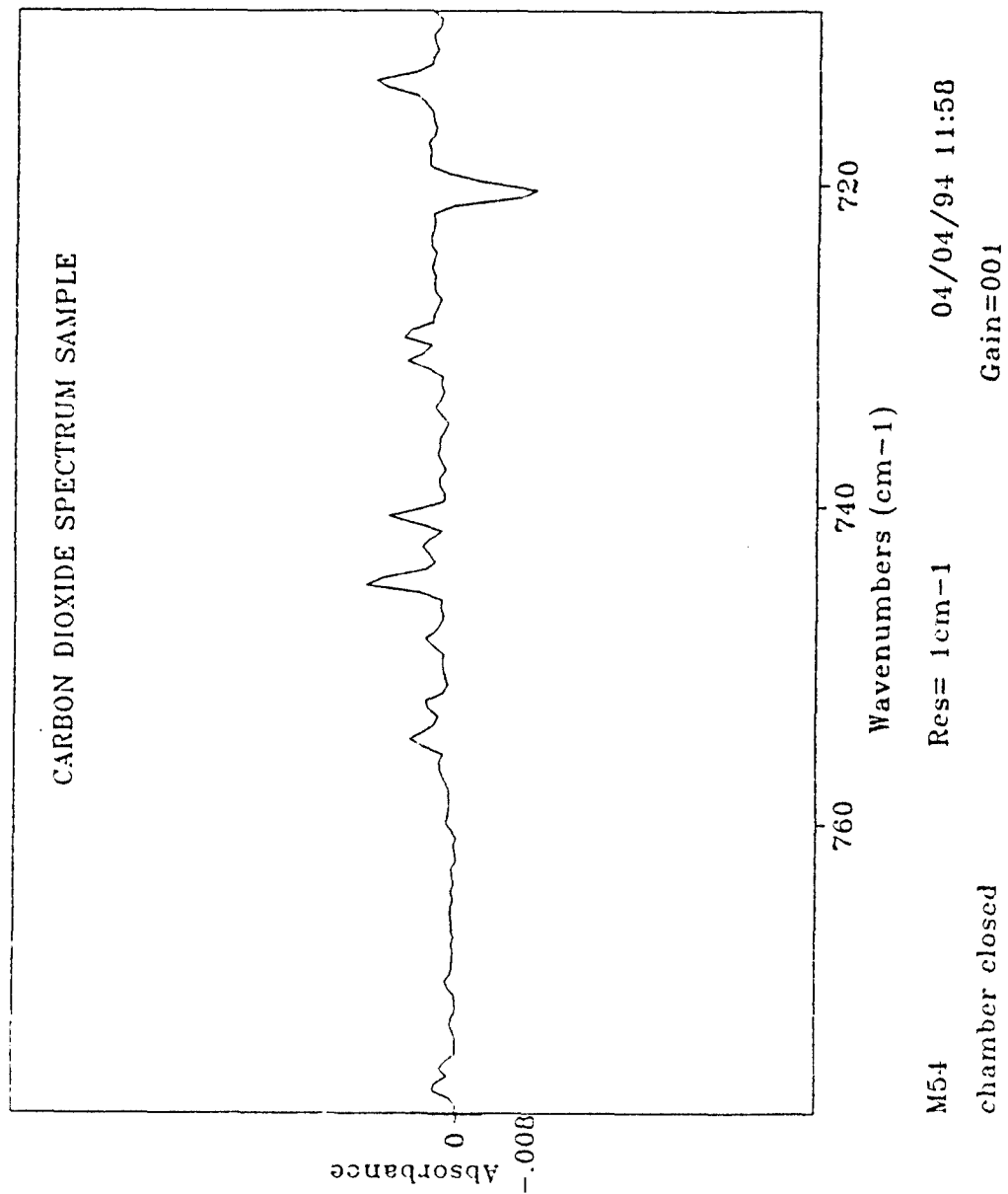


FIGURE 8. CARBON DIOXIDE SPECTRUM EXAMPLE.

Δ in relative concentration of phenol (concentration at or below the detection limit) at 1176 cm^{-1} as evident in figure 6. The Δ in relative concentration (decrease) of carbon dioxide over time was monitored using the 720 cm^{-1} band. Due to our experimental observations, we decided to change the parameters for the next trial. Next, we monitored the chamber after surface application of 1000 ml of contaminant (toluene and water). As before, methane was injected to track the leak rate. The increase in toluene concentration was readily detectable and resulted in spectra similar to the toluene spectrum in figure 9. Comparing the spectrum in figure 9 with the spectrum in figure 7 confirmed our use of the band at 729 cm^{-1} for this compound. Once again, we were unable to observe phenol in the acquired spectra and the relative Δ in carbon dioxide concentration was monitored at 720 cm^{-1} .

To ensure we could in fact detect phenol, we designed a simple trial exclusively, to monitor phenol. The chamber was sealed, 1 ml of phenol (.90) was injected into treatment system, and the atmosphere above the plants was monitored periodically for two hours. Methane (10 ml) was also injected to track leak rate. The spectrum with the largest relative concentration of phenol based upon absorbance (1176 cm^{-1}) is in figure 10. This test demonstrated our ability to observe small quantities of phenol. Data gathered up to this point, allowed us to make some general observations. The relative concentration of toluene present in the vapor phase was less than the concentration of toluene being introduced in the contaminated groundwater and the phenol in the

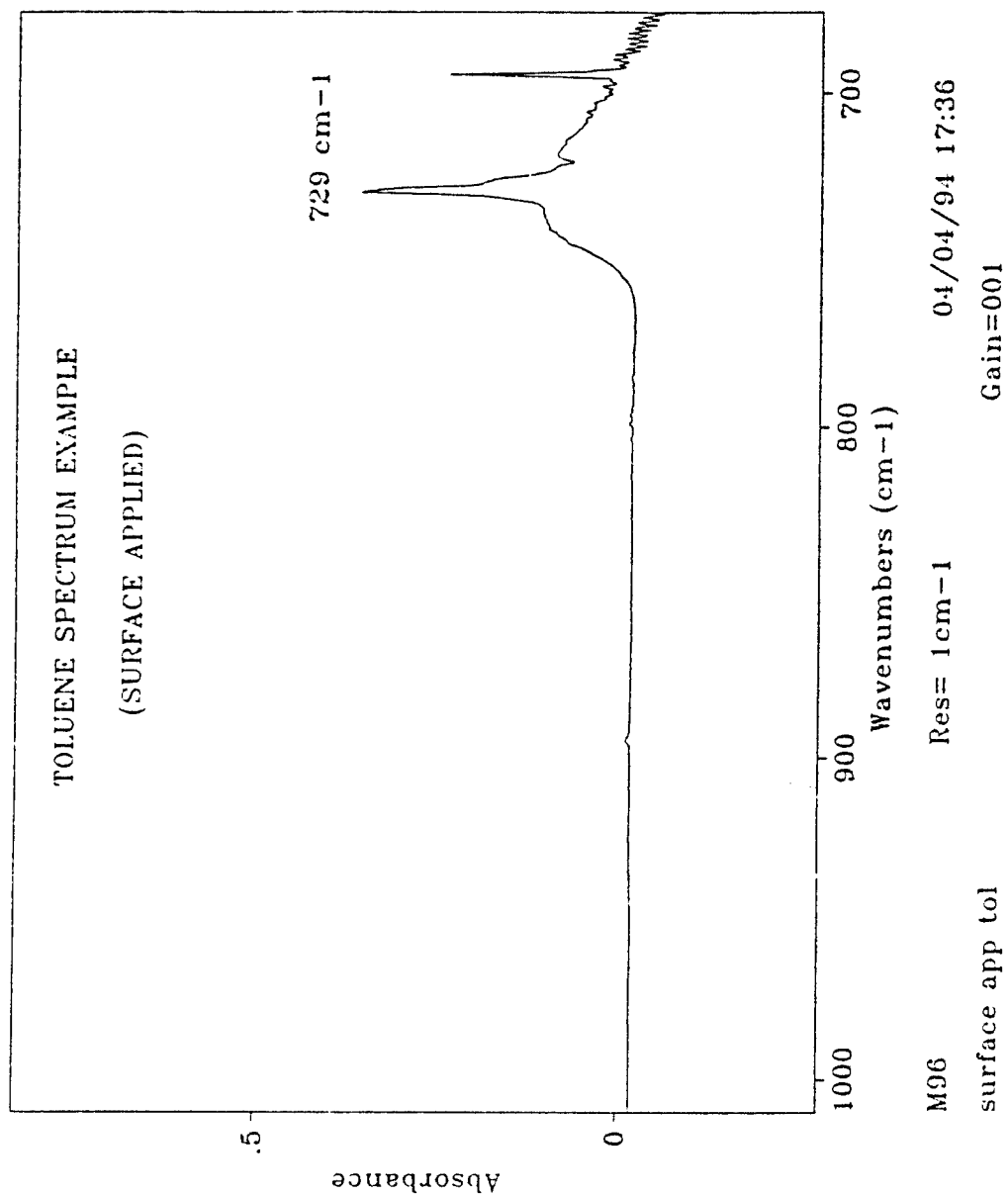


FIGURE 9. TOLUENE SPECTRUM EXAMPLE.

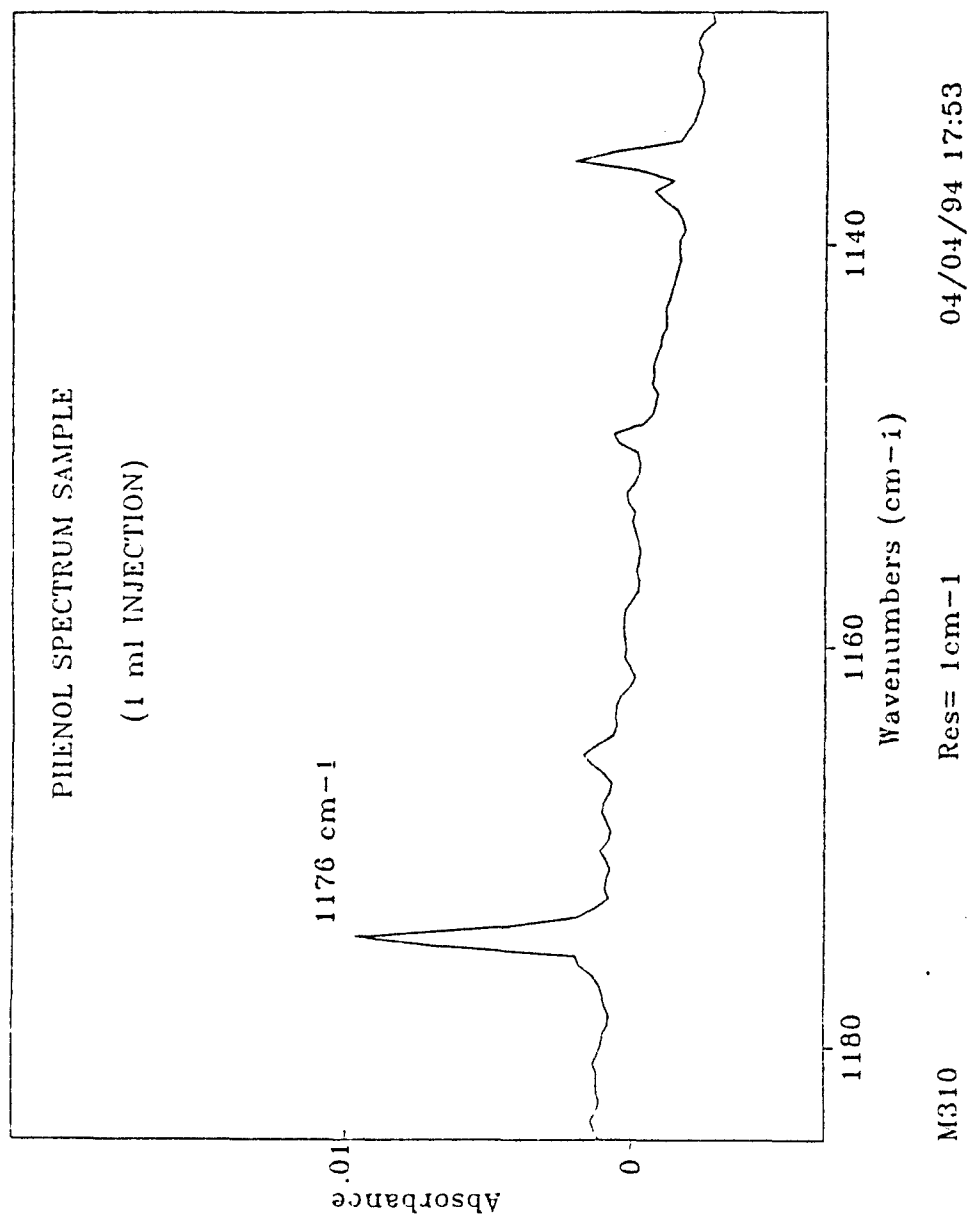


FIGURE 10. PHENOL SPECTRUM EXAMPLE.

groundwater was not detectable in the vapor phase. In short, these two contaminant compounds were not being transferred from the groundwater into the vapor phase in the same concentrations. The lower relative atmospheric concentrations of toluene and phenol, suggest and support that some type of degradative process is underway.

Satisfied with our ability to monitor toluene, phenol and methane we focussed our attention on carbon dioxide. An experiment was conducted to monitor relative Δ in carbon dioxide concentration. The chamber was closed off and 10 spectra were collected at fifteen minute intervals. At the conclusion of the tenth spectrum, three injections of 29 ml of CO_2 (≈ 200 ppm) were introduced in 15 minute intervals and in between spectral acquisition. An absorbance file was created for each of the spectra using the first spectrum as a reference. The absorbance units were determined by using integrated area. The integrated area and a calibration file were used to calculate the concentration in parts per million (ppm). The calibration process will be outlined in chapter 5. A graph of the rate of relative Δ in carbon dioxide concentration (0 is atmospheric concentration) versus time is shown in figure 11. The normal atmospheric carbon dioxide concentration is approximately 333 ppm based upon components of atmospheric air as listed in the CRC Handbook of Chemistry and Physics³.

Up to this point, we obtained favorable results even though our work was mostly qualitative in nature. For this technique to become a viable

monitoring tool for bioremediation studies, we needed to demonstrate its quantitative value. To accomplish this goal, a calibration study was conducted and a small library of calibration files was generated. The calibration process and files are the subject of the subsequent chapter.

RATE OF CO2

15 MARCH 93

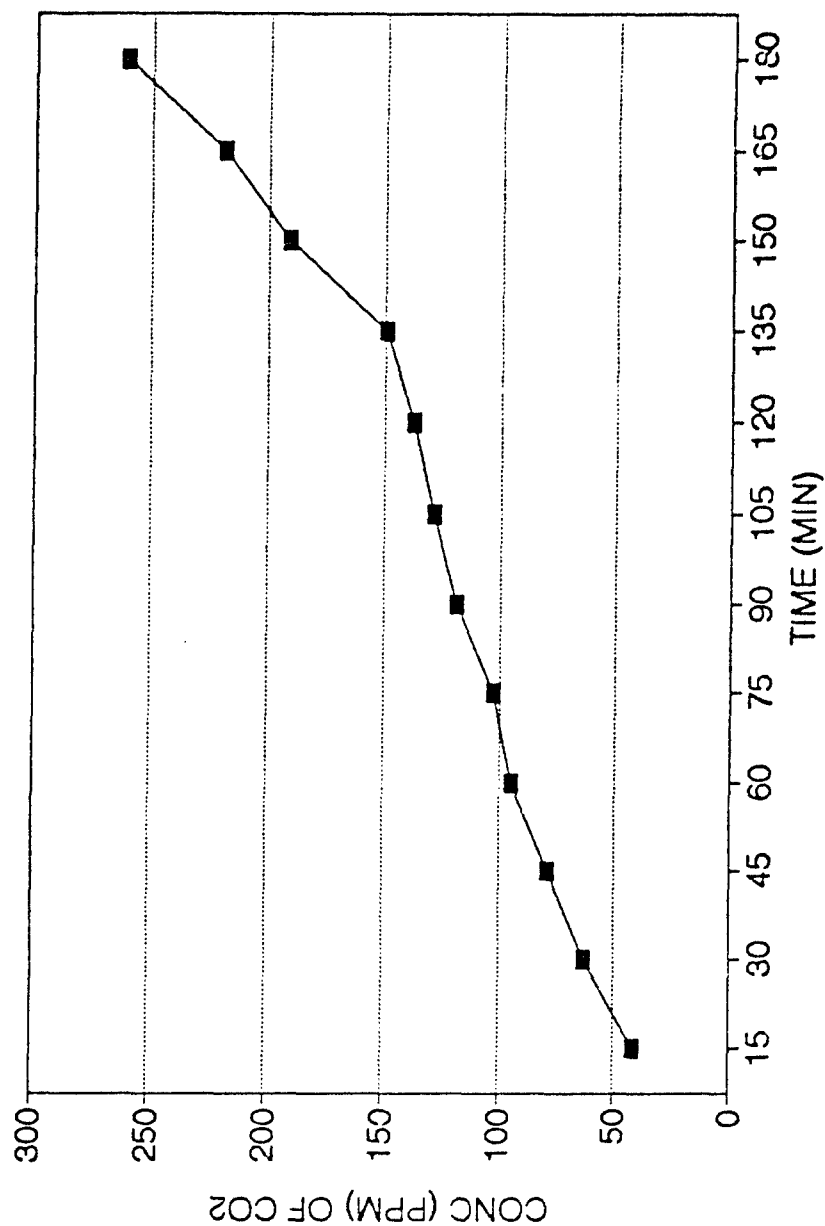


FIGURE 11. GRAPH OF RELATIVE Δ IN CO₂ CONCENTRATION

REFERENCES:

1. Davis, L.C., Chaffin, C.T., Muralidharan, N., Visser, V.P., Fateley, W.G., Erickson, L.E. and Hammaker, R.M., "Monitoring the Beneficial Effects of Plants in Bioremediation of Volatile Organic Compounds" In: L.E. Erickson, D. Tillison, S.C. Grant and J.P. McDonald (eds.), Proceedings of the 8th Annual Hazardous Waste Research, Engineering Extension Service, Kansas State University, Manhattan, Kansas, pp. 236-249, (1993).
2. Davis, p. 239.
3. Weast, Robert C. (ed.), CRC Handbook of Chemistry and Physics, 64th ed., Boca Raton, Florida, p. F-162, (1983).

CHAPTER FIVE

CALIBRATION AND QUANTIFICATION PROCEDURES

This chapter will present experimental procedures for calibration files, steps followed for quantitative interpretation of spectral information, Beer's Law plots of calibration work and a representative spectrum of the region used for the calibration standards of each compound. The methodology utilized for quantitative analysis was clearly outlined by Dr. Witkowski¹ and originally formulated by Dr. Spartz², both former members of the Fateley and Hammaker research group at Kansas State University. First, a succinct review of calibration procedures is provided.

Calibration spectra may be used to identify and quantify the volatile organic compounds present in the collected spectra and to make estimates about the detection limits corresponding to the absorption bands in the IR spectrum of each compound³. The minimum detectable absorbance (detection limit) is three times the peak to peak noise at the wavenumber of the absorption band in the baseline of the background spectrum of the atmosphere over the pathlength (i.e. chamber pathlength of 2.44 m). The calibration spectra presented were collected in a fixed path cell with a length of either 50 cm or 5 cm assuming obedience of Beer's Law⁴ ($A = abc$, where A is the absorbance of the band, a is absorption coefficient in units of $[\text{pathlength} \cdot \text{concentration}^{-1}]$, b is the pathlength and c is the concentration⁵). To determine whether or not Beer's Law applies, calibration spectra are collected at four different concentrations. The absorbance is measured at the band used to identify the compound being calibrated and the absorbance is

plotted versus concentration*pathlength. Linear regression analysis is done and the absorption coefficient is determined. These plots are then used to calculate a concentration in parts per billion (ppb) using the following equation⁶:

$$C_{\text{atm}}(\text{ppb}) = \frac{C_{\text{cell}}(\text{M}) b_{\text{cell}}(\text{m}) R(\text{L} \cdot \text{atm} \cdot \text{mol}^{-1} \cdot \text{K}^{-1}) T_{\text{atm}}(\text{K}) 10^9}{b_{\text{atm}}(\text{m}) P_{\text{atm}}(\text{atm})}$$

The rigorous solution of this equation is available in the aforementioned references^{1,2}. An example demonstrating how the information contained in this equation is used for the calibration of trichloroethylene (TCE) is described below.

Four different spectra are collected. The four spectra used for the calibration of TCE are shown in figure 12. Each of the four samples are made by introducing a known pressure of compound being calibrated into the sample cell and backfilling the cell with nitrogen until atmospheric pressure (~ 740 torr in Manhattan, Kansas) is attained in a 50 cm cell. The measured volume of the 50 cm cell is 697 ml. The concentration is calculated from the pressure, as measured on the vacuum system manostat, using the equation:

$$C_{\text{cell}}(\text{moles/L}) = P_{\text{cell}}(\text{torr}) / [R(\text{L} \cdot \text{atm} / \text{K} \cdot \text{mol}) T_{\text{cell}}(\text{K}) (760 \text{ torr/1 atm})]$$

Once determined, the molar concentrations are then multiplied by the pathlength. A four point calibration curve (Beer's Law plot) in figure 13 is

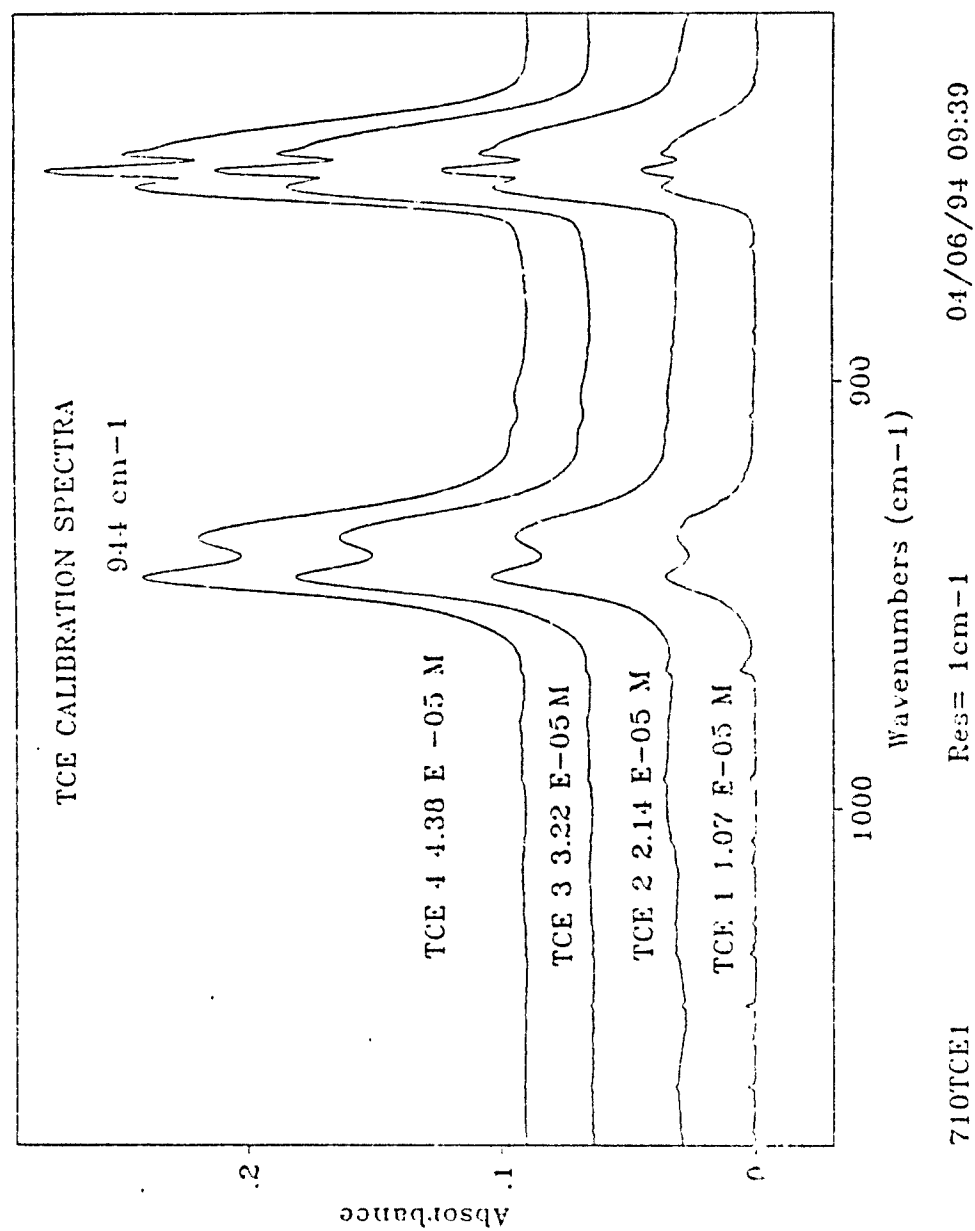


FIGURE 12. FOUR CALIBRATION SPECTRA OF
TRICHLOROETHYLENE.

Beer's Law Plot

Trichloroethylene, 1 cm^{-1} , $b=0.5 \text{ meters}$

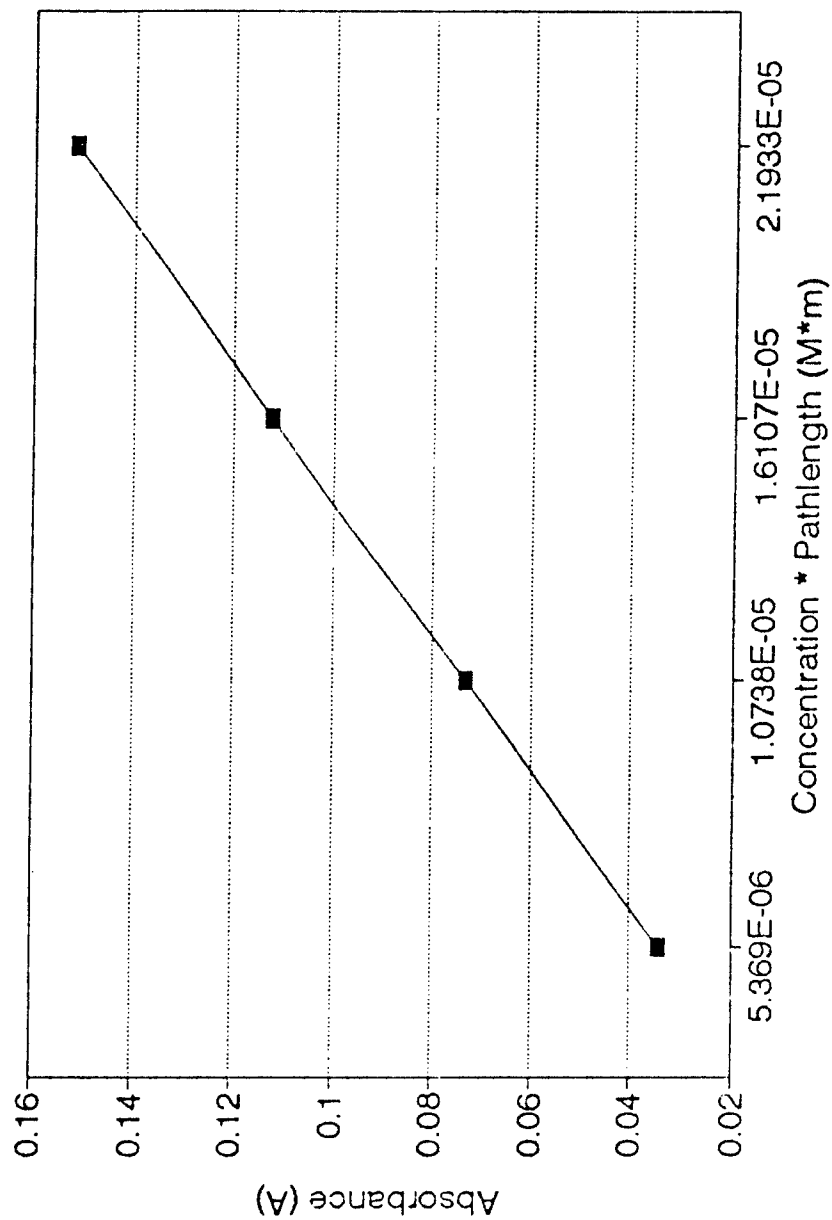


FIGURE 13. FOUR POINT CALIBRATION CURVE FOR TCE.

then generated with the information in the spreadsheet shown in figure 14 using Quattro Pro software. Linear regression yields the absorption coefficient. We are then able to use this calibration file to determine the atmospheric concentration (C_{atm}) in ppb by completing the calculation shown at the top of page 44. For example, substituting the information in the table below into this equation, we find C_{atm} (ppb) = 4002. This calculation is also represented in the spreadsheet presented in figure 14.

TABLE 2: EXPERIMENTAL DATA FOR EXAMPLE CALCULATION

VARIABLE	VALUE AND UNITS
C_{cell}	8.17 E-07 M
b_{cell}	0.5 m
R	0.0821 L*atm/mol*K
T_{atm}	295.6 K
b_{atm}	2.44 m
P_{atm}	0.986 atm

trichloroethylene
Cell Pathlength 0.5 meters

peak absorbance 944 cm-1 A	Concentration * Pathlength C*b	Absorptivity a
0.034638	5.369E-06	6451.48072267
0.07152	1.0738E-05	6660.45818588
0.115055	1.6107E-05	7143.1675669
0.15029	2.1933E-05	6652.23179684

Regression Output:

Constant	-0.003
Std Err of Y Est	0.00336
R Squared	0.99705
No. of Observations	4
Degrees of Freedom	2
X Coefficient(s)	7085.55
Std Err of Coef.	272.473

Measured Absorbance
0.002895

Calc. Concentration(M)
8.17E-07

Cell Pathlength(m)
0.5

Measured Temperature(K)
295.6

Atmospheric Concentration(ppb)
4002

Atmospheric Pressure(atm)
0.986

Atmospheric Pathlength(m)
2.44

FIGURE 14. CALIBRATION SPREADSHEET FOR
TRICHLOROETHYLENE.

During the course of this research, a number of calibrations were prepared for use in our study of bioremediation. The calibrations of each compound identified in table 3 were accomplished by the author using a 50 cm cell. With exception of phenol, the calibrations of each compound in table 4 were accomplished by members of our research group and were extracted from our laboratory calibration file library. Each of the calibrations in table 4 were prepared using a 5 cm cell.

TABLE 3. CALIBRATIONS USING 50 CM CELL

COMPOUND	CAS #	SPECTRUM	CAL.	SHEET
1,1,1-Trichloroethane	71-55-6	p. 82	p. 83	p. 84
1,1,2-Trichloroethane	79-00-5	p. 85	p. 86	p. 87
Trichloroethylene	79-01-6	p. 45	p. 46	p. 48
Carbon Dioxide	124-38-9	p. 52	p. 53	p. 54
1,1-Dichloroethane	75-34-3	p. 58	p. 59	p. 60
1,2-Dichloroethane	107-06-2	p. 61	p. 62	p. 63
1,1-Dichloroethylene	75-35-4	p. 64	p. 65	p. 66
cis-1,2-Dichloroethylene	156-59-2	p. 67	p. 68	p. 69
trans-1,2-Dichloroethylene	156-60-5	p. 70	p. 71	p. 72

Information provided in tables 3 and 4 include compound name, Chemical Abstracts Service registry number (CAS #), page number of actual calibration spectrum (SPECTRUM), page number of the calibration curve (CAL) and the page number of the generated calibration spreadsheet (SHEET).

TABLE 4. CALIBRATIONS USING 5 CM CELL

COMPOUND	CAS #	SPECTRUM	CAL	SHEET
Methane	74-82-8	p. 73	p. 74	p. 75
Chloroform	865-49-6	p. 55	p. 56	p. 57
Vinyl Chloride	75-01-4	p. 88	p. 89	p. 90
Toluene	108-88-3	p. 79	p. 80	p. 81
Phenol	108-95-2	p. 76	p. 77	p. 78

The calibrations, except for phenol, in table 4 above were collected at $.5 \text{ cm}^{-1}$ resolution. A quick reference which indexes the figure numbers of all calibration spectra, calibration curves and spreadsheets organized by compound name in alphanumeric order is listed in table 5.

TABLE 5. INDEX OF CALIBRATION INFORMATION FIGURE
NUMBERS

<u>COMPOUND NAME</u>	<u>FIGURE NUMBERS</u>		
	<u>SPECTRUM</u>	<u>CALIB CURVES</u>	<u>S. SHEET</u>
Carbon Dioxide	15	16	17
Chloroform	18	19	20
1,1-Dichloroethane	21	22	23
1,2-Dichloroethane	24	25	26
1,1-Dichloroethylene	27	28	29
cis-1,2-Dichloroethylene	30	31	32
trans-1,2-Dichloroethylene	33	34	35
Methane	36	37	38
Phenol	39	40	41
Toluene	42	43	44
1,1,1-Trichloroethane	45	46	47
1,1,2-Trichloroethane	48	49	50
Trichloroethylene	12	13	14
Vinyl Chloride	51	52	53

The calibration spectrum, calibration curves, and calibration spreadsheets are printed in figures 12 through 56. The trichloroethylene information included earlier in the chapter will not be reprinted here.

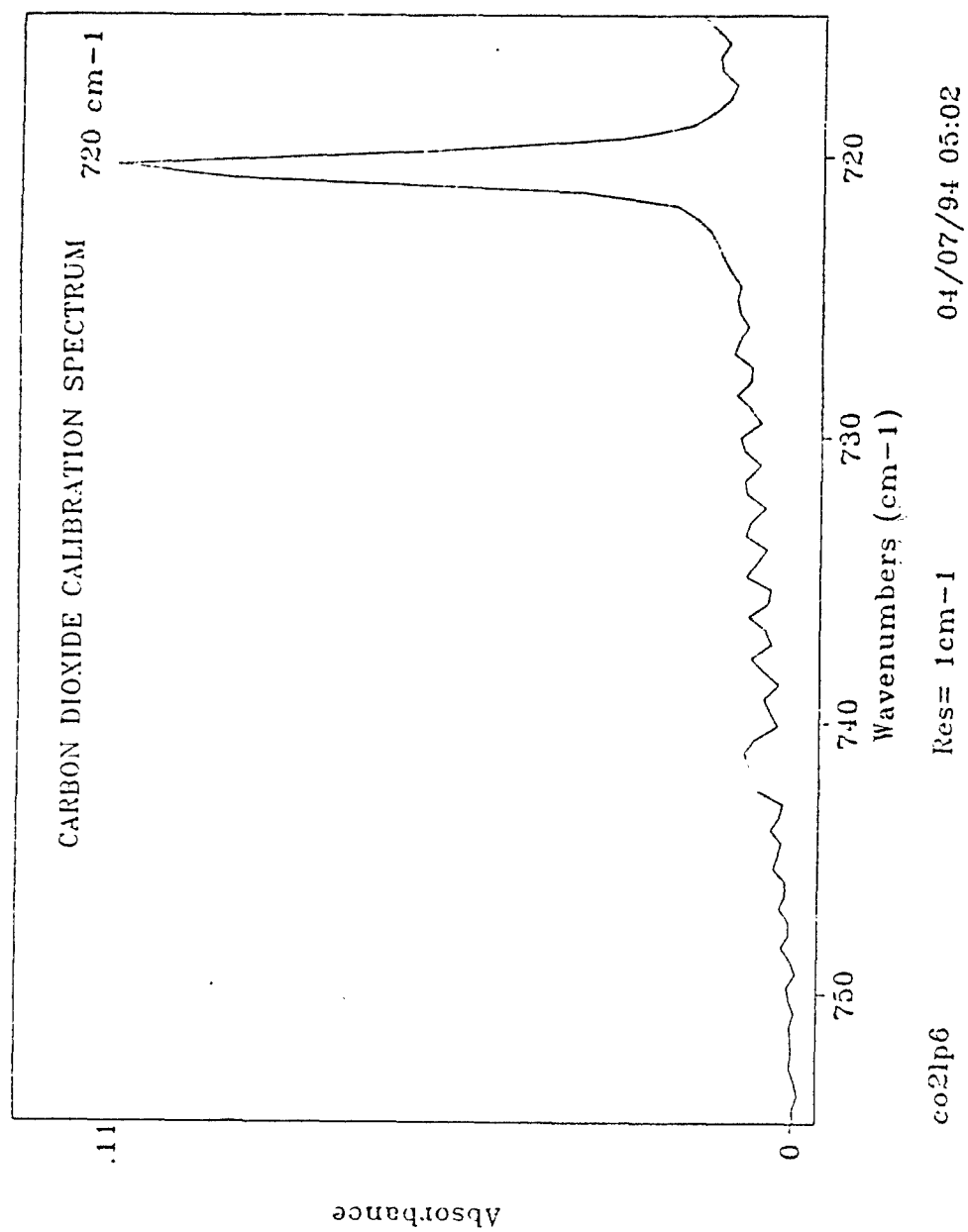


FIGURE 15. CALIBRATION SPECTRUM OF CARBON DIOXIDE.

Beer's Law Plot

CO₂, Res. 1 cm-1, b=0.5 meters

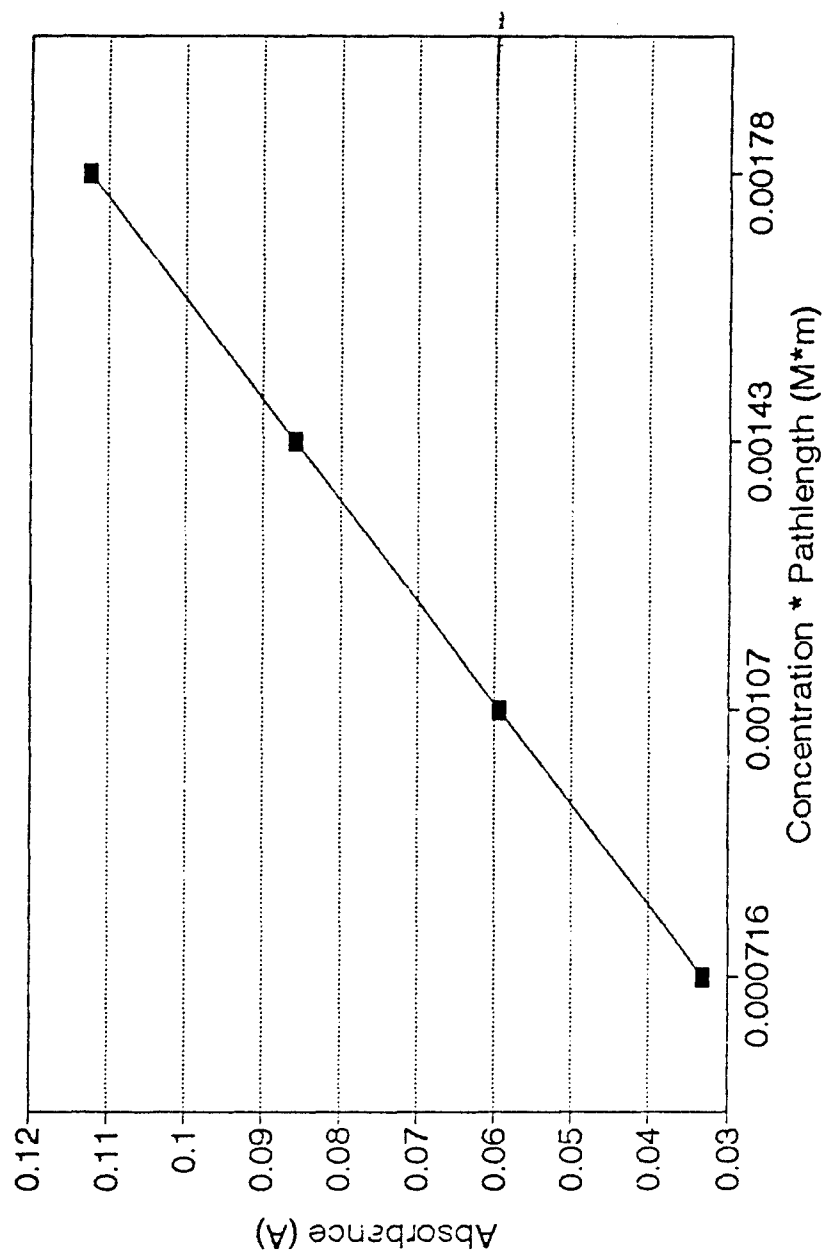


FIGURE 16. FOUR POINT CALIBRATION CURVE FOR CO₂.

Carbon Dioxide
Cell Pathlength 0.50 meters

peak absorbance 720 cm-1

A
0.029124
0.061434
0.09424
0.106036

Concentration * Pathlength

C*b
0.000716
0.00107
0.00143
0.00178

Absorptivity

a
40.6759776536
57.414953271
65.9020979021
59.5707865169

Regression Output:

Constant	-0.02
Std Err of Y Est	0.00784
R Squared	0.96589
No. of Observations	4
Degrees of Freedom	2
X Coefficient(s)	74.2532
Std Err of Coef.	9.86652

Measured Absorbance
0.00405

Calc. Concentration(M)
1.09E-04

Cell Pathlength(m)
0.5

Measured Temperature(K)
295

Atmospheric Concentration(ppb)
533166

Atmospheric Pressure(atm)
0.986

Atmospheric Pathlength(m)
2.44

FIGURE 17. CALIBRATION SPREADSHEET FOR CARBON DIOXIDE.

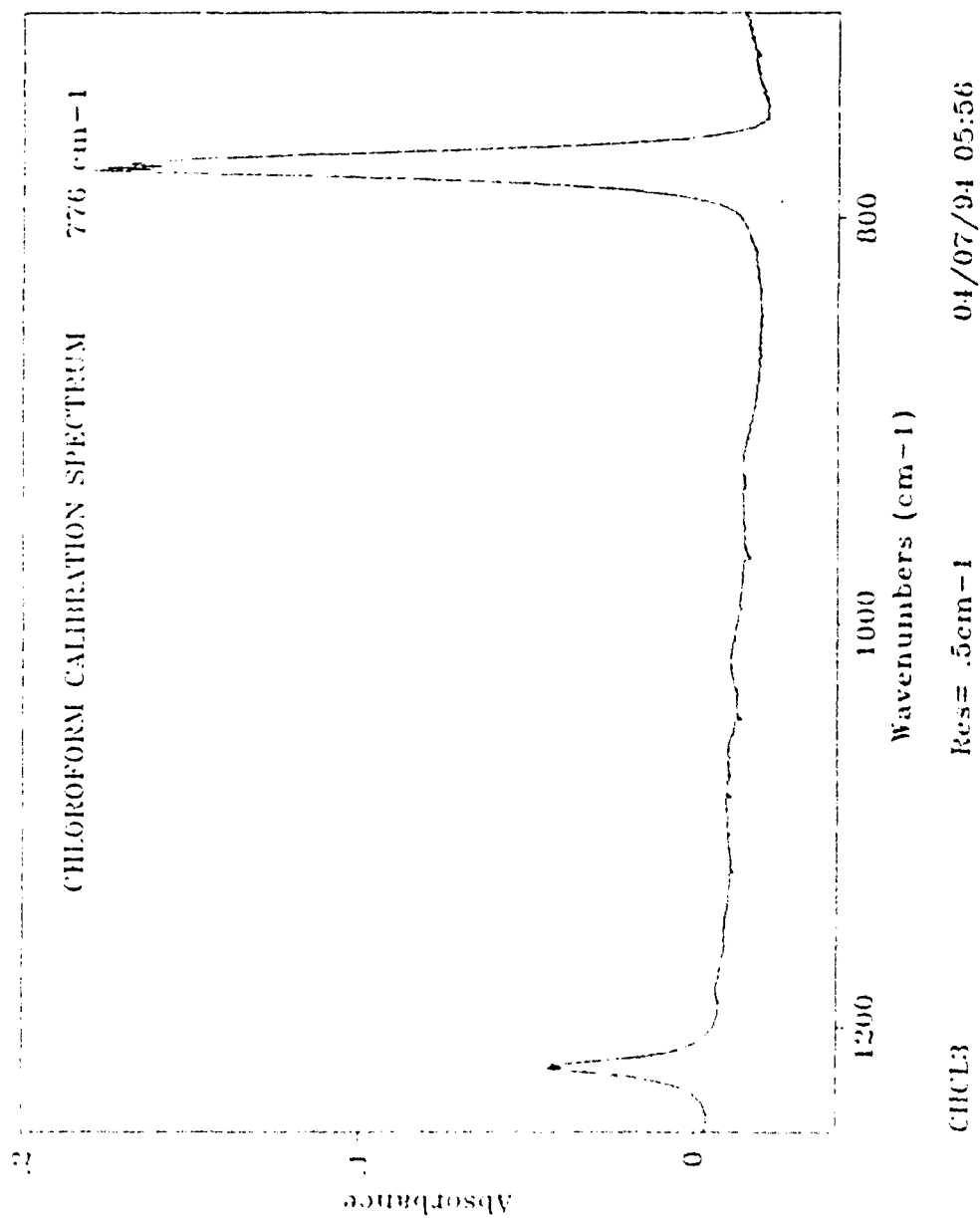
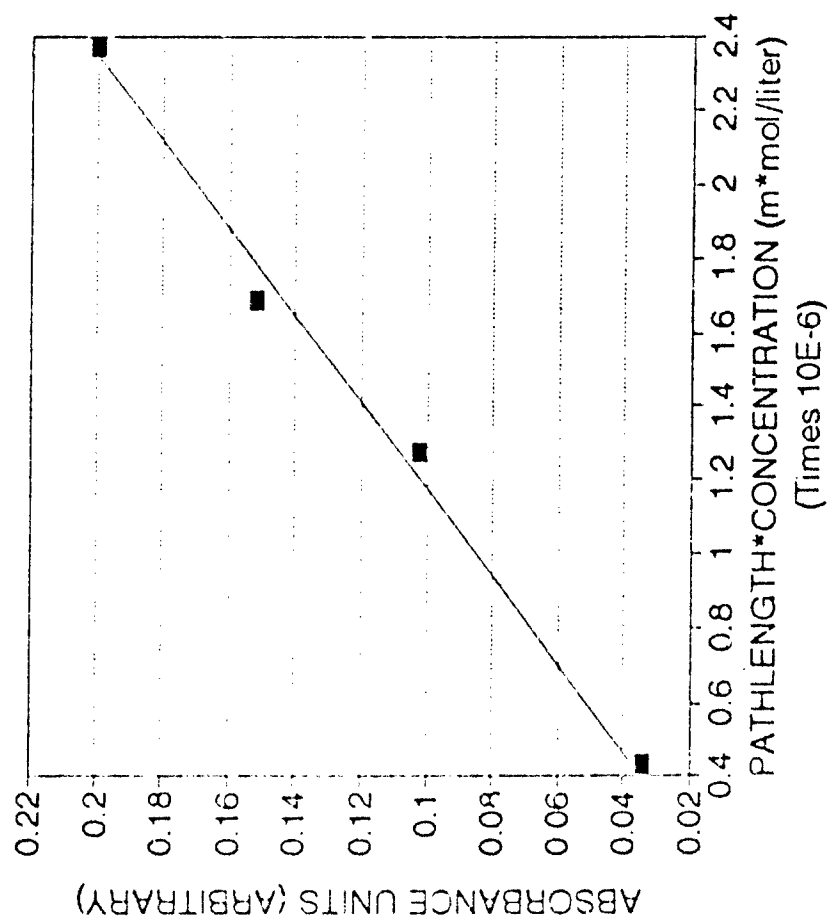


FIGURE 18. CALIBRATION SPECTRUM OF CHLOROFORM.

Chloroform

776.7 cm⁻¹ 0.5 cm⁻¹



■	R-squared =
—	0.9924
—	ABS COEF =
—	8.507E+04
—	DL at 100 m (ppb) =
—	8.9

FIGURE 19. FOUR POINT CALIBRATION CURVE FOR CHLOROFORM.

Chloroform

FILE = 05c06abs
 Peak Resolution
 776.7 cm-1 0.5 cm-1
 # OF SCANS = 128
 DETECTOR = MCT
 SOURCE = SiC
 BEAMSPUTTER = ZnSe
 b - CELL LENGTH (m) = 0.05
 TEMPERATURE (K) = 291
 DATE = Feb3.93

Regression Output:

Constant 0
 Std Err of Y Est 0.006158
 R Squared 0.9924
 No. of Observations 4
 Degrees of Freedom 3

X Coefficient(s) 85070.265398
 Std Err of Coef. 1917.4691196

$$y = 85070.27 * x + 0$$

DETECTION LIMIT AT 3 TIMES PEAK TO PEAK NOISE

NOISE = 0.001
 CALC CONC = 7.05E-07
 CONC (ppb at 10cm) = 8.9

FILE	ABS	TORR	b*(n/V)	ABS1-ABS2	ABS COEF
05c05abs	0.1801	0.8626	2.38E-06	0.19996 0.202073	8.418E+04
	-0.01988		1.89E-06	0.15193 0.143789	8.989E+04
05c07abs	0.14868	0.6138	1.27E-06	0.10251 0.108345	8.049E+04
	-0.00325		4.38E-07	0.034254 0.037247	7.823E+04
05c08abs	0.10158	0.4625			
	-0.00093				
05c09abs	0.025104	0.159			
	-0.00615				
				AVE =	8.320E+04
				From Regression =	8.507E+04

FIGURE 20. CALIBRATION SPREADSHEET FOR CHLOROFORM.

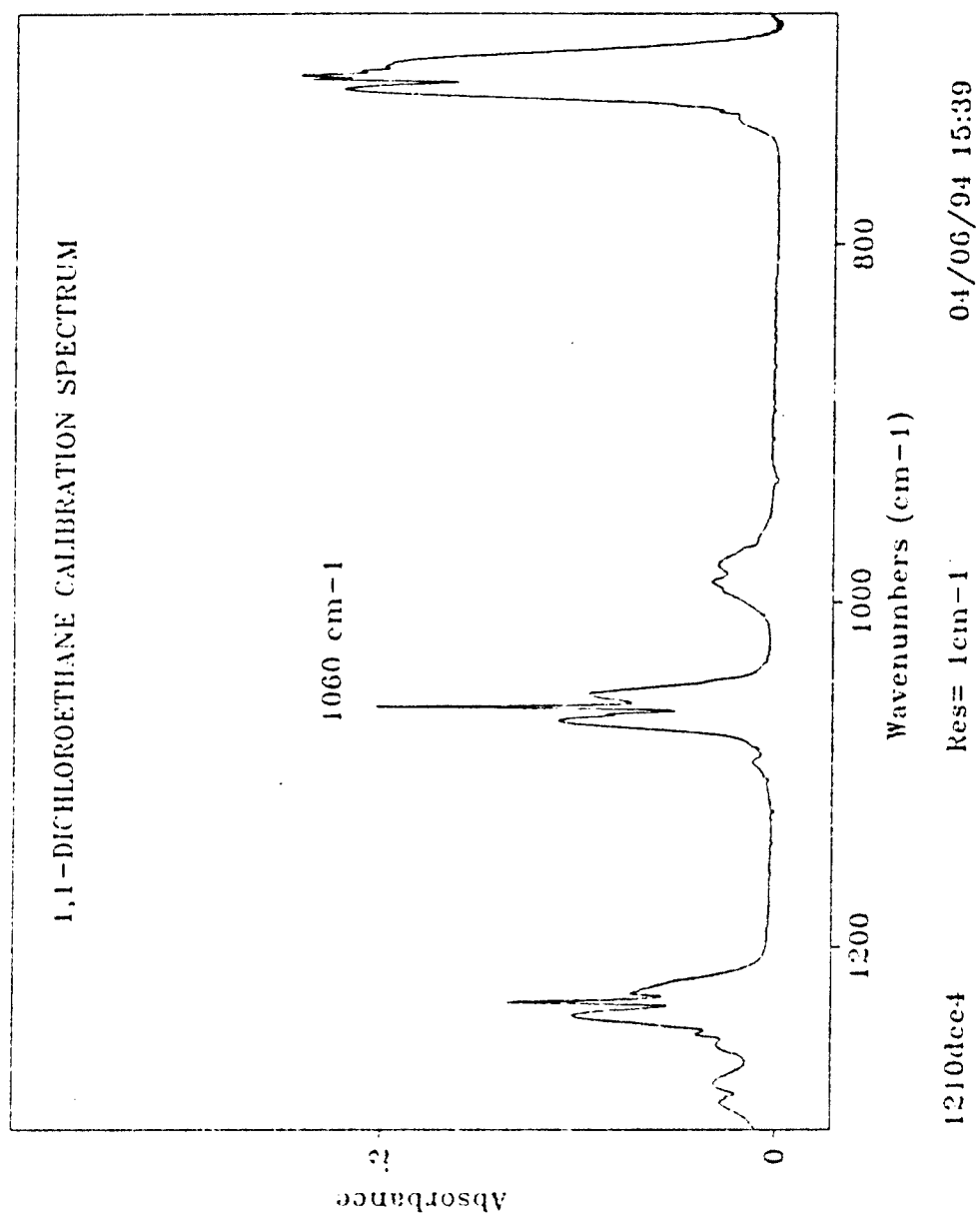


FIGURE 21. CALIBRATION SPECTRUM OF 1,1-DICHLOROETHANE.

Beer's Law Plot

1,1-Dichloroethane, 1 cm^{-1} , $b=0.5\text{ meters}$

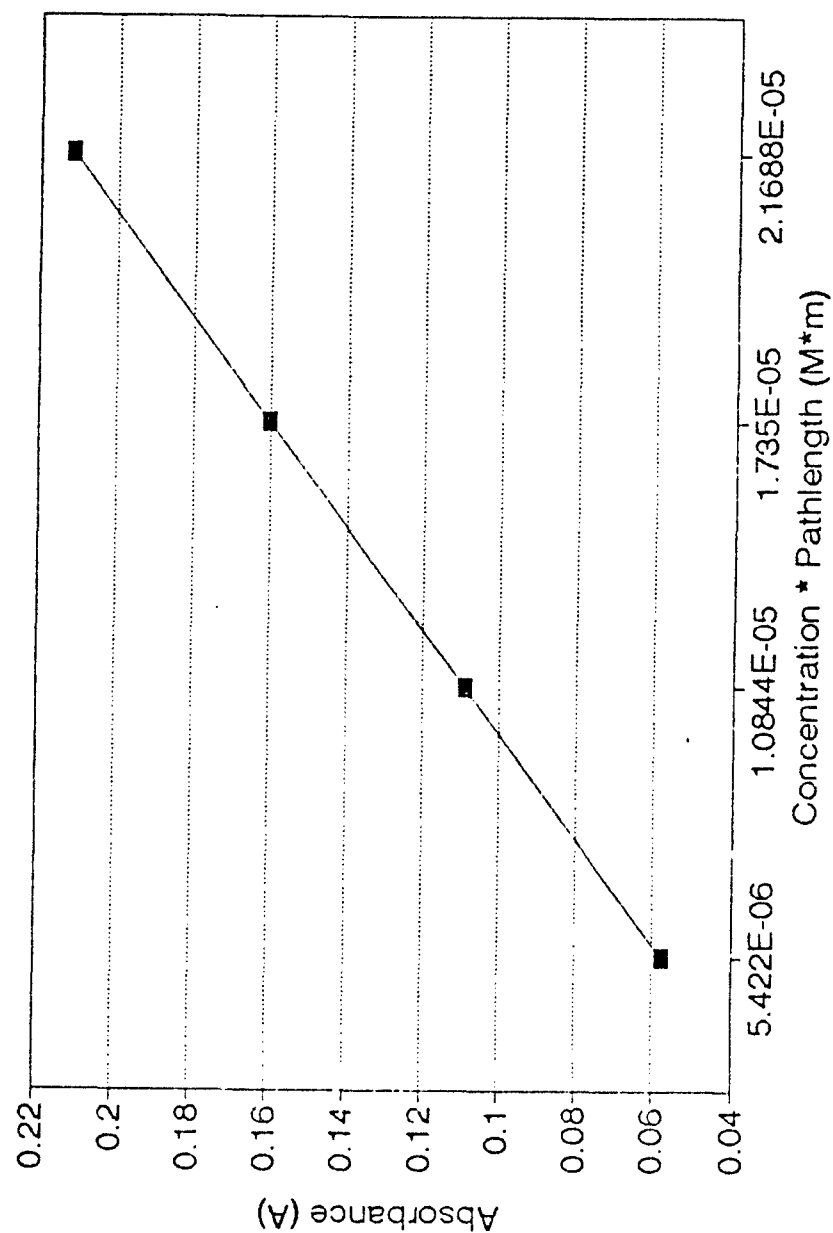


FIGURE 22. FOUR POINT CALIBRATION CURVE FOR
1,1-DICHLOROETHANE.

1,1-Dichloroethane
Cell Pathlength 0.5 meters

peak absorbance 1000 cm ⁻¹ A	Concentration * Pathlength C*b	Absorptivity a
0.052021	5.422E-05	9686.646293729
0.111631	1.0514E-05	10312.76742301
0.171097	1.735E-05	9359.78945245
0.200109	2.1090E-05	9375.643518259

Regression Output:

Constant	0.000399
Std Err of Y Est	0.00603
R Squared	0.994536
No. of Observations	4
Degrees of Freedom	2

X Coefficient(s)	9276.911
Std Err of Coef	460.318

Measured Absorbance
0.060075

Calc. Concentration (M)
0.24807

Cell Pathlength(m)
0.5

Measured Temperature(M)
295

Atmospheric Concentration(ppb)
20.5

Atmospheric Pressure(atm)
0.930

Atmospheric Pathlength(m)
2.41

FIGURE 23. CALIBRATION SPREADSHEET FOR
1,1-DICHLOROETHANE.

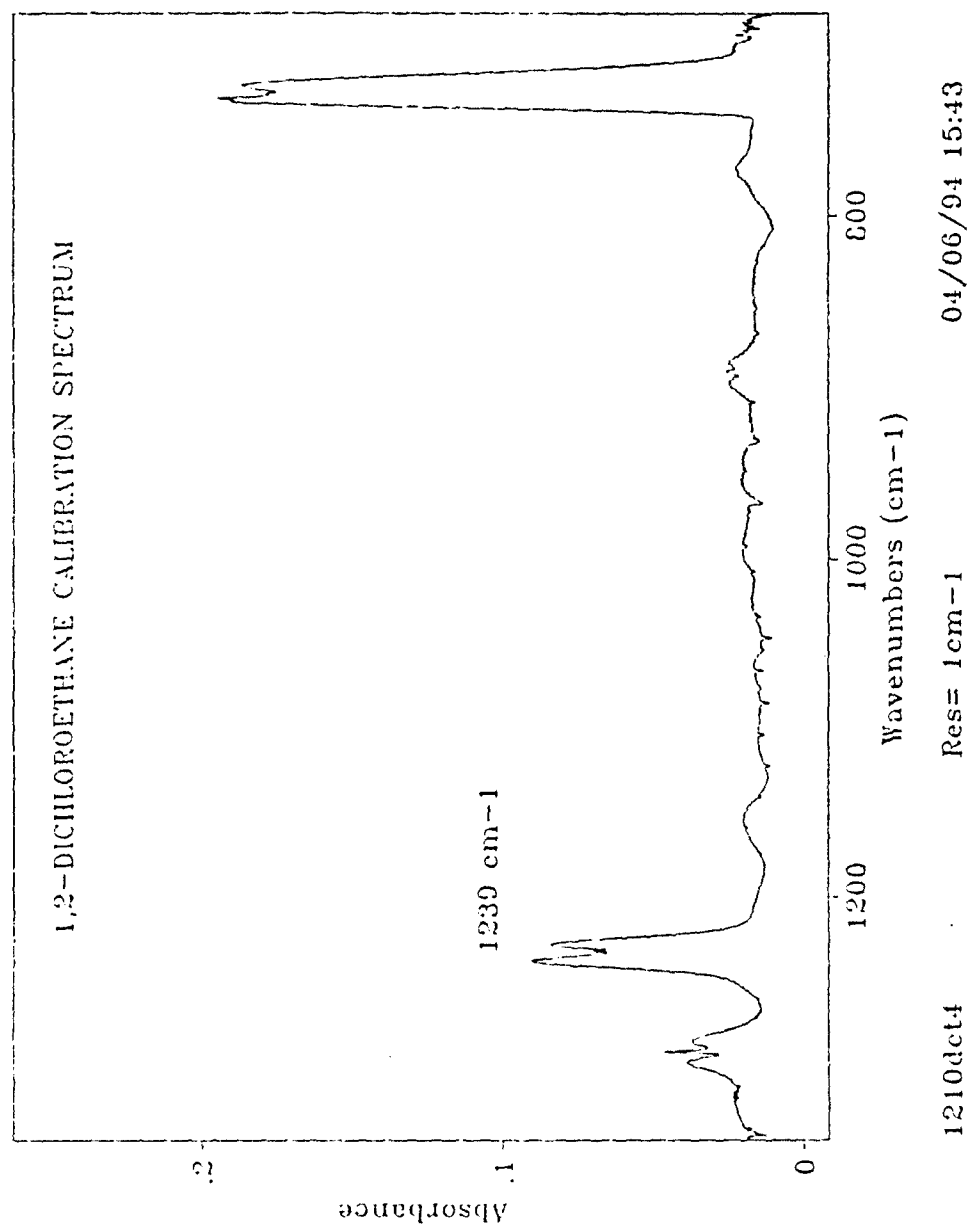


FIGURE 24. CALIBRATION SPECTRUM OF 1,2-DICHLOROETHANE.

Beer's Law Plot

1,2-Dichloroethane, 1 cm^{-1} , $b = .5\text{ meters}$

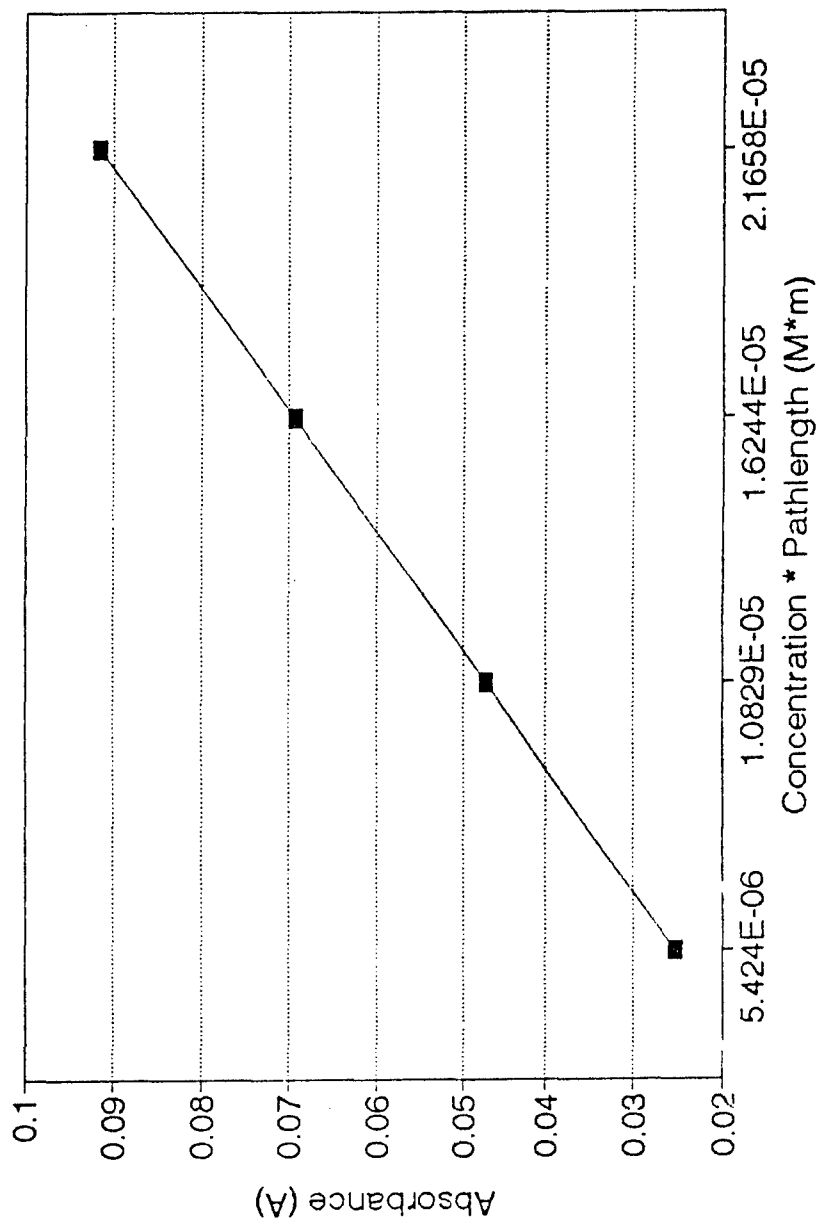


FIGURE 25. FOUR POINT CALIBRATION CURVE FOR
1,2-DICHLOROETHANE.

1,2-Dichloroethane
Cell Pathlength 0.5 meters

peak absorbance 1239 cm-1 A	Concentration * Pathlength C*b	Absorptivity a
0.02594	5.424E-06	4782.448377581
0.043131	1.0829E-05	3982.91624342
0.075795	1.6244E-05	4666.030534351
0.088578	2.1658E-05	4089.851325145

Regression Output:

Constant	0.003177
Std Err of Y Est	0.0058
R Squared	0.973091
No. of Observations	4
Degrees of Freedom	2

X Coefficient(s)	4076.011
Std Err of Coef.	479.2865

Measured Absorbance
0.002895

Calc. Concentration(M)
1.42E-05

Cell Pathlength(m)
0.5

Measured Temperature(K)
295

Atmospheric Concentration(ppb)
634

Atmospheric Pressure(atm)
0.986

Atmospheric Pathlength(m)
2.44

FIGURE 26. CALIBRATION SPREADSHEET FOR
1,2-DICHLOROETHANE.

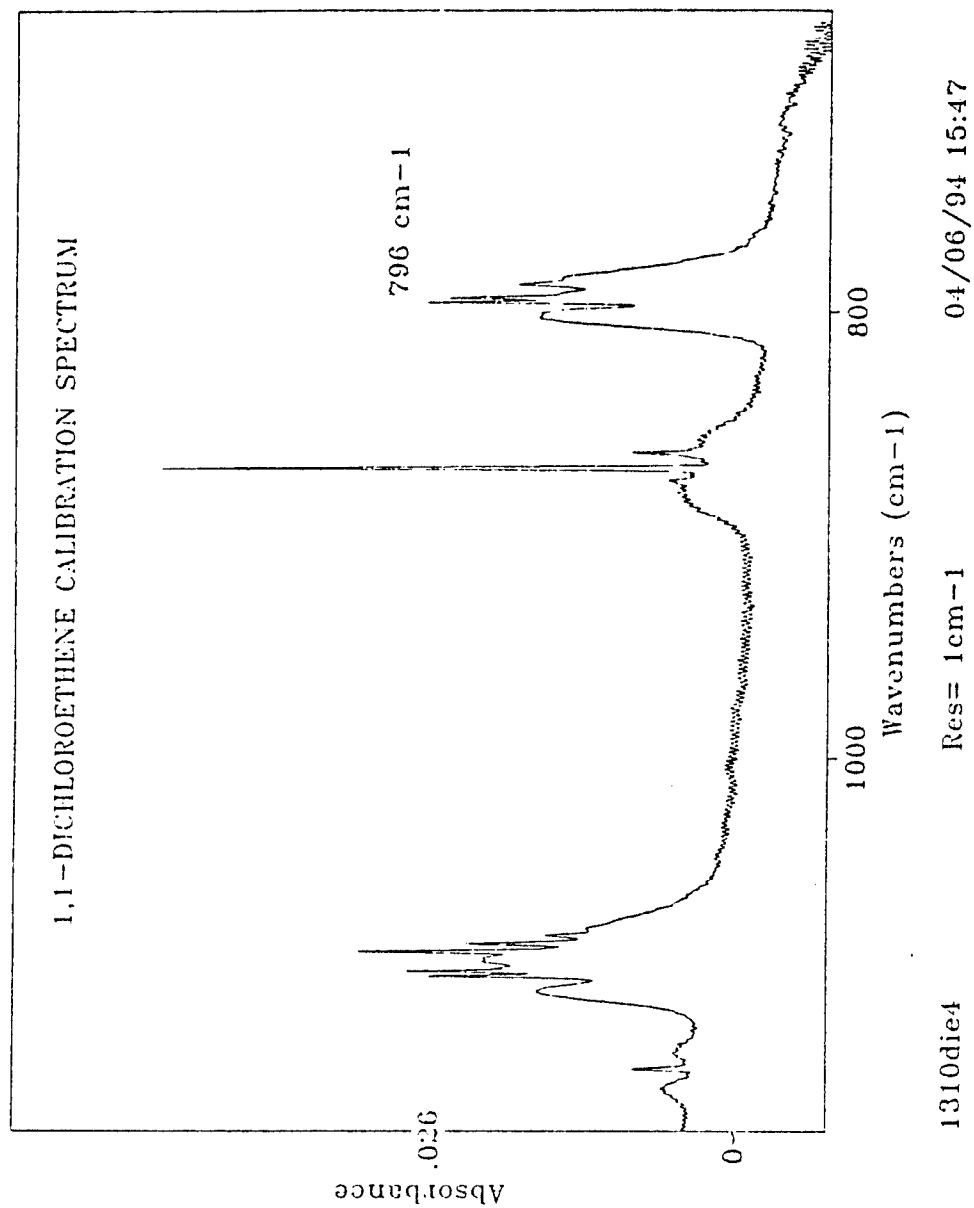


FIGURE 27. CALIBRATION SPECTRUM OF 1,1-DICHLOROETHYLENE.

Beer's Law Plot
1,1-Dichloroethylene, 1 cm-1, b=.5 m

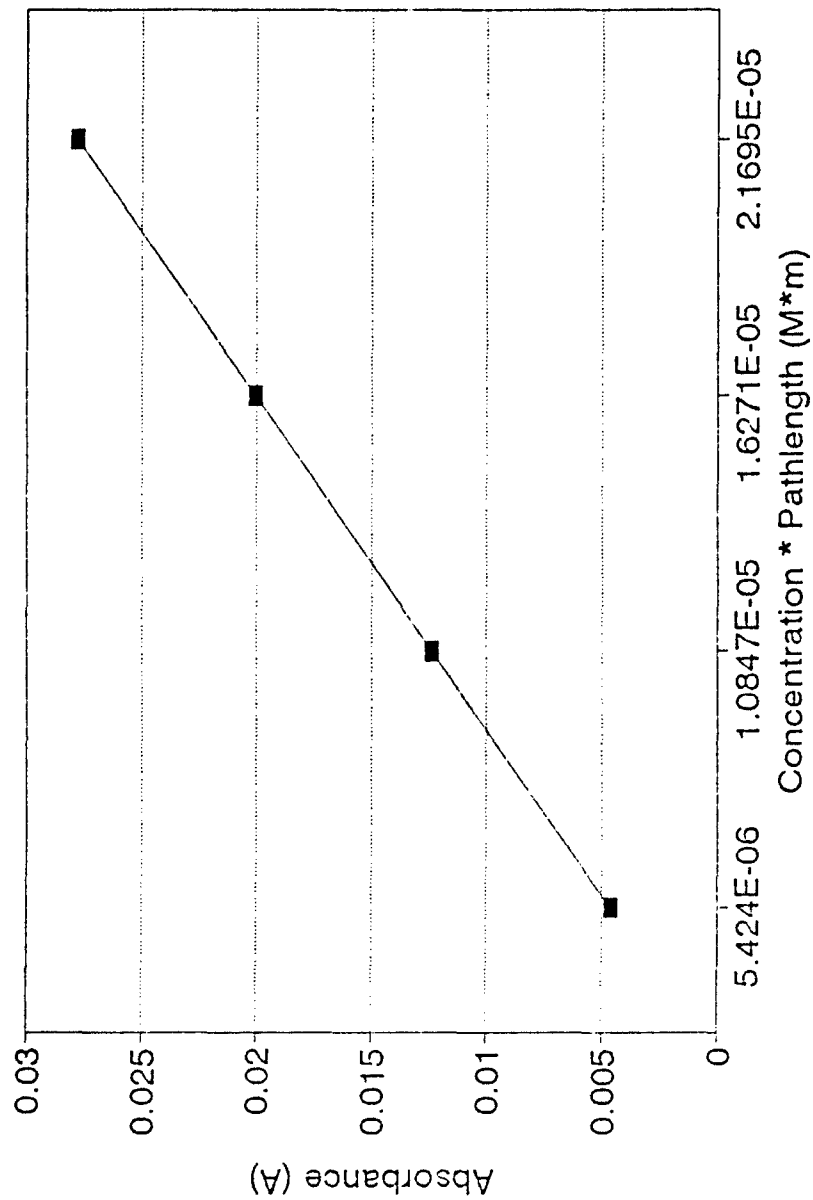


FIGURE 28. FOUR POINT CALIBRATION CURVE FOR
1,1-DICHLOROETHYLENE.

1,1-Dichloroethylene
Cell Pathlength 0.5 meters

peak absorbance 798 cm-1

A

0.004694

0.010598

0.023423

0.026184

Concentration * Pathlength

C*b

5.424E-06

1.0847E-05

1.6271E-05

2.1695E-05

Absorptivity

a

865.412979351

977.0443440583

1439.555036568

1206.914035492

Regression Output:

Constant

-0.0031

Std Err of Y Est

0.002906

R Squared

0.946474

No. of Observations

4

Degrees of Freedom

2

X Coefficient(s)

1425.135

Std Err of Coef

239.6458

Measured Absorbance

0.002895

Calc. Concentration(M)

4.06E-06

Cell Pathlength(m)

0.5

Measured Temperature(K)

295

Atmospheric Concentration(ppb)

9690

Atmospheric Pressure(atm)

0.986

Atmospheric Pathlength(m)

0.5

FIGURE 29. CALIBRATION SPREADSHEET FOR

1,1-DICHLOROETHYLENE

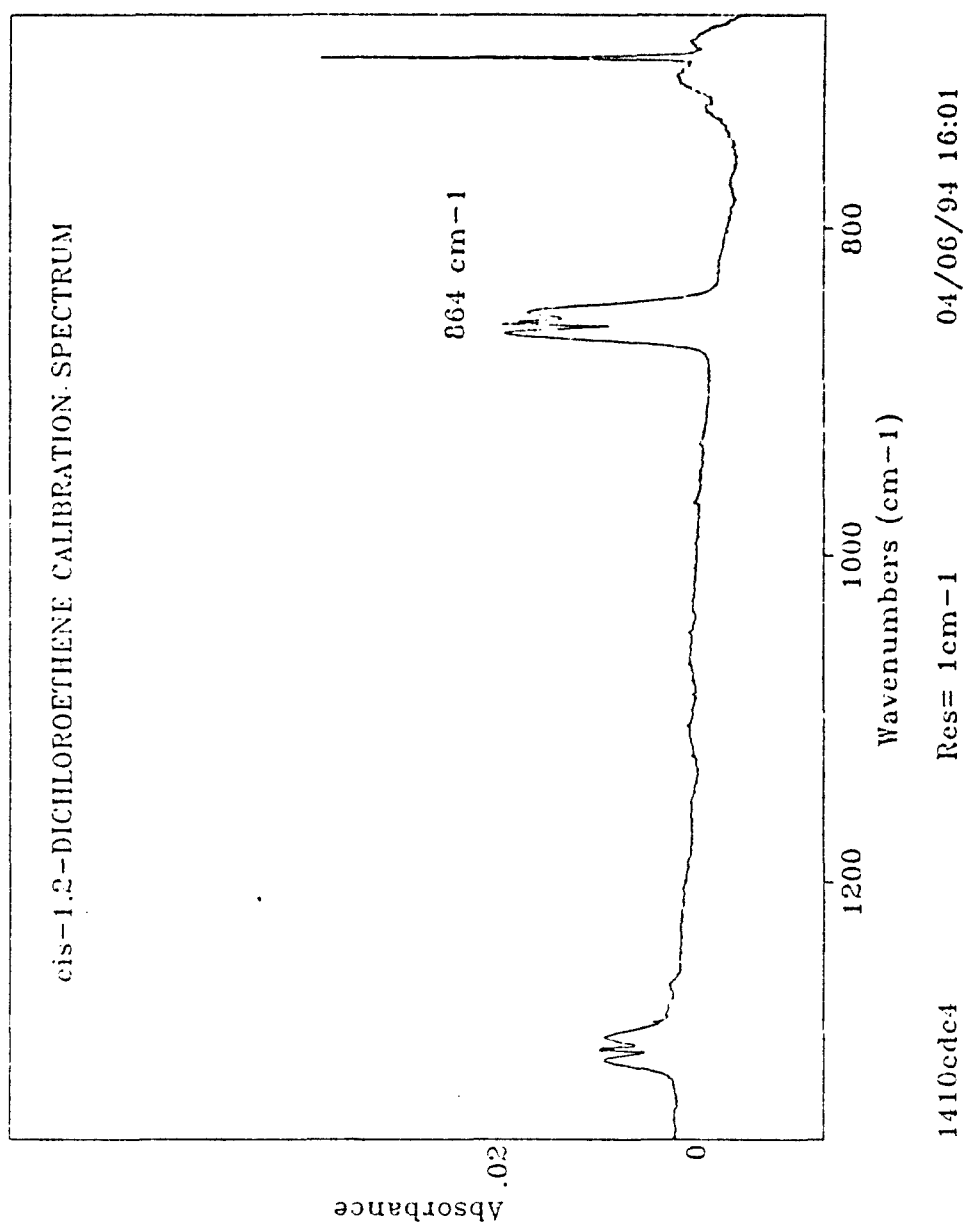


FIGURE 30. CALIBRATION SPECTRUM OF
cis-1,2-DICHLOROETHYLENE.

Beer's Law Plot

cis-1,2-Dichloroethene, 1 cm-1, b=.5 m

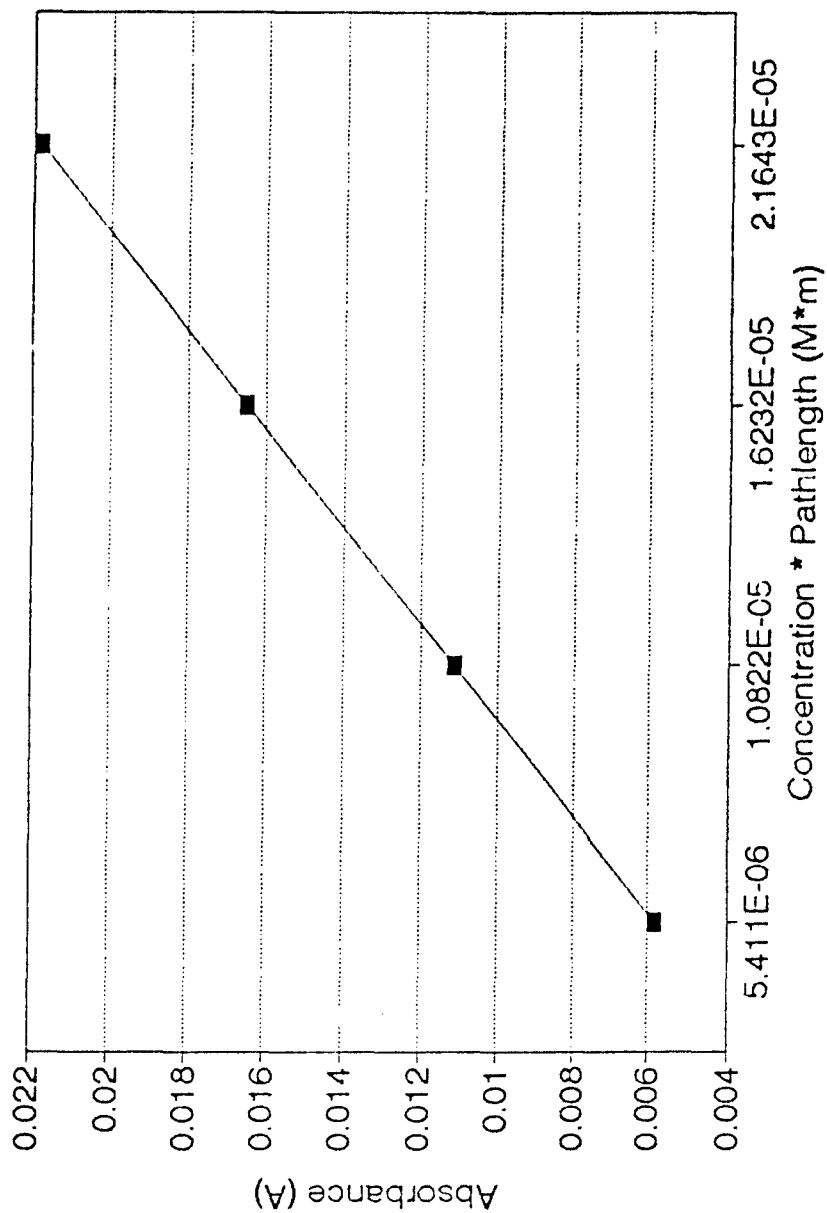


FIGURE 31. FOUR POINT CALIBRATION CURVE FOR
cis-1,2-DICHLOROETHYLENE.

cis-1,2-Dichloroethene
Cell Pathlength 0.5 meters

peak absorbance 864 cm-1

A

0.005609

0.011467

0.016545

0.021662

Concentration * Pathlength

C*b

5.411E-05

1.0822E-05

1.7332E-05

2.1643E-05

Absorptivity

a

1036.592127148

1053.600813159

1019.232807979

1000.877881994

Regression Output

Constant

0.000511

Std Err of Y Est

0.000292

R Squared

0.998797

No. of Observations

4

Degrees of Freedom

2

X Coefficient(s)

943.9395

Std Err of Coef

24.14373

Measured Absorbance

0.002895

Calc. Concentration(1/l)

5.88E-06

Cell Pathlength(m)

0.5

Measured Temperature(K)

295

Atmospheric Concentration (ppb)

2875

Atmospheric Pressure(atm)

0.986

Atmospheric Pathlength(m)

2.44

FIGURE 32. CALIBRATION SPREADSHEET FOR
cis-1,2-DICHLOROETHYLENE.

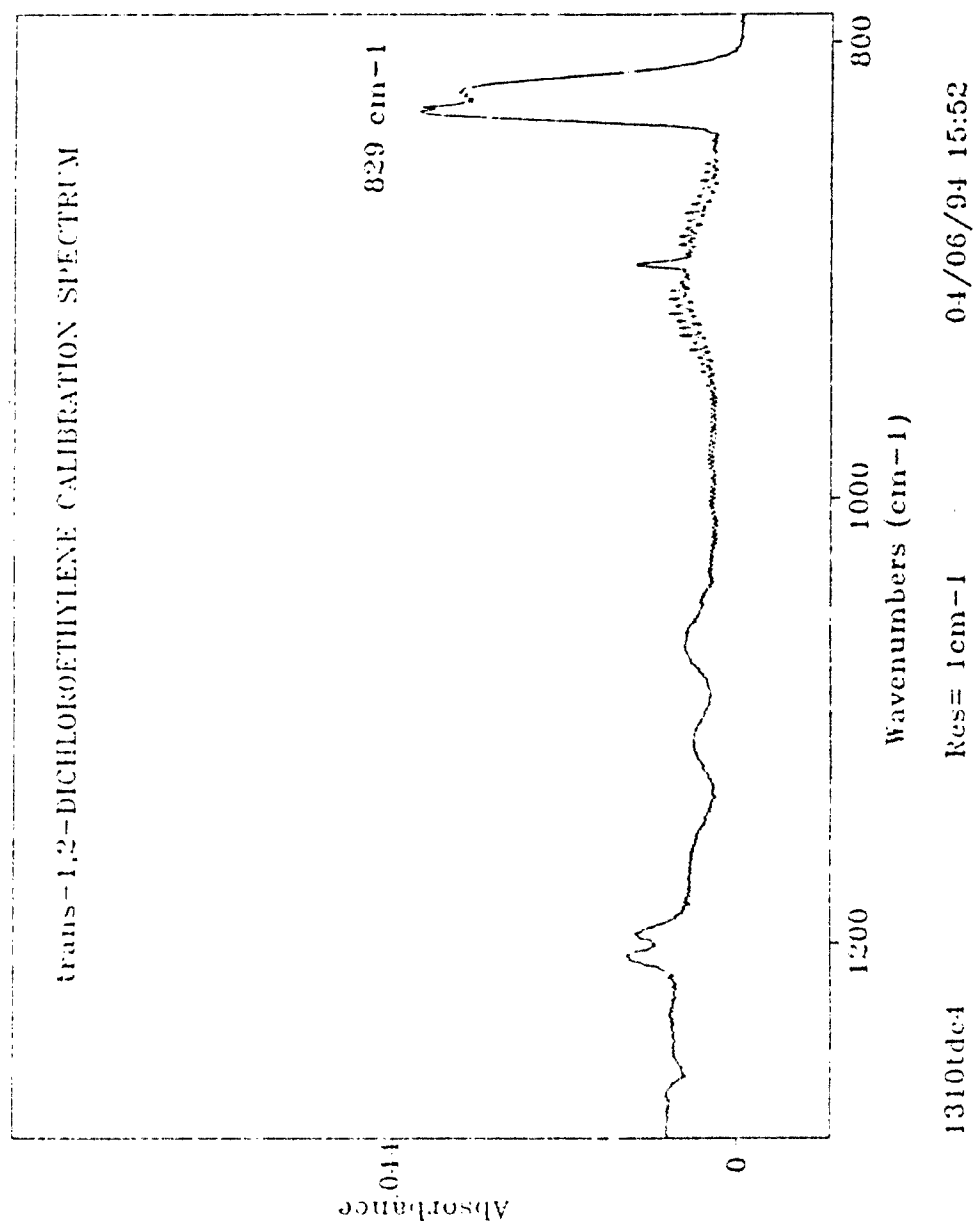


FIGURE 33. CALIBRATION SPECTRUM OF
trans-1,2-DICHLOROETHYLENE

Beer's Law Plot

trans 1,2-Dichloroethene, 1 cm-1, b=.5 m

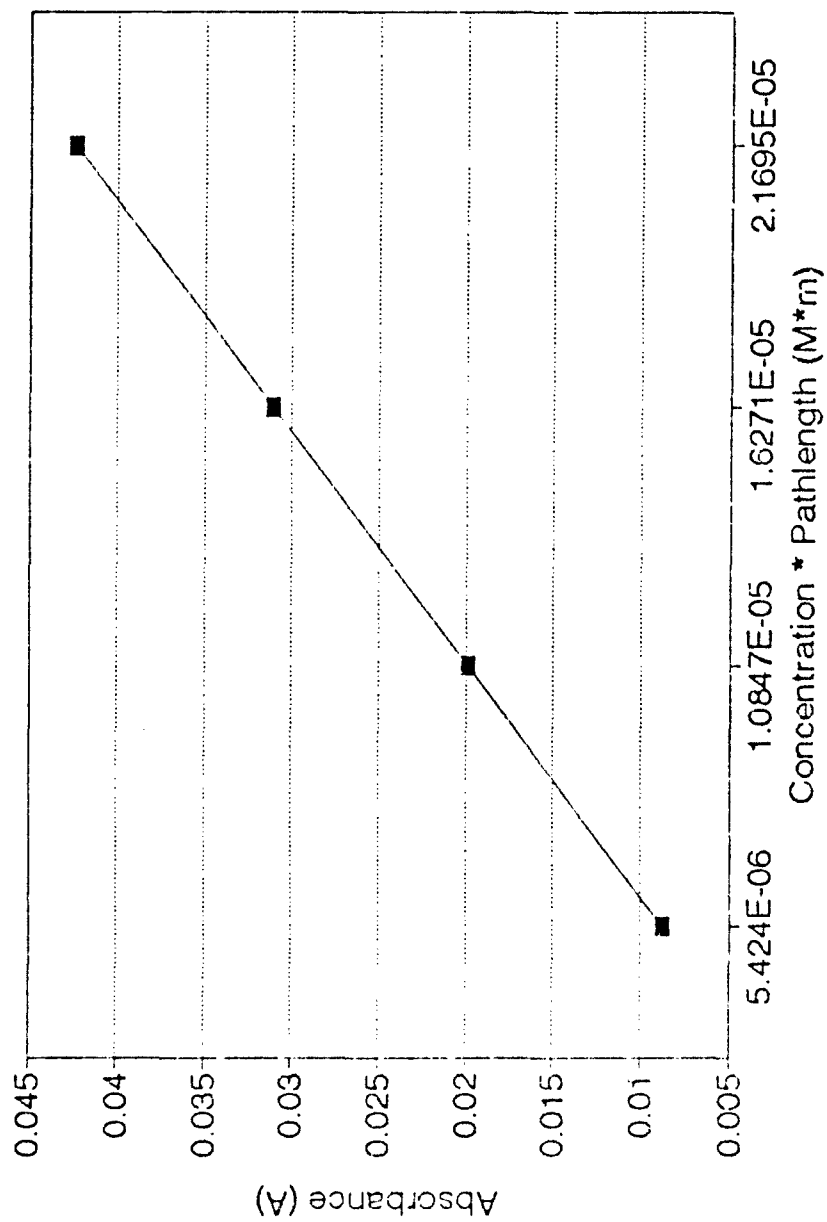


FIGURE 34. FOUR POINT CALIBRATION CURVE FOR
trans-1,2-DICHLOROETHYLENE

trans 1,2-Dichloroethylene
Cell Pathlength 0.5 meters

peak absorbance 829 cm-1

A

0.009511

0.020418

0.027995

0.044248

Concentration * Pathlength

C*b

5.424E-06

1.0847E-05

1.6271E-05

2.1695E-05

Absorptivity

a

1753.502349853

1882.363787222

1720.545756253

2039.548283015

Regression Output:

Constant

-0.0024

Std Err of Y Est

0.002679

R Squared

0.977551

No. of Observations

4

Degrees of Freedom

2

X Coefficient(s)

2061.107

Std Err of Coef

220.8598

Measured Absorbance

0.018348

Calc. Concentration(M)

1.78E-05

Cell Pathlength(m)

0.5

Measured Temperature(K)

295

Atmospheric Concentration(ppb)

42465

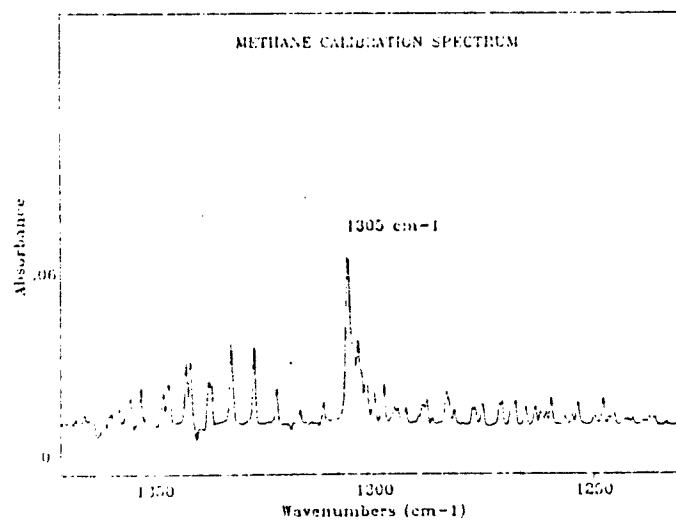
Atmospheric Pressure(atm)

0.986

Atmospheric Pathlength(m)

0.5

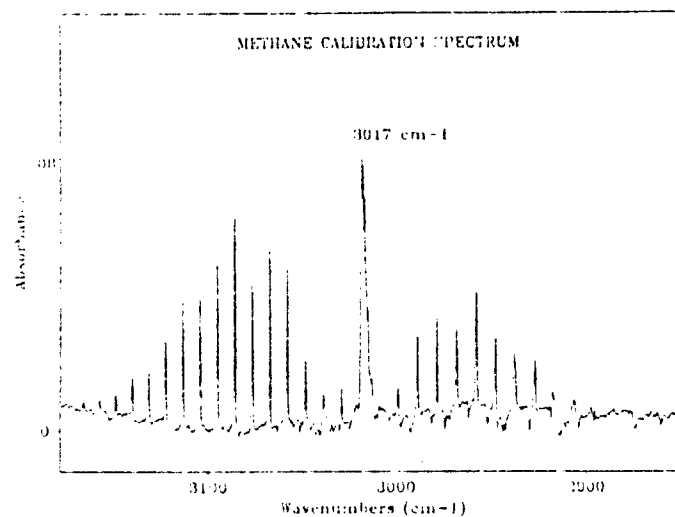
FIGURE 35. CALIBRATION SPREADSHEET FOR
trans-1,2-DICHLOROETHYLENE.



METHANE

Res= .5cm⁻¹

04/07/94 05:24



METHANE

Res= .5cm⁻¹

04/07/94 05:30

FIGURE 36. CALIBRATION SPECTRUM OF METHANE.

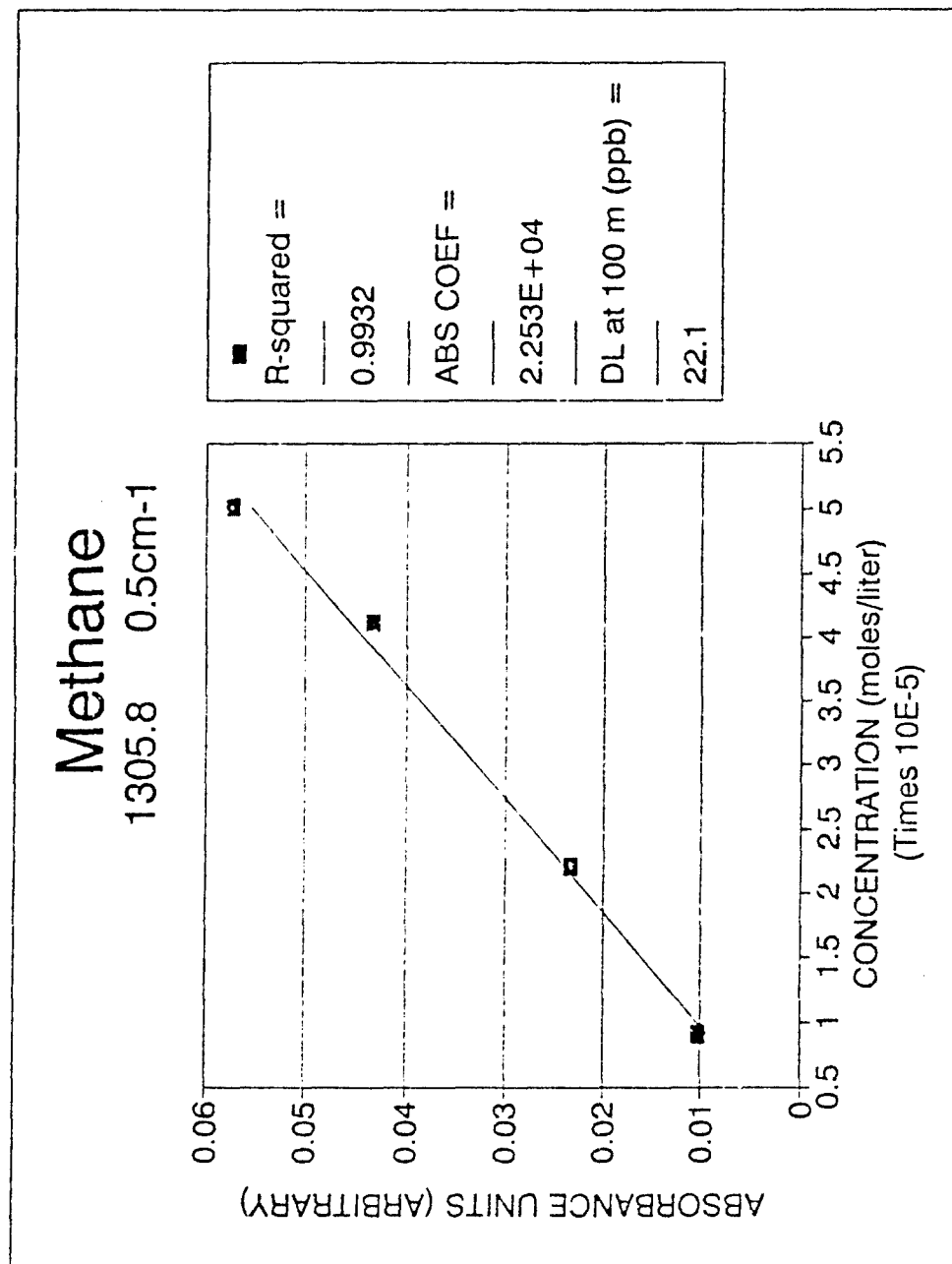


FIGURE 37. FOUR POINT CALIBRATION CURVE FOR METHANE.

Methane

FILE = 05c1Gabs
 Peak Resolution
 1305.8 0.5cm-1
 # OF SCANS = 128
 DETECTOR = MCT
 SOURCE = SiC
 BEAMSPLITTER = ZnSe
 CELL LENGTH (m) = 0.05
 TEMPERATURE (K) = 297
 DATE = 020493

Regression Output:

Constant
 Std Err of Y Est
 R Squared
 No. of Observations
 Degrees of Freedom
 X Coefficient(s) 1126.6631332
 Std Err of Coef. 66.07185591

$$y = 1126.663 * x +$$

DETECTION LIMIT AT 3 TIMES PEAK T
 NOISE =
 CALC CONC =
 CONC (ppb at 100m) =

FILE	ABS	TORR	n_V	ABS1-ABS2		ABS COEF
05mcal51	0.014375	0.1695	9.15E-03	0.010187	0.009327	2.228E+04
	0.004188		2.21E-05	0.023357	0.023942	2.112E+04
05mcal52	0.031851	0.4099	4.12E-05	0.04337	0.045489	2.103E+04
	0.008194		5.01E-05	0.057364	0.05552	2.288E+04
05mcal53	0.053445	0.7643				
	0.010075					
05mcal54	0.066516	0.9293				
	0.003152					
AVE =						2.183E+04
From Regression =						2.253E+04

FIGURE 38. CALIBRATION SPREADSHEET FOR METHANE.

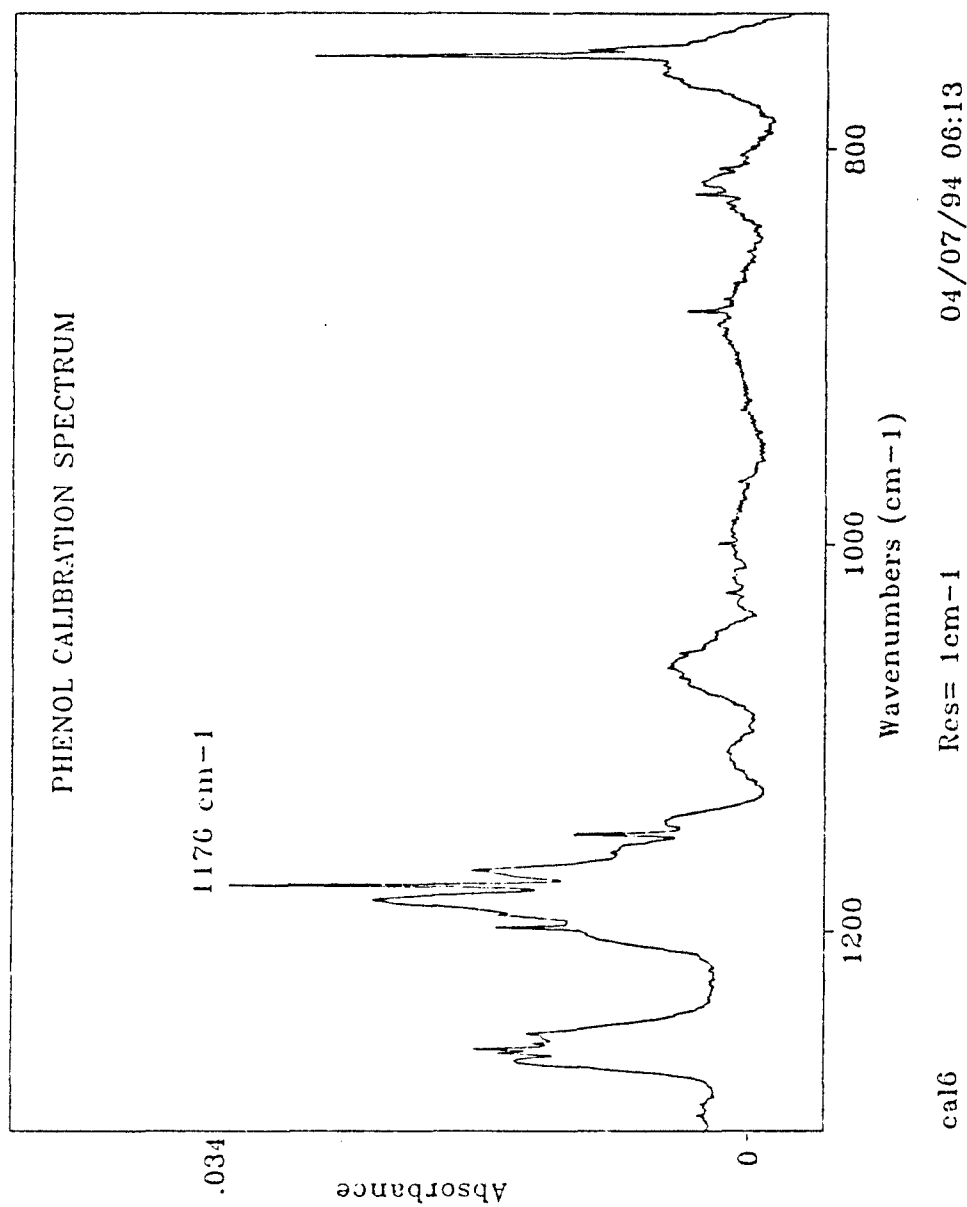


FIGURE 39. CALIBRATION SPECTRUM OF PHENOL.

Beer's Law Plot

Phenol, Res. 1 cm-1, b=0.05 meters

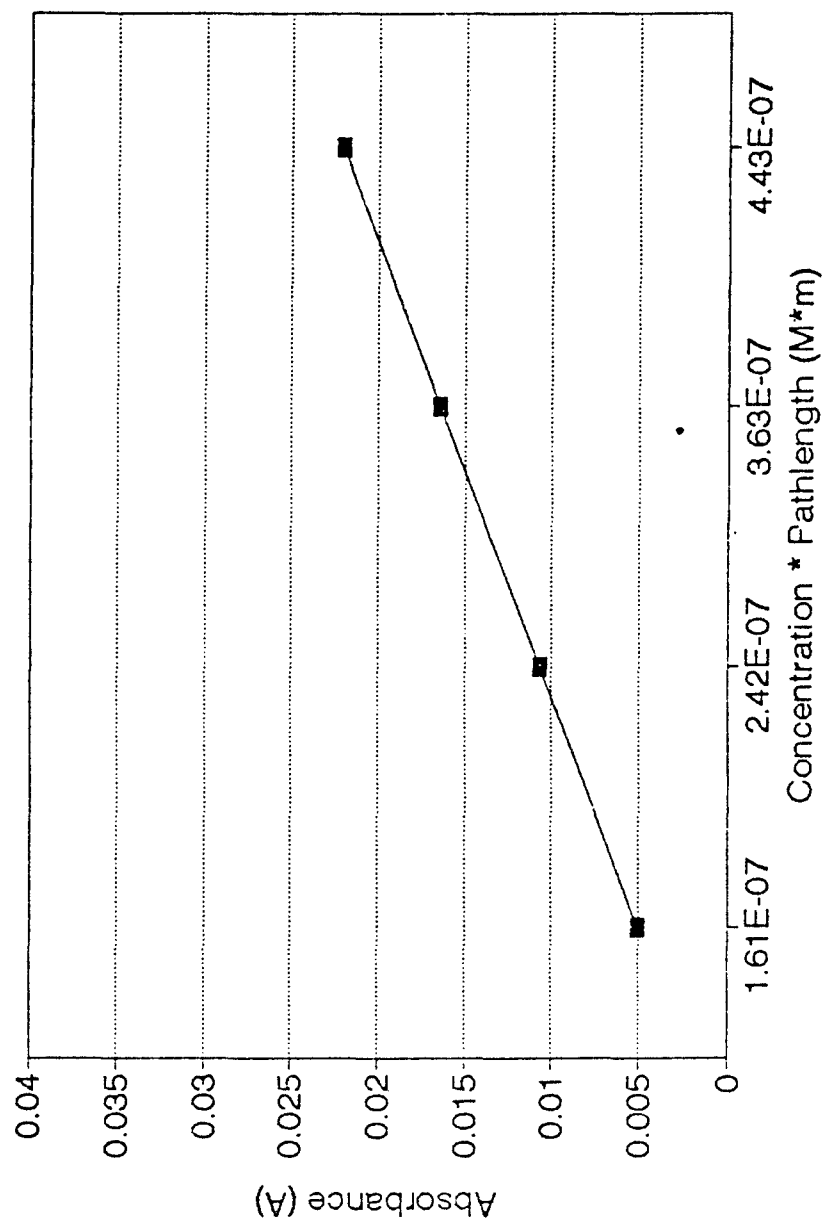


FIGURE 40. FOUR POINT CALIBRATION CURVE FOR PHENOL.

phenol
Cell Pathlength 0.05 meters

peak absorbance 1176 cm-1

A
0.005953
0.00977
0.015787
0.022789

Concentration * Pathlength

C*b
1.61E-07
2.42E-07
3.63E-07
4.43E-07

Absorptivity

a
36975.1552795
40371.9008264
43490.3581267
51442.4379233

Regression Output:

Constant	0.00109
Std Err of Y Est	0.00038
R Squared	0.99961
No. of Observations	4
Degrees of Freedom	2

X Coefficient(s)	31352.9
Std Err of Coef.	437.455

Measured Absorbance

0.0011

Calc. Concentration(M)

7.02E-07

Cell Pathlength(m)

0.05

FIGURE 41. CALIBRATION SPREADSHEET FOR PHENOL.

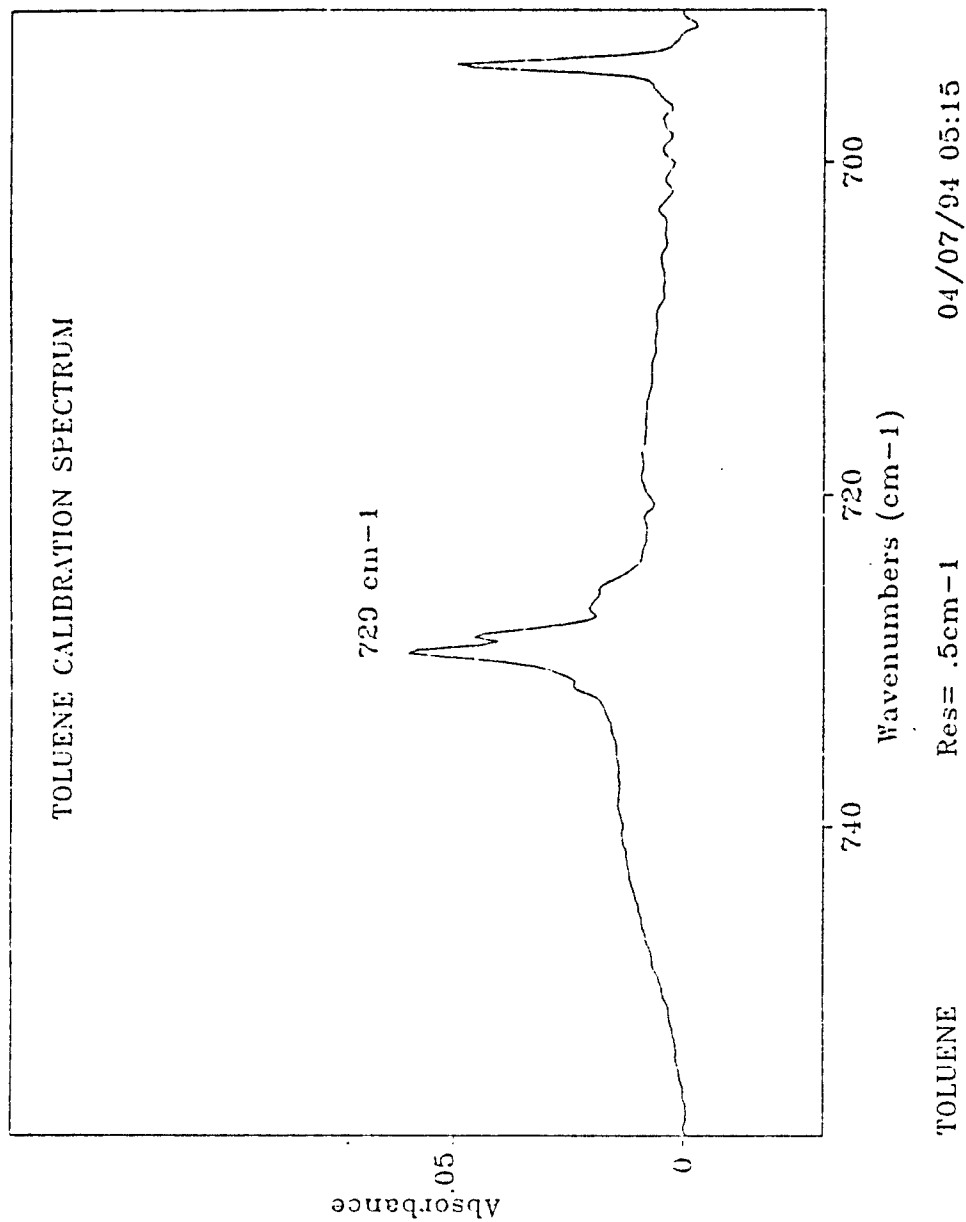
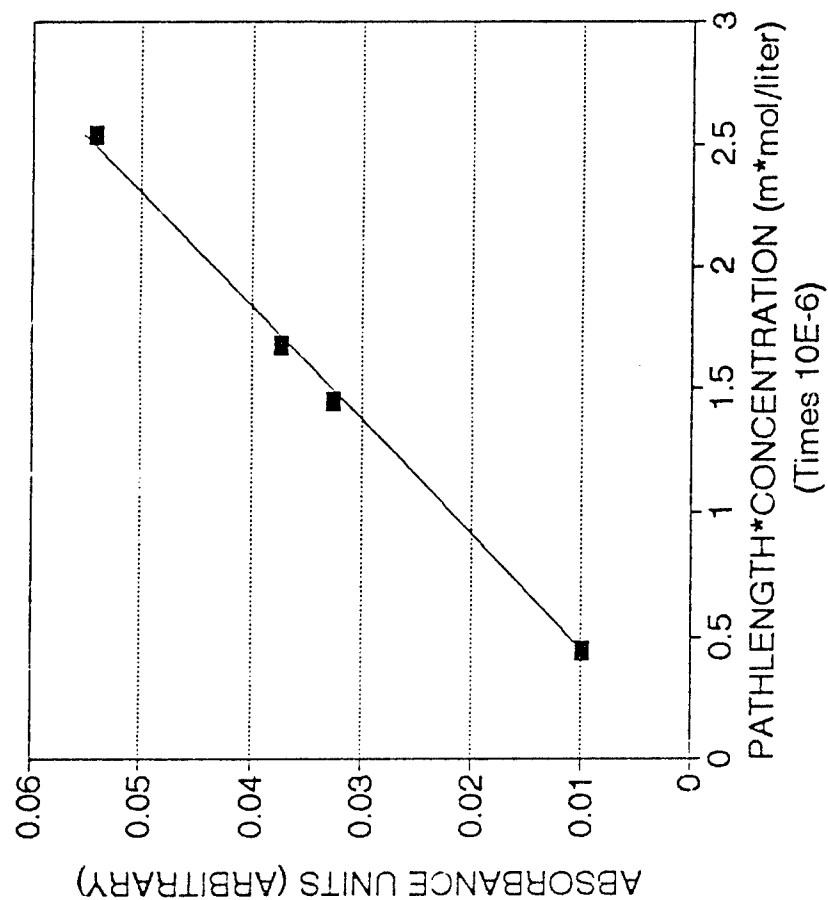


FIGURE 42. CALIBRATION SPECTRUM OF TOLUENE.

Toluene 729.5 cm-1 0.5 cm-1



■
R-squared =
0.9973
ABS COEF =
2.174E+04
DL at 100 m (ppb) =
34.7

FIGURE 43. FOUR POINT CALIBRATION CURVE FOR TOLUENE.

Toluene

Regression Output:

FILE =	05c11abs	Constant	0
Peak Resolution		Std Err of Y Est	0.000962
729.5 cm-1 0.5 cm-1		R Squared	0.9973
# OF SCANS =	128	Nr of Observations	4
DETECTOR =	MCT	Degrees of Freedom	3
SOURCE =	SiC	X Coefficient(s)	21737.93666
BEAMSPLITTER =	ZnSe	Std Err of Coef.	252.17034267
b - CELL LENGTH (m) =	0.05		
TEMPERATURE (K) =	297	y =	21737.94 * x + 0
DATE =	Feb4.93		

DETECTION LIMIT AT 3 TIMES PEAK TO PEAK NOISE

NOISE = 0.001

CALC CONC = 2.76E-06

GCNC (ppb at 100m) = 34.7

FILE	ABS	TORR	b*(m/V)	ABS1-ABS2	ABS COEF
05c11abs	0.051907	0.913	2.54E-06	0.054247	0.055218
	0.00466		1.08E-06	0.037287	0.036557
05c12abs	0.022327	0.6233	1.45E-06	0.032622	0.031572
	-0.01496		4.51E-07	0.009753	0.009871
05c13abs	0.046015	0.5303			
	0.013393				
05c14abs	0.020001	0.1633			
	0.010248				

AVE = 2.186E+04

From Regression = 2.174E+04

FIGURE 44. CALIBRATION SPREADSHEET FOR TOLUENE.

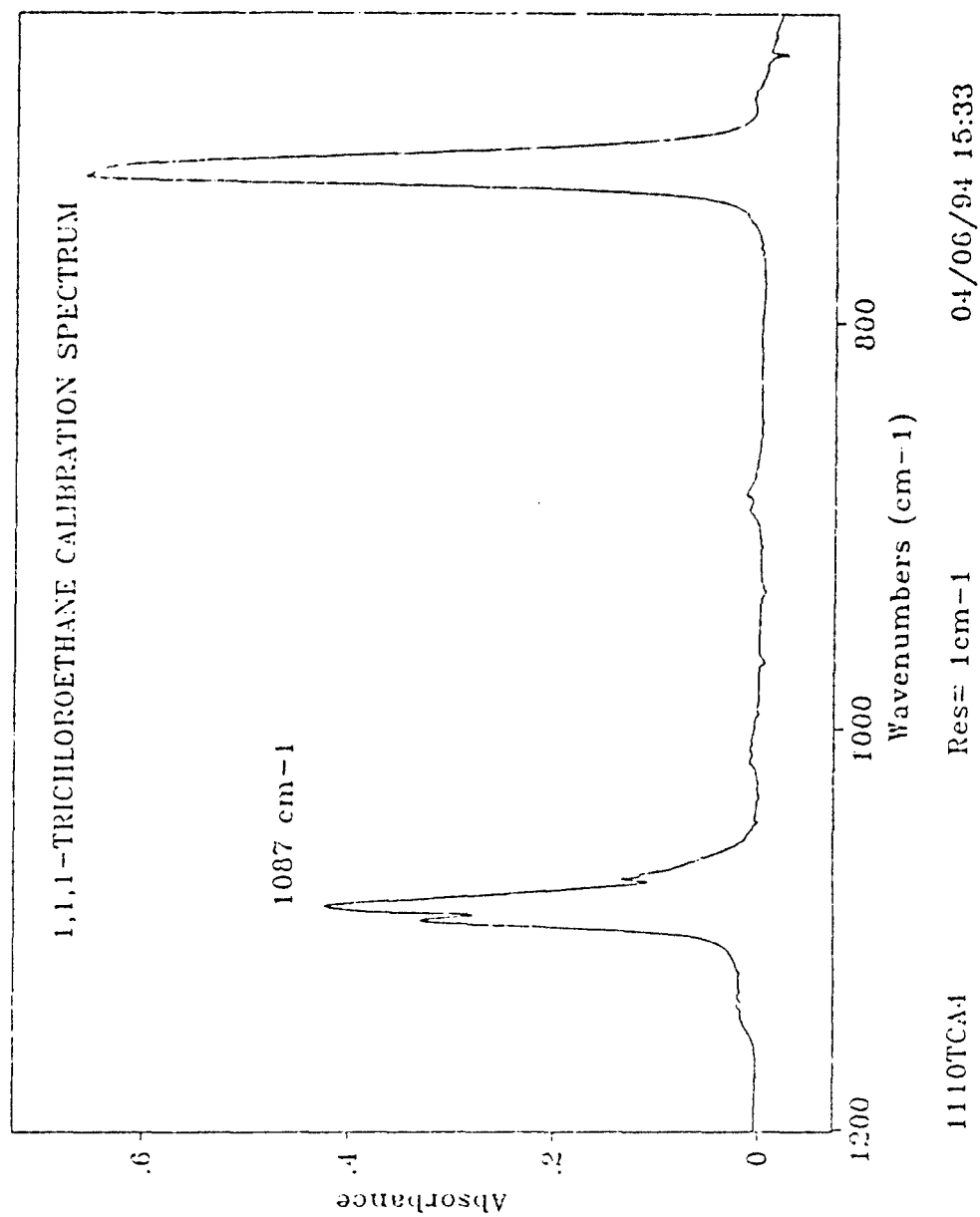


FIGURE 45. CALIBRATION SPECTRUM OF
1,1,1-TRICHLOROETHANE.

Beer's Law Plot

1,1,1-TCA, Res. 1 cm-1, b=0.5 meters

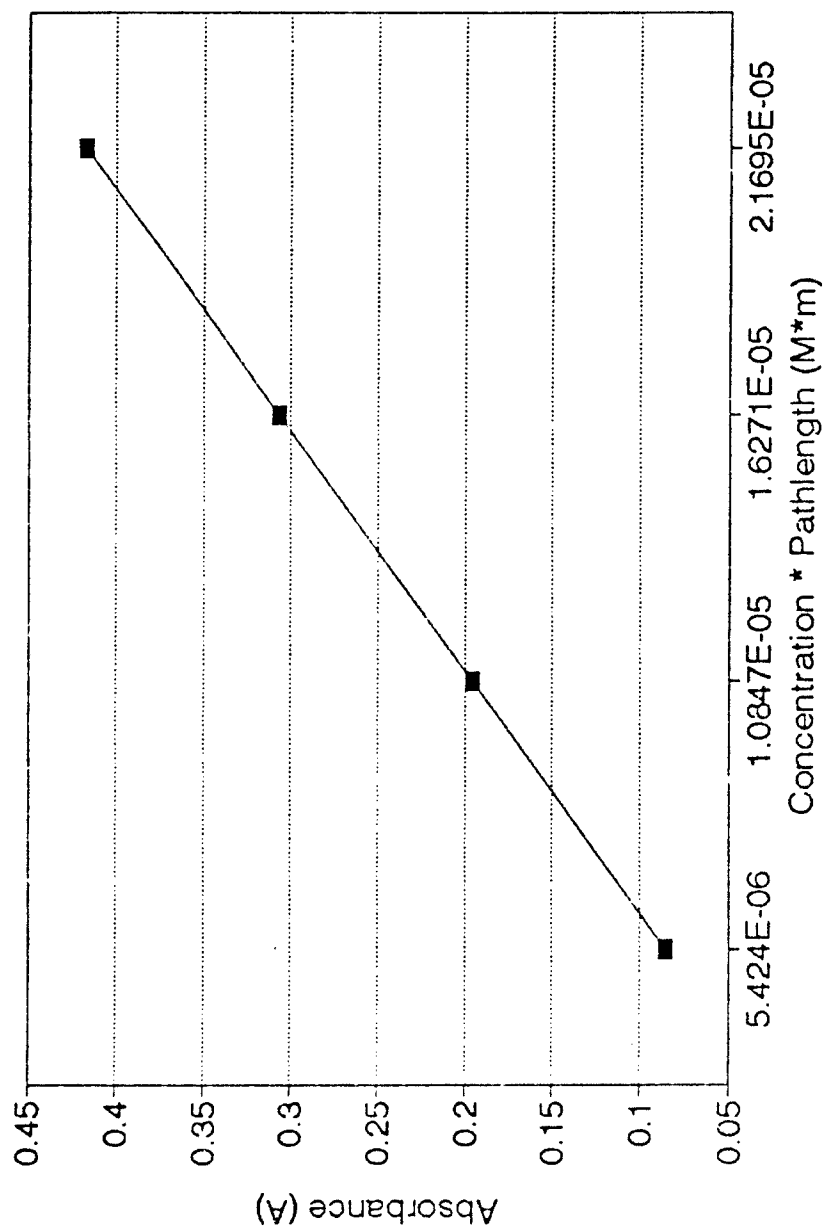


FIGURE 46. FOUR POINT CALIBRATION CURVE FOR
1,1,1-TRICHLOROETHANE.

1,1,1-trichloroethane
Cell Pathlength 0.5 meters

peak absorbance 1087 cm-1 A	Concentration * Pathlength C*b	Absorptivity a
0.094224	5.424E-06	17371.68141593
0.188601	1.0847E-05	17387.38821794
0.297785	1.6271E-05	18301.57949727
0.426223	2.1695E-05	19646.13966352

Regression Output:

Constant	-0.02459
Std Err of Y Est	0.012056
R Squared	0.995263
No. of Observations	4
Degrees of Freedom	2

X Coefficient(s)	20376.94
Std Err of Coef.	994.0738

Measured Absorbance
0.003221

Calc. Concentration(M)
3.16E-07

Cell Pathlength(m)
0.5

Measured Temperature(K)
295.6

Atmospheric Concentration(ppb)
1546

Atmospheric Pressure(atm)
0.986

Atmospheric Pathlength(m)
2.44

FIGURE 47. CALIBRATION SPREADSHEET FOR
1,1,1-TRICHLOROETHANE.

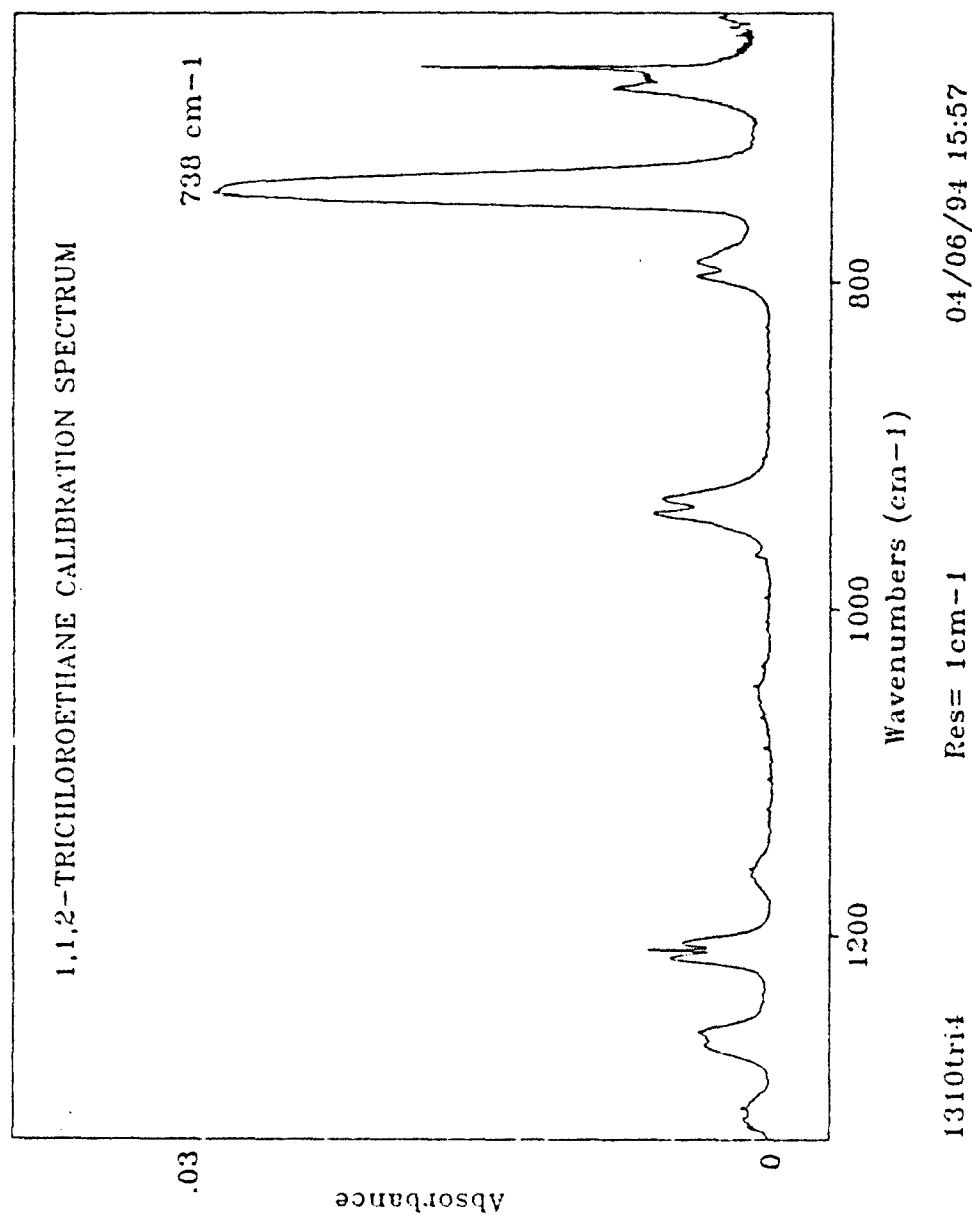


FIGURE 48. CALIBRATION SPECTRUM OF 1,1,2-TRICHLOROETHANE.

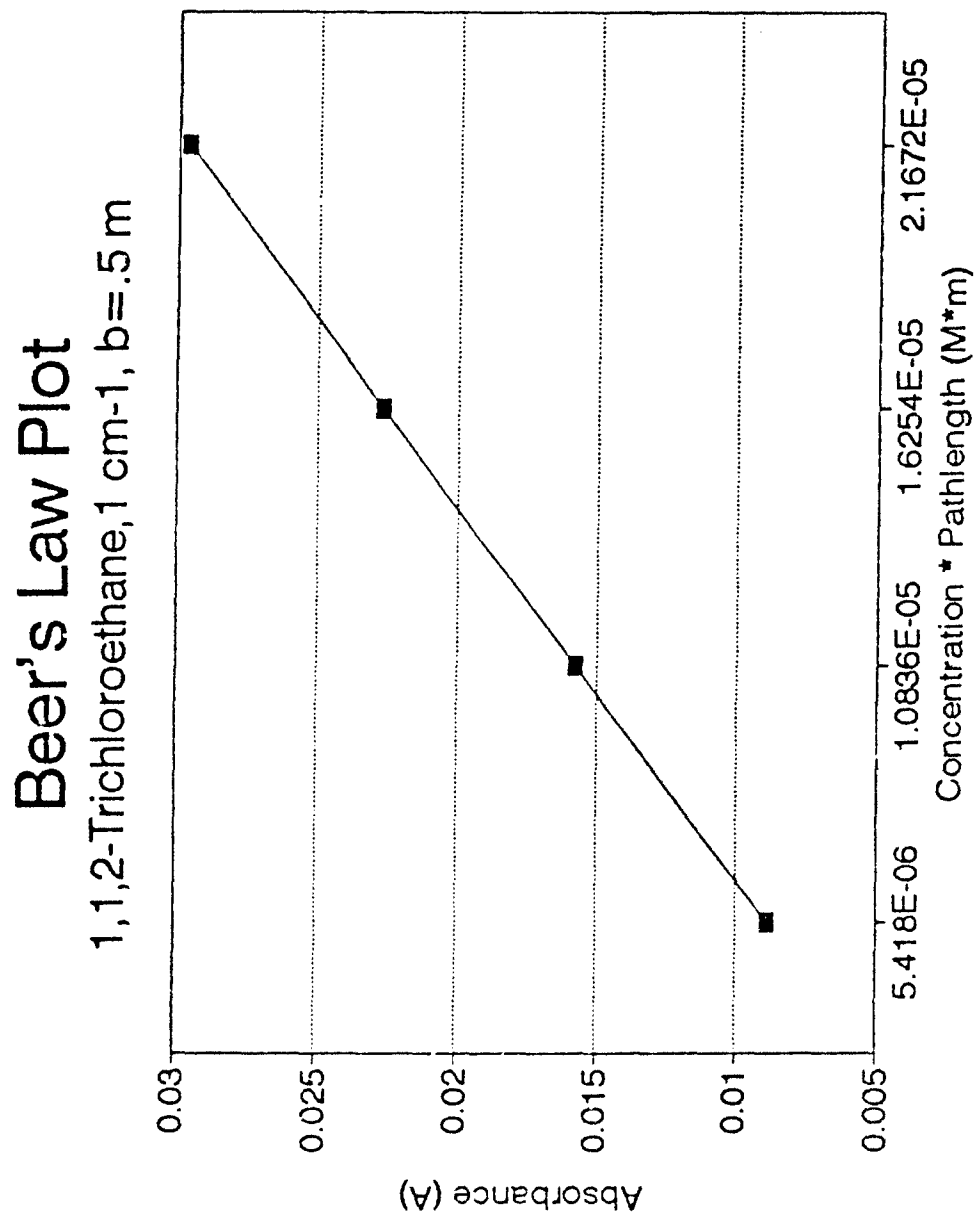


FIGURE 49. FOUR POINT CALIBRATION CURVE FOR
1,1,2-TRICHLOROETHANE.

1,1,2-Trichloroethane
Cell Pathlength 0.5 meters

peak absorbance 738 cm-1 A	Concentration * Pathlength C*b	Absorptivity a
0.008847	5.418E-06	1632.890365449
0.01689	1.0836E-05	1558.69324474
0.020349	1.6254E-05	1251.937984498
0.030728	2.1672E-05	1417.774086379

Regression Output:	
Constant	0.001929
Std Err of Y Est	0.001997
R Squared	0.987665
No. of Observations	4
Degrees of Freedom	2
X Coefficient(s)	1275.305
Std Err of Coef.	184.8437

Measured Absorbance
0.002895

Calc. Concentration(M)
4.54E-06

Cell Pathlength(m)
0.5

Measured Temperature(K)
295

Atmospheric Concentration(ppb)
2219

Atmospheric Pressure(atm)
0.988

Atmospheric Pathlength(m)
2.44

FIGURE 50. CALIBRATION SPREADSHEET FOR
1,1,2-TRICHLOROETHANE.

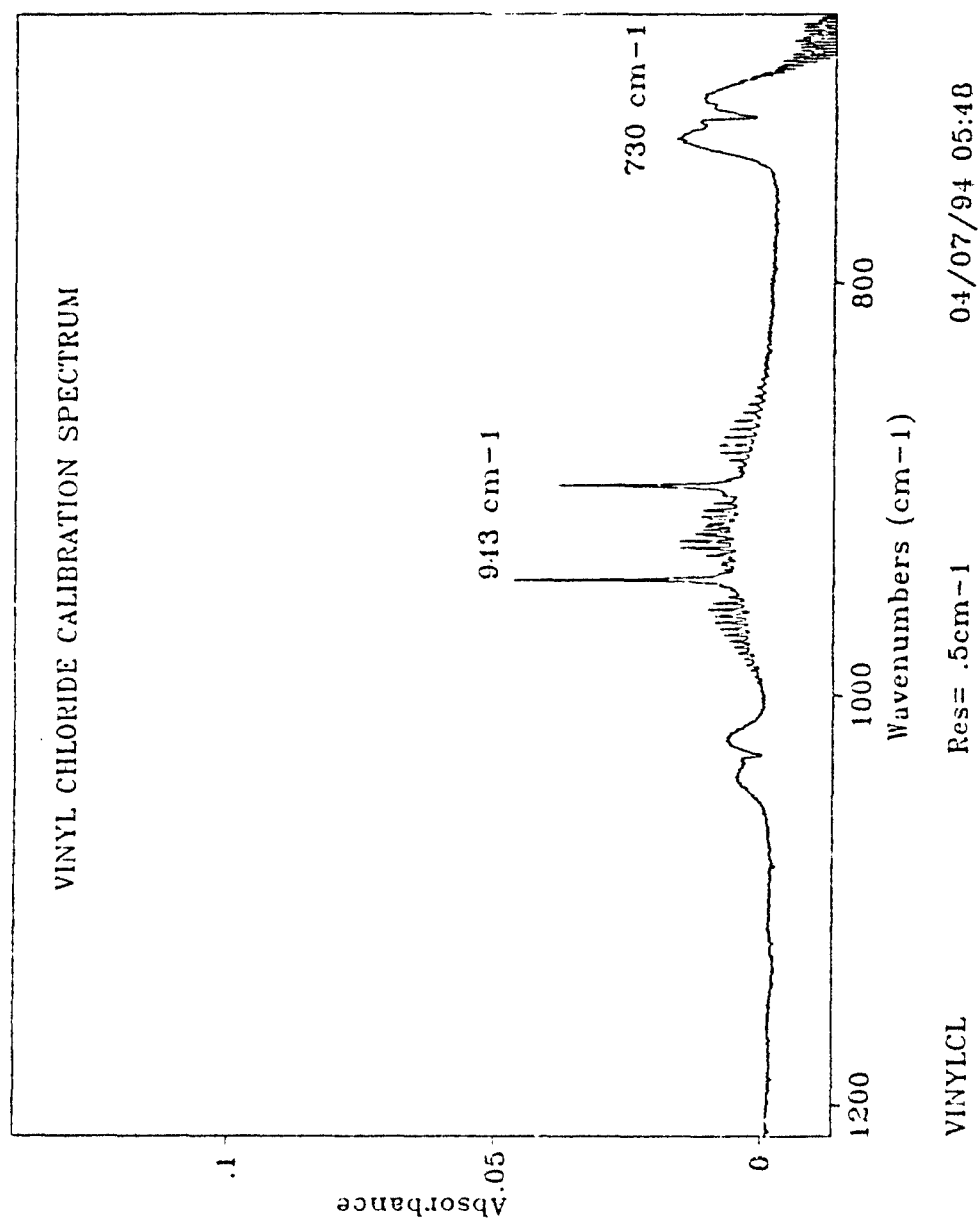
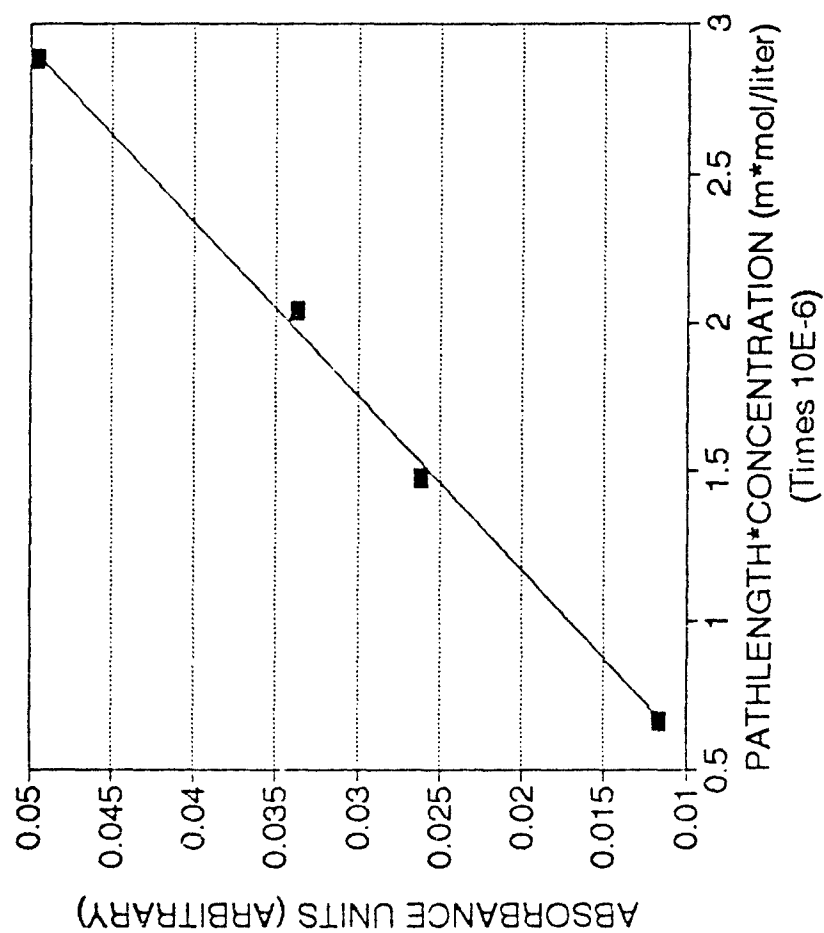


FIGURE 51. CALIBRATION SPECTRUM OF VINYL CHLORIDE.

Vinyl Chloride 942.1 cm-1 0.5 cm-1



R-squared =
0.9970
ABS COEF =
1.708E+04
DL at 100 m (ppb) =
44.1

FIGURE 52. FOUR POINT CALIBRATION CURVE FOR VINYL CHLORIDE.

Vinyl Chloride

FILE =
 Peak Resolution
 942.1 cm-1 0.5 cm-1
 # OF SCANS =
 DETECTOR =
 SOURCE =
 BEAMSPLITTER =
 b - CELL LENGTH (m) =
 TEMPERATURE (K) =
 DATE =

vinylcl1
 128
 MCT
 SiC
 ZnSe
 0.05
 298
 Jun22,93

Regression Output:

Constant 0
 Std Err of Y Est 0.00086
 R Squared 0.9970
 No. of Observations 4
 Degrees of Freedom 3
 X Coefficient(s) 17083.070448
 Std Err of Coef. 221.25889791
 y = 17083.07 * x + 0

DETECTION LIMIT AT 3 TIMES PEAK TO PEAK NOISE
 NOISE = 0.001
 CALC CONC = 3.51E-06
 CONC (ppb at 100m) = 44.1

FILE	ABS	TORR	b*(n/V)	ABG1	ABG2	ABS COEF
vinylcl1	0.00913	0.248	6.67E-07	0.011663	0.011392	1.750E+04
vinylcl2	-0.00254		1.48E-06	0.026155	0.025219	1.772E+04
vinylcl3	0.022382	0.549	2.04E-06	0.031765	0.034866	1.654E+04
vinylcl4	-0.00377		2.89E-06	0.019527	0.04929	1.717E+04
vinylcl5	0.033545	0.759				
vinylcl6	-0.00022					
vinylcl7	0.047198	1.073				
vinylcl8	-0.00233					
AVE =						1.723E+04
From Regression =						1.708E+04

FIGURE 53. CALIBRATION SPREADSHEET FOR VINYL CHLORIDE.

Historically, the members of our research group have prepared calibration files using a 5 cm cell as discussed earlier. Initially, I also used a 5 cm cell for calibration files, however, use of the 5 cm cell quickly caused some difficulties in the calibration process. It was during the preparation of a carbon dioxide calibration using a 5 cm cell that I encountered these problems. Since carbon dioxide is an important component in the atmosphere and one of the compounds of interest in our study, it was necessary to overcome this calibration problem.

As previously addressed, carbon dioxide is present in the atmosphere; therefore, analyzing and quantifying the relative changes in the carbon dioxide concentration using open path FT-IR can be challenging. Ultimately, we desired to monitor the change in carbon dioxide concentration within the plant chamber. This ability would enable us to track assimilation, consumption of CO₂ through photosynthesis and accumulation of CO₂ generated by the respiration of microbial biomass utilizing the root derived material from the alfalfa plants in the rhizosphere.

A carbon dioxide calibration file was generated using a 5 cm cell and we had trouble acquiring a linear calibration curve. The nonlinear calibration curve is shown in figure 54. After analysis of this futile effort, the work was repeated, in hopes that some experimental error was responsible for this nonlinear calibration. Once again, a similar nonlinear calibration curve (figure 55) resulted.

Beer's Law Plot

CO₂, Res. 1 cm⁻¹, b=.05 meters

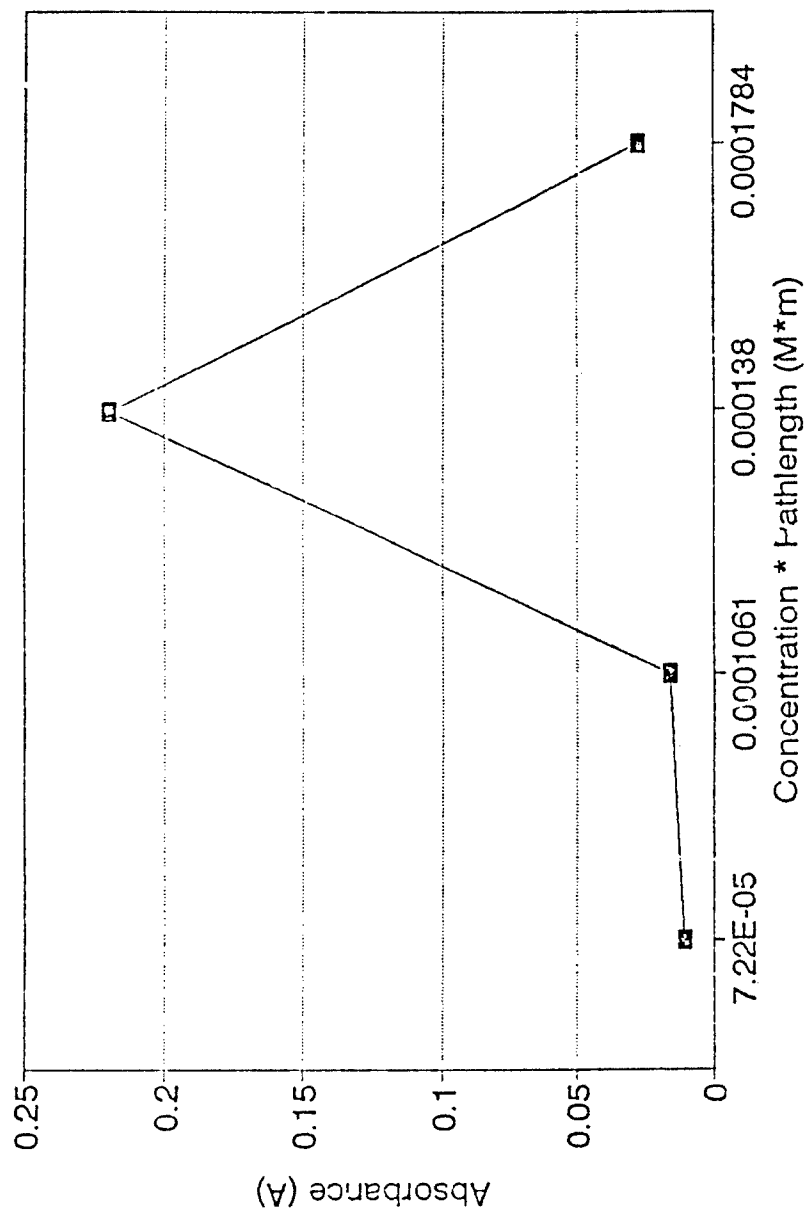


FIGURE 54. NONLINEAR CALIBRATION CURVE OF CARBON DIOXIDE.

Beer's Law Plot

CO₂, Res. 1 cm-1, b=.05 meters

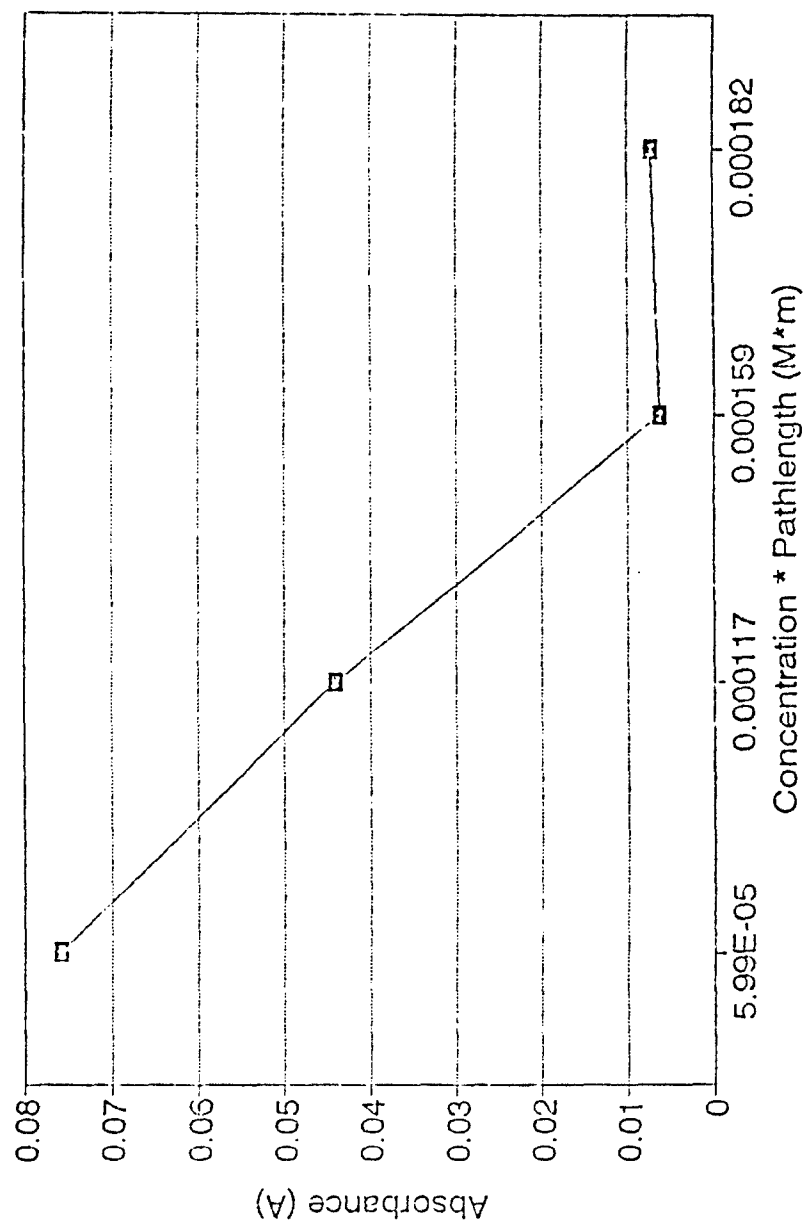
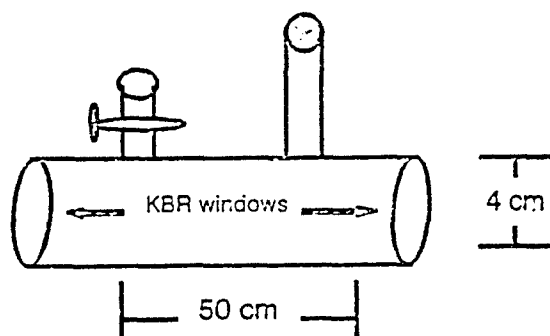


FIGURE 55. NONLINEAR CALIBRATION CURVE OF CARBON DIOXIDE.

The calibration work was unsuccessfully repeated, persuading us that there may be another reason for this problem. Subsequent to careful consideration, convinced that the short pathlength of the cell relative to the ambient pathlength was the problem, a 50 cm cell was developed. The cell design is illustrated in figure 56. The cell was made by Master Glass Blower, Mr. Mitsugi Ohno, a member of the Kansas State University Department of Chemistry faculty.

FIGURE 56. DIAGRAM OF 50 cm CELL.



The design features of this cell are a matter of convenience and forethought. The design provides for convenient attachment to and use with the available vacuum system in our lab. The additional extension with a septum enables introduction of a variety of samples by injection through the septum while the cell is under a vacuum. This capability will facilitate analysis of groundwater and plant material head space gas samples, which will be discussed later.

The use of the longer, 50 cm pathlength cell resulted in a linear calibration curve (refer to figure 16). This result can be attributed to the

higher ambient concentration of carbon dioxide CO_2 present relative to the carbon dioxide concentration present in the 5 cm cell when the shorter cell is utilized. When using the 50 cm cell, the increase in the contained pathlength overcomes the shortfall observed using the 5 cm cell, by minimizing the influence the ambient carbon dioxide concentration has upon the calibration. For this calibration the absorbance band at 720 cm^{-1} was used as shown in figure 15. Further experimental efforts demonstrated that practical use of the 720 cm^{-1} band for CO_2 quantification is precluded because there are a myriad of volatile organic compounds which have absorption bands in close proximity to this 720 cm^{-1} band.

To avoid the possibility of overlapping bands and regions of the spectra where CO_2 may be totally absorbing, we had to investigate the carbon dioxide spectrum in a more rigorous fashion. The 667 cm^{-1} and 2349 cm^{-1} bands are two extremely strong infrared absorption bands and these two bands coupled with the strong Raman band at 1340 cm^{-1} are the fundamentals of carbon dioxide⁷. A complete outline of the infrared and Raman absorption bands is found in Herzberg's text⁸. In addition to these two IR fundamental bands identified above, the bands at 2076 cm^{-1} and 2284 cm^{-1} were also investigated. The band at 2284 cm^{-1} became the band of choice. Ultimately, we found that by integrating the area under the P-branch of the rotational band of C-O stretch in the region of 2235 cm^{-1} to 2283 cm^{-1} , shown in figure 57, we were able to obtain a linear calibration curve (figure 58). The four point calibration

spreadsheet is provided in figure 59. Utilizing this new calibration we were able to quantify the relative concentration changes of carbon dioxide in the plant treatment system and demonstrate clear trends in a series of experiments which ensued.

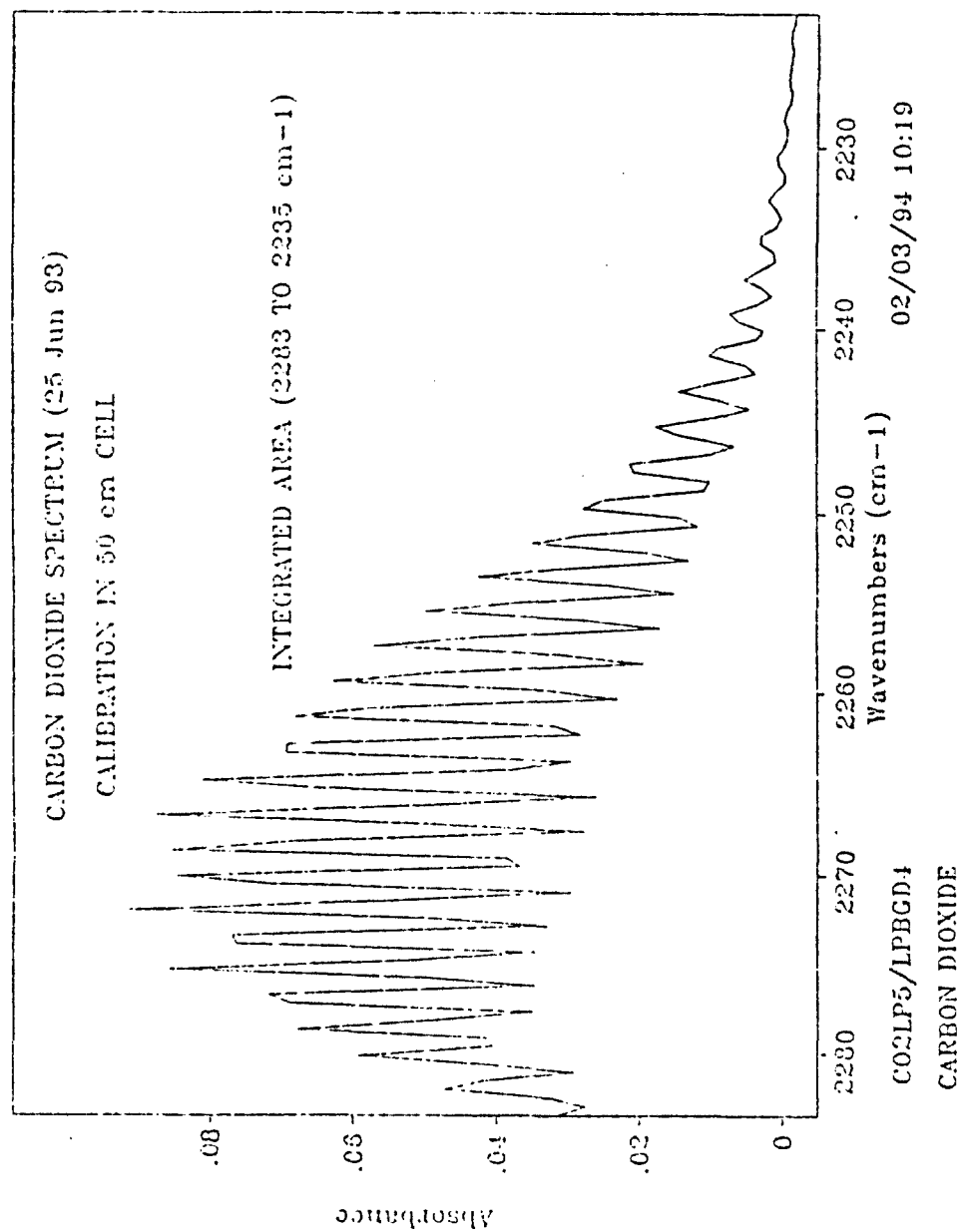


FIGURE 57. CALIBRATION SPECTRUM CARBON DIOXIDE.

Beer's Law Plot

Carbon Dioxide, 1 cm^{-1} , $b=0.5 \text{ meters}$

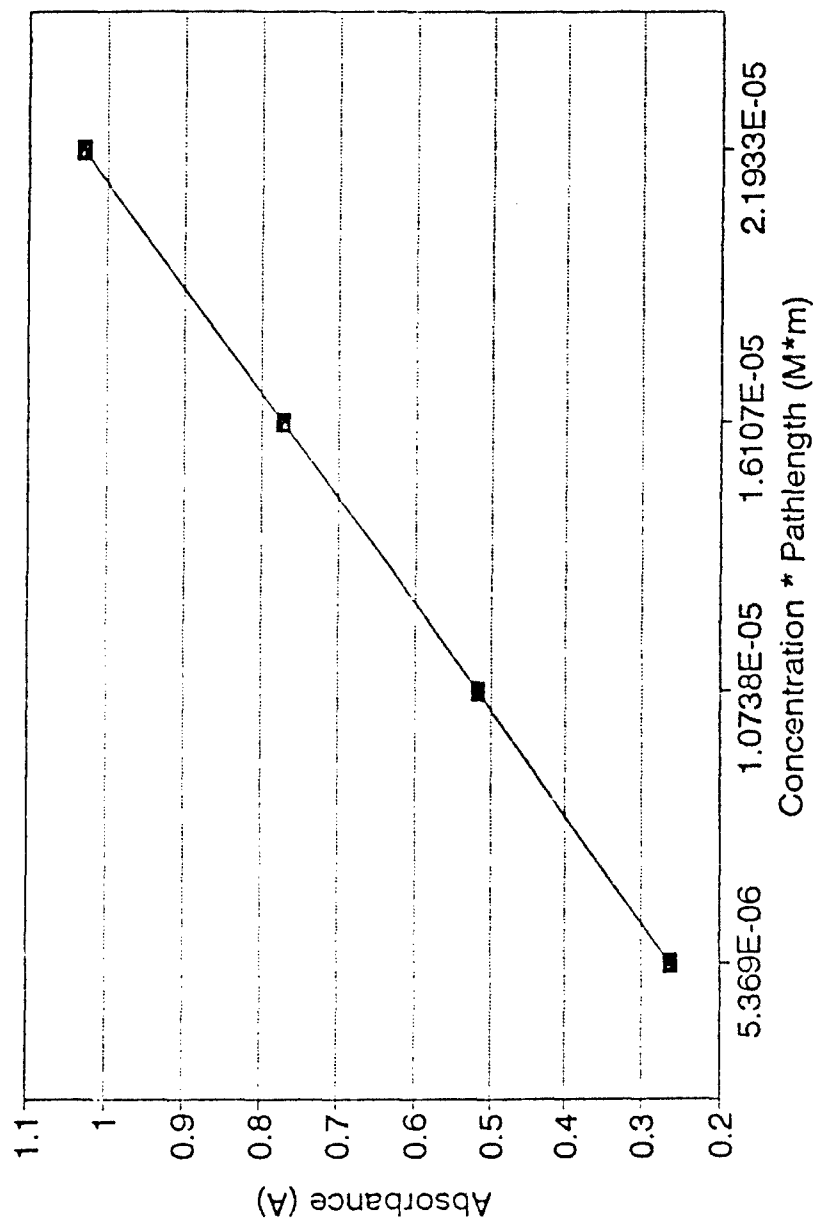


FIGURE 58. FOUR POINT CALIBRATION CURVE FOR CARBON DIOXIDE.

Carbon Dioxide
Cell Pathlength 0.5 meters

peak absorb. (2283-2235 cm-1) A	Concentration * Pathlength C*b	Absorptivity a
0.266434	5.369E-06	49624.5110821
0.483772	1.0738E-05	45052.337493
0.830328	1.6107E-05	51550.7543304
1.00253	2.1933E-05	45708.7493731

Regression Output:

Constant	0.019
Std Err of Y Est	0.05645
R Squared	0.98077
No. of Observations	4
Degrees of Freedom	2
X Coefficient(s)	46301.3
Std Err of Coef.	4583.86

Measured Absorbance
0.118966

Calc. Concentration(M)
5.14E-06

Cell Pathlength(m)
0.5

Measured Temperature(K)
295.6

Atmospheric Concentration(ppb)
25167

Atmospheric Pressure(atm)
0.986

Atmospheric Pathlength(m)
2.44

FIGURE 59. CALIBRATION SPREADSHEET FOR CARBON DIOXIDE.

REFERENCES:

1. Witkowski, Mark R., Testing and Optimization of a Mobile Fourier Transform Infrared (FT-IR) Spectrometer System for the Monitoring of Volatile Organic Compounds (VOCs). Diss. Kansas State University, Manhattan, Kansas, (1992).
2. Spartz, M.L., Witkowski, M.R., Fateley, J.H., Jarvis, J.M., White, J.S., Paukstelis, J.V., Hammaker, R.M., Fateley, W.G., Carter, R.E., Thomas, M., Lane, D.D., Marotz, G.A., Fairless, B.J., Holloway, T., Hudson, J.L. and Gurka, D.F., "Evaluation of a Mobile FT-IR System for Rapid VOC Determination", American Environmental Laboratory, November 1989, pp. 15-30, (1989).
3. Spartz, p. 19.
4. Strong, Frederick C., "Theoretical Basis of the Bouguer-Beer Law of Radiation Absorption", Analytical Chemistry, vol 24, no 2, February 1952, p. 341, (1952).
5. Spartz, p. 20.
6. Spartz, p. 20.
7. Herzberg, Gerhard, Molecular Spectra and Molecular Structure Volume II Infrared and Raman Spectra of Polyatomic Molecules, Krieger Publishing Co., Malabar, Florida, p. 272, (1991).
8. Herzberg, p. 278.

CHAPTER 6

PRACTICAL APPLICATIONS OF FT-IR MONITORING OF BIOREMEDIATION MEAT AND POTATOES

Armed with the calibration information presented in the previous chapter, we are able to make a number of practical observations about the bioremediation process using FT-IR spectrometry. This chapter will present the methodology and results attained from a number of different types of experiments conducted during this study. It will briefly demonstrate how open path FT-IR spectrometry was used to study the remediation of volatile organic compounds in the monitoring analysis of the atmosphere above the plants, ground water samples, and plant samples.

One experiment designed to monitor the relative CO₂ concentration present in the chamber before and after the plants were harvested clearly demonstrated the practical capacity for monitoring fluctuations in the relative carbon dioxide concentrations using the spectral regions defined in chapter 5. The spectrometer is set up as shown in figure 3 and all observations are made with the plant treatment chamber sealed. It was evident that the relative carbon dioxide concentration decreased with the plants present (figure 60) and we were also able to demonstrate an accumulation in relative carbon dioxide concentration after the plants were harvested (figure 61). The toluene and phenol, both groundwater contaminants, were removed from the groundwater. Pure water was introduced into the plant chamber until the soil and ground water samples were completely purged of these contaminants. The focal point of our research efforts then extended the use FT-IR in the study of the remediation of chlorinated compounds, specifically 1,1,1-trichloroethane (TCA)

CO₂ CONCENTRATION CHANGE WITH PLANTS

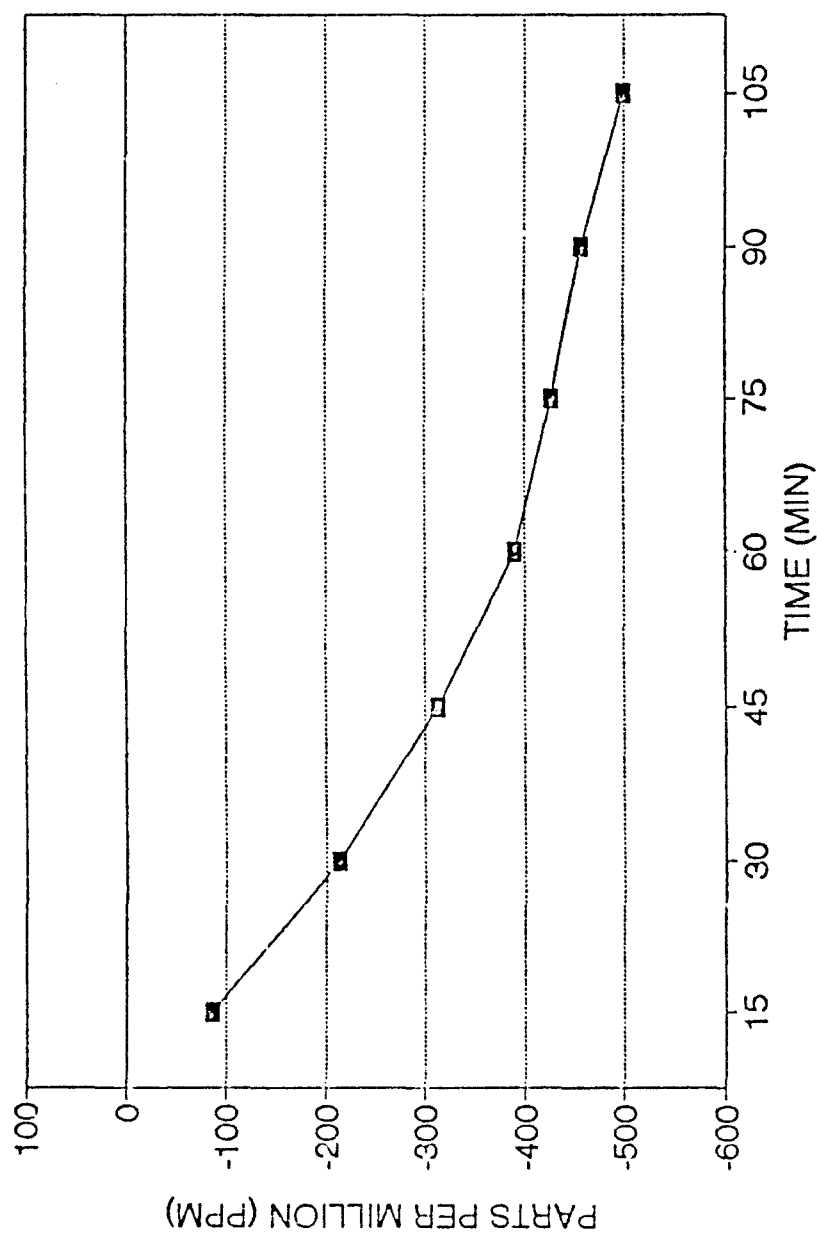


FIGURE 60. GRAPH OF CHANGE IN RELATIVE CO₂
CONCENTRATION WITH PLANTS.

CO₂ CONCENTRATION CHANGE CUT PLANTS

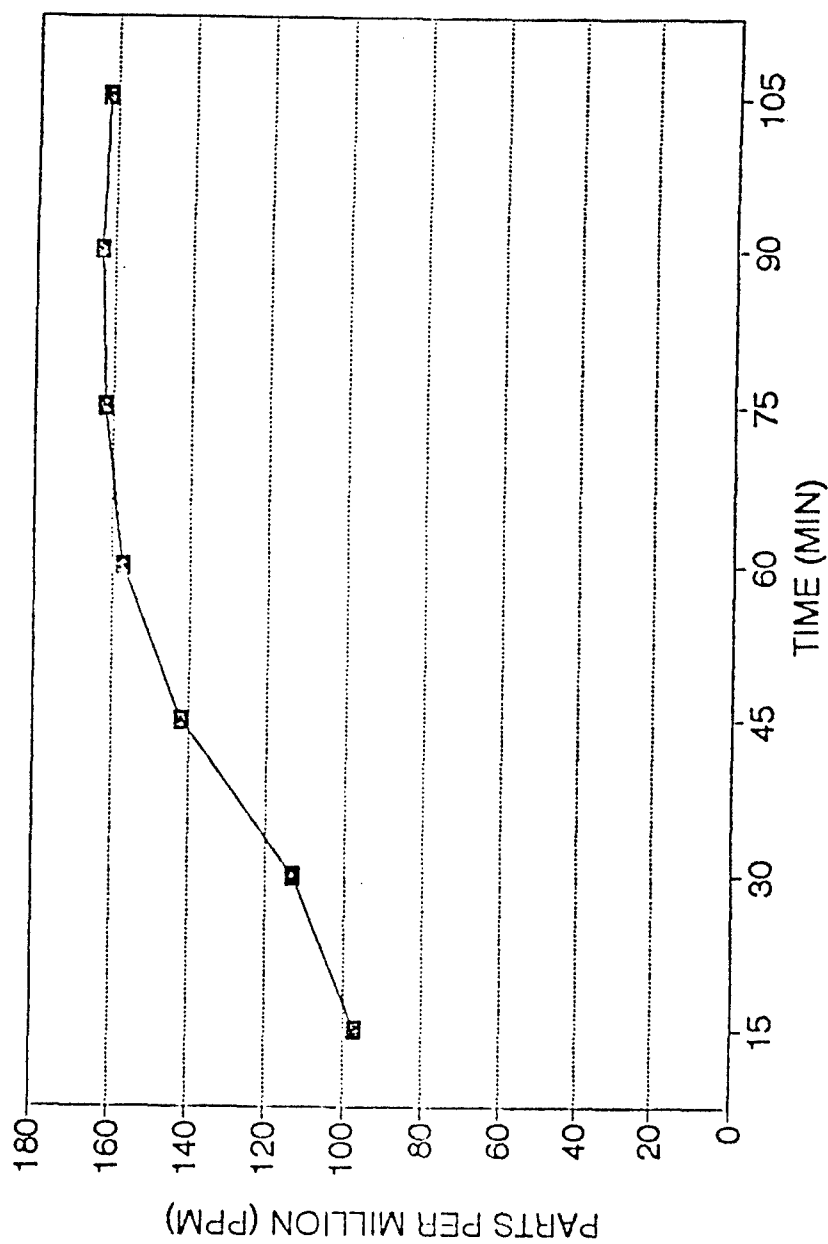


FIGURE 61. GRAPH OF CHANGE IN RELATIVE CO₂ CONCENTRATION WITHOUT PLANTS.

and trichloroethylene (TCE).

In order to establish that we were capable of monitoring these two compounds simultaneously in our chamber, 100 μ l of each compound was injected into the chamber and the atmosphere above the plants was monitored for a period of two hours. Figure 62, a representative spectrum, illustrates that both TCA and TCE are present. Also, pictured are overlays of calibration spectra for both TCA and TCE. Certain that we could spectrally distinguish between the two compounds, both compounds were introduced into the plant chamber groundwater as contaminants. The alfalfa plants and microorganisms present in the rhizosphere were given time to adapt to the presence of these chlorinated hydrocarbons in the soil and groundwater.

Coincident with this period of adaptivity, the entire midwest experienced the most severe flood in recent history. In addition to the impact the flood caused in terms of damage and destruction, it served as a reminder to people throughout the entire region of how dependent we are upon the purity of our groundwater sources. As we watched waste of all types get carried away by the high water levels, this natural disaster clearly demonstrated why it is so necessary to eliminate the contamination that presently endangers the groundwater sources of the United States. Kansas, like many other states, gets much of its potable water from wells. This dependence upon well water makes Kansans especially sensitive to the health hazards contaminated groundwater may present. This disastrous flood further justified continued research in this

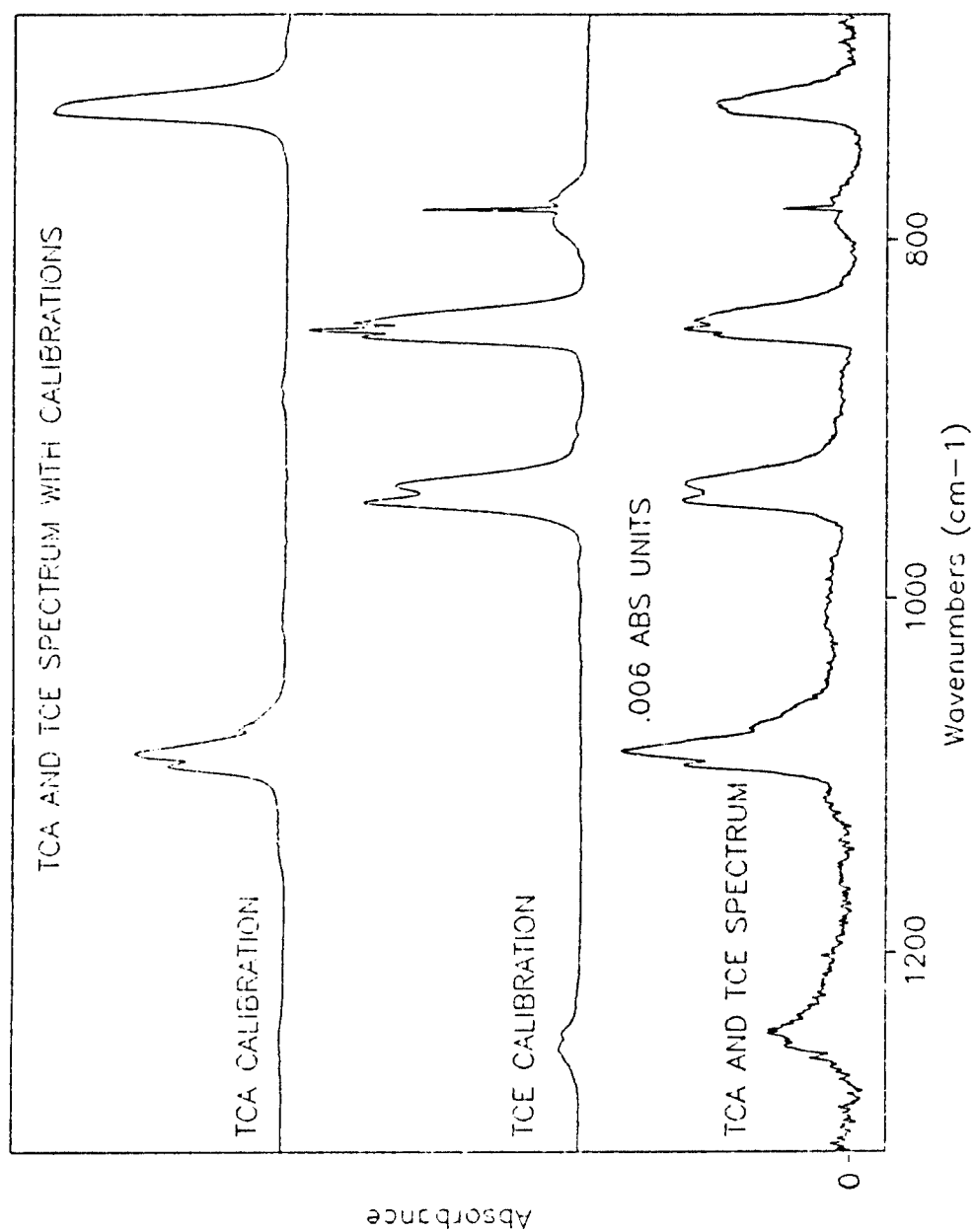


FIGURE 62. SPECTRUM CONTAINING TCA AND TCE WITH
OVERLAID CALIBRATION SPECTRA

arena.

Research efforts continued centered on the monitoring of bioremediation of TCA and TCE. We monitored the atmosphere above the plants to observe the rate of accumulation of TCA and TCE over time. The relative change in CO_2 concentration was also analyzed. Essentially, the procedure remained consistent with previous work except hexane was used to monitor the leak rate in lieu of methane. The absorbance band at 2964 cm^{-1} was used to monitor for hexane (figure 63). Over time, we observed a decrease in absorbance at this band for hexane as shown in the spectra in figure 64. This switch to hexane from methane was done to facilitate monitoring of methane which may be accumulating in the plant chamber if methanogenic bacteria are involved in the biodegradation pathways of these two compounds. The spectra in figure 64 demonstrate an observed decrease in the intensity of the hexane absorbance band (2964 cm^{-1}) over four specified time intervals.

Some of the most interesting information we found came from a similar experiment designed to monitor the accumulation of TCA and TCE in the plant chamber with plants in the chamber and after the alfalfa plants were harvested. Harvesting the plants resulted in cutting the plants back to a height of 5 cm. The chamber was monitored for a period of two hours with the plants present and subsequently, monitored for two hours after the plants were harvested. The absorbance for each file was used to determine the relative

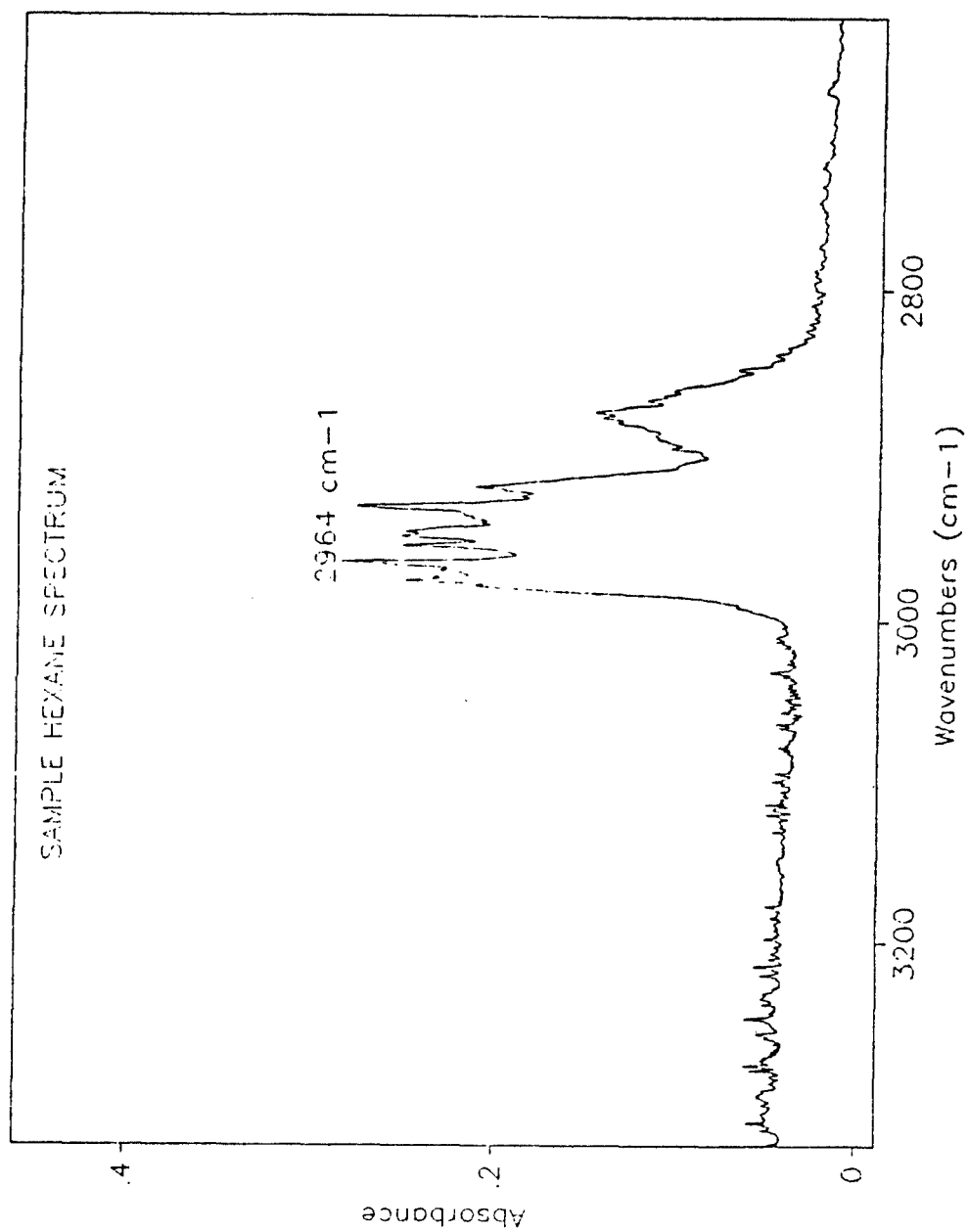


FIGURE 63. SPECTRUM OF HEXANE (2964 cm^{-1}).

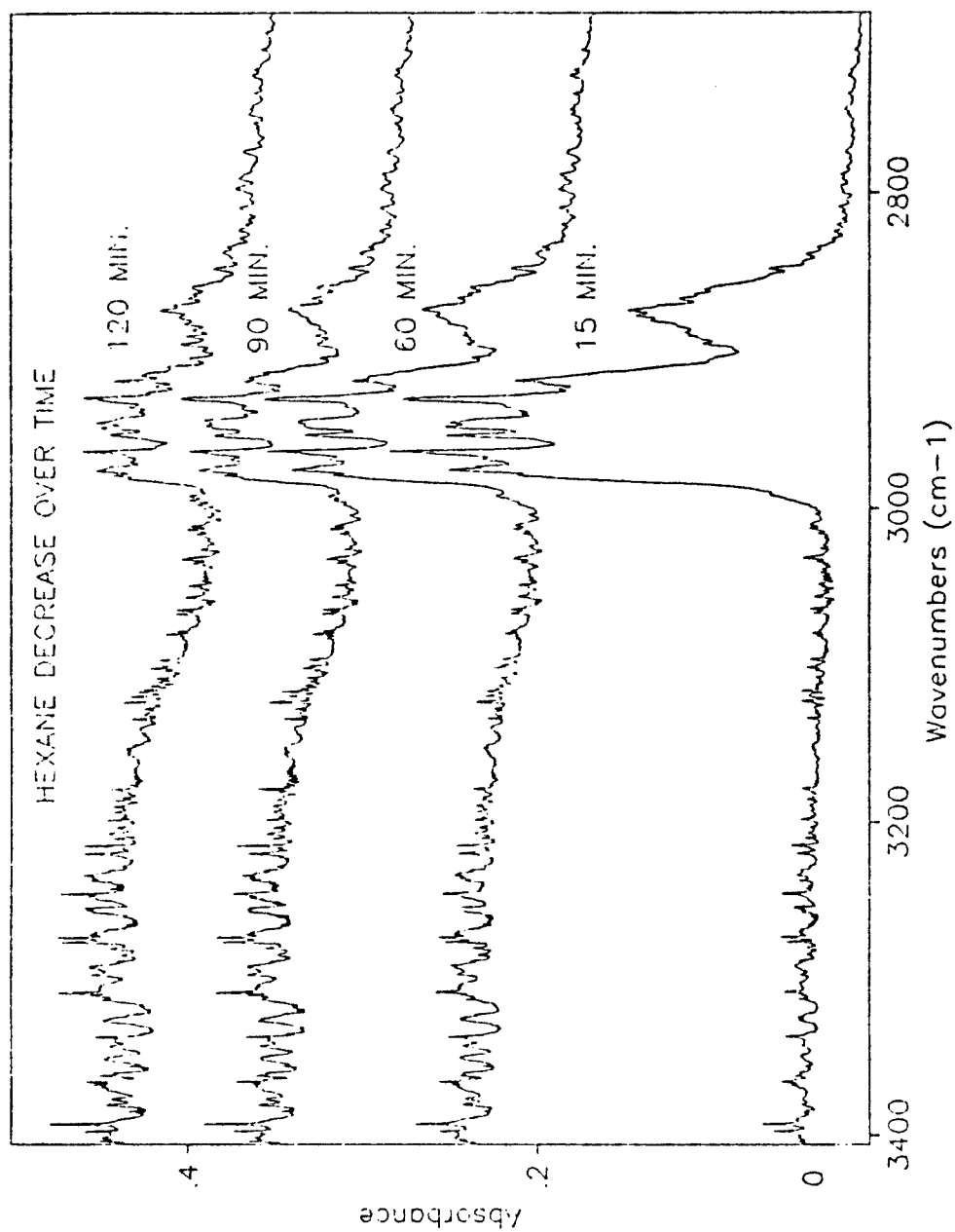


FIGURE 64. HEXANE SPECTRA SHOWS ABSORBANCE DECREASE OVER TIME.

concentration of TCA and TCE in each spectrum using the absorption bands shown in the calibrations of each of these compounds, respectively. The spectra in figure 65 illustrate the absorbance increases observed over time with the plants present. The spectra in figure 66 illustrates a very similar increase observed over time after the plants were harvested. Close examination shows that the two spectral collections are almost identical. The spectra shown were collected at the same three time intervals of 15 minutes, 45 minutes, and 1 hour, 45 minutes.

Graphing the rate of TCA and TCE accumulation (ppb versus time) with and without the plants makes it much easier to see this similarity. The graph of TCA is in figure 67 and the graph of TCE is in figure 68. In each of the graphs the squares represent the points in the series with plants and the crosses represent the points in the series without the plants. The data represented in the graphs is outlined in table 6. Analysis of the information consistently shows an approximate 4 to 1 ratio of TCE to TCA. This ratio is compatible with the concentrations of the two compounds being introduced in the groundwater, 200 μ l per liter TCE and 50 μ l per liter TCA. In both of the experiments, prior to the each of the last three spectra, 10 μ l of TCA and 10 μ l of TCE were injected into the chamber. These stepwise increases in relative concentration of both compounds manifest themselves as a linear increase in each graph. The significance of this should not be overlooked. It suggests that the plants themselves are not transpiring the volatile organic compounds and

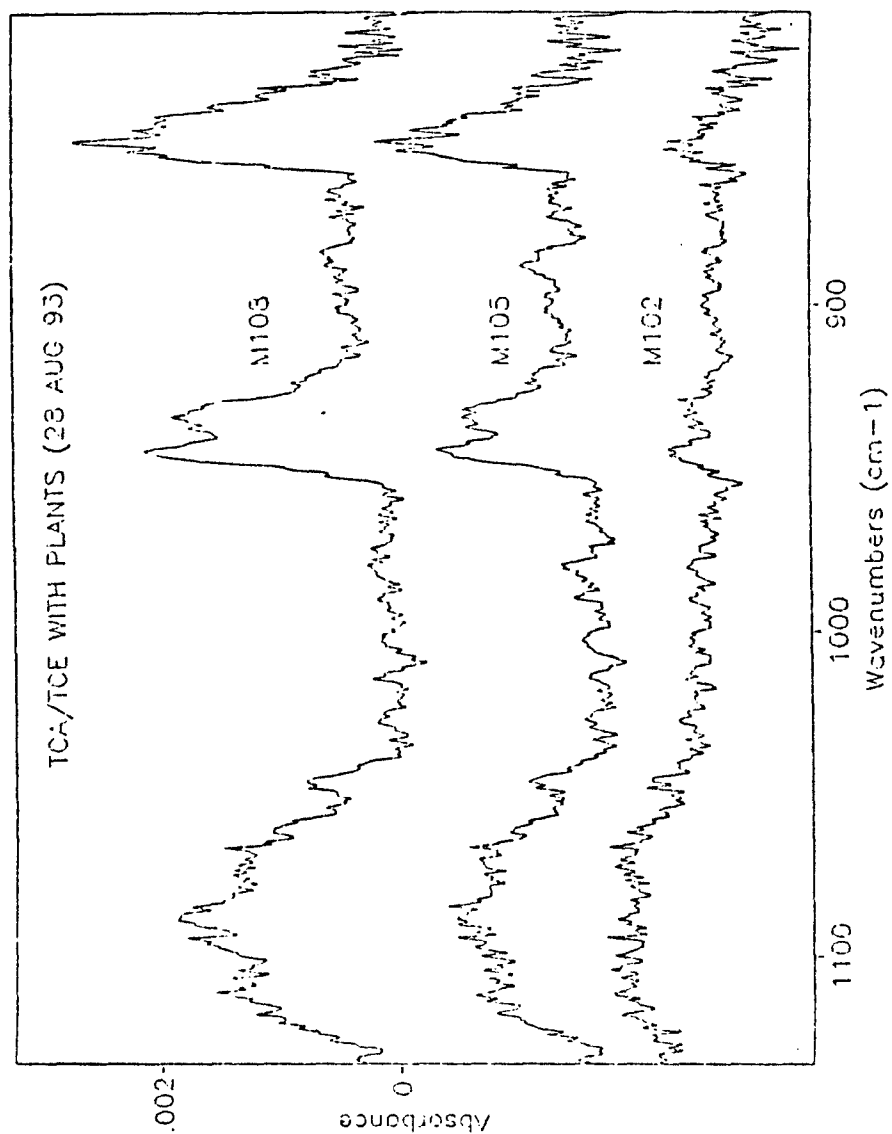


FIGURE 65. TCA AND TCE SPECTRA WITH PLANTS.

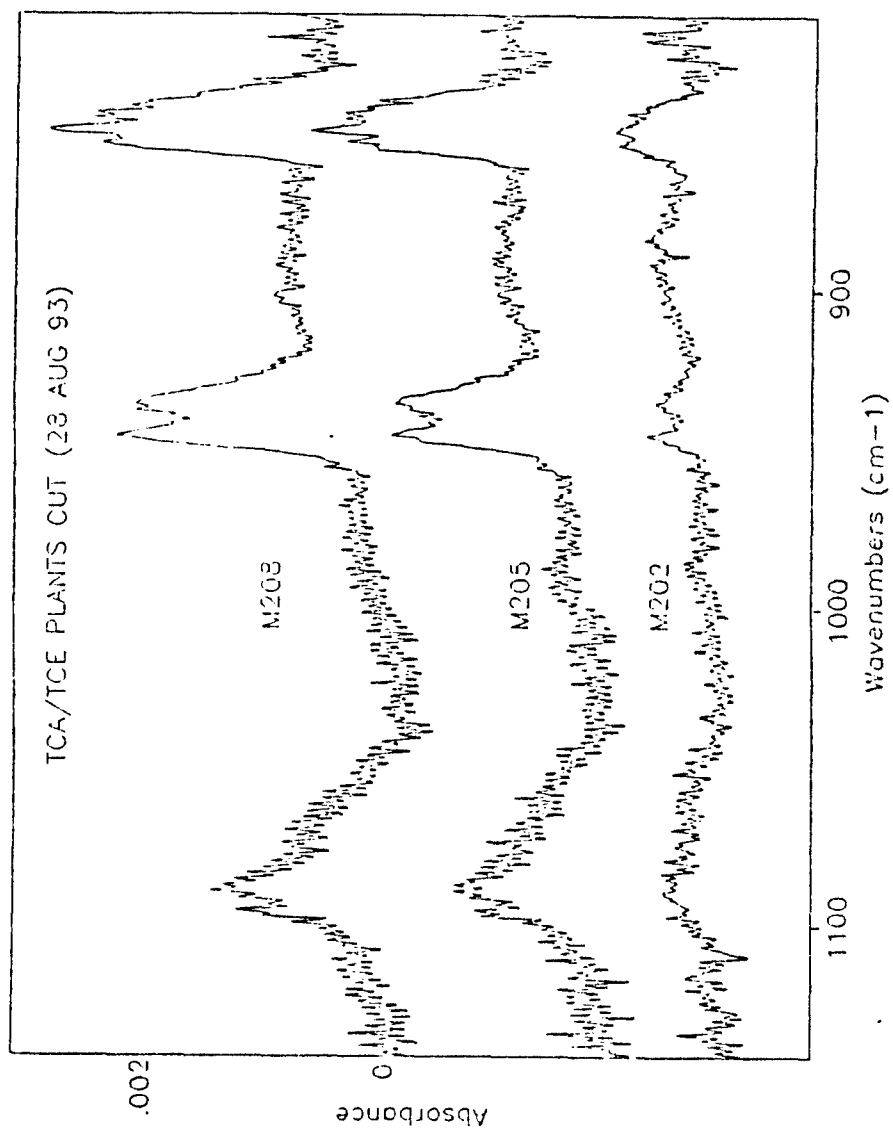


FIGURE 66. TCA AND TCE SPECTRA WITH PLANTS CUT.

TCA ACCUMULATION

28 AUG 93

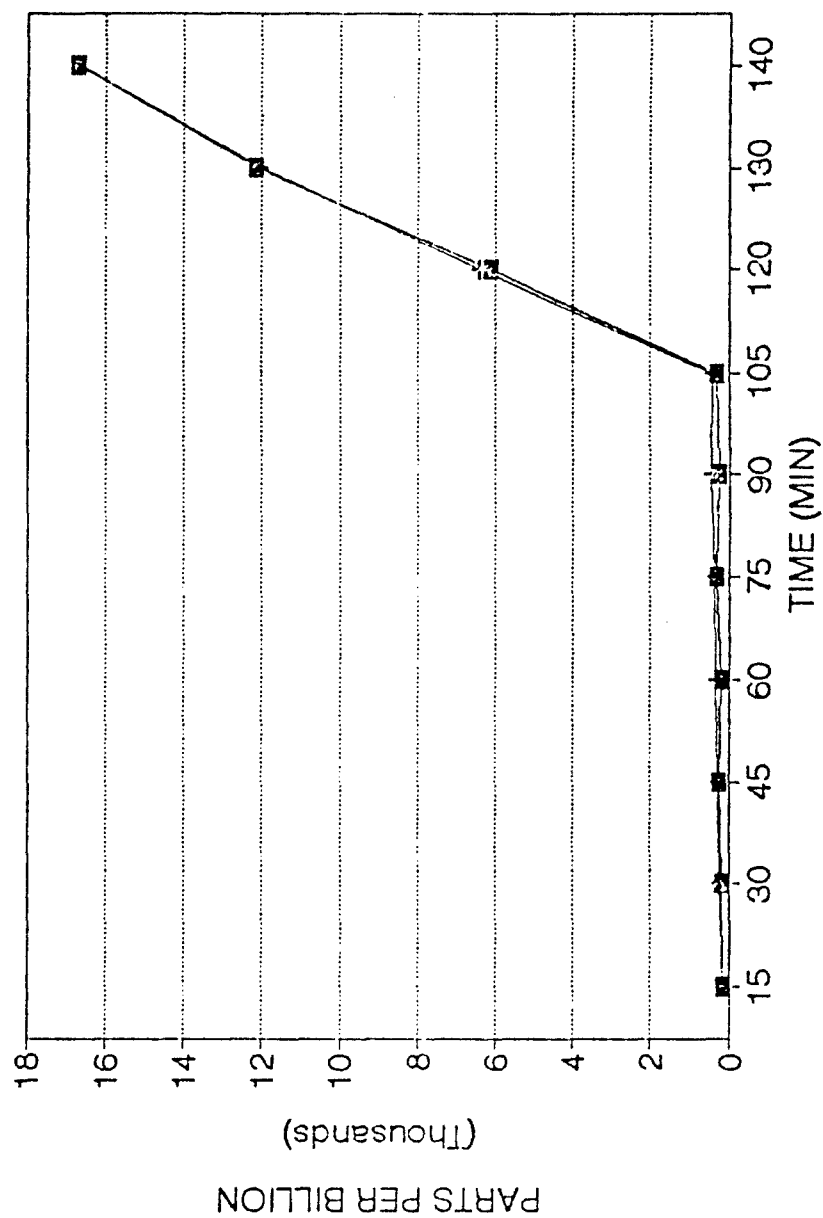


FIGURE 67. GRAPH OF TCA ACCUMULATION OVER TIME.

TCE ACCUMULATION

28 AUG 93

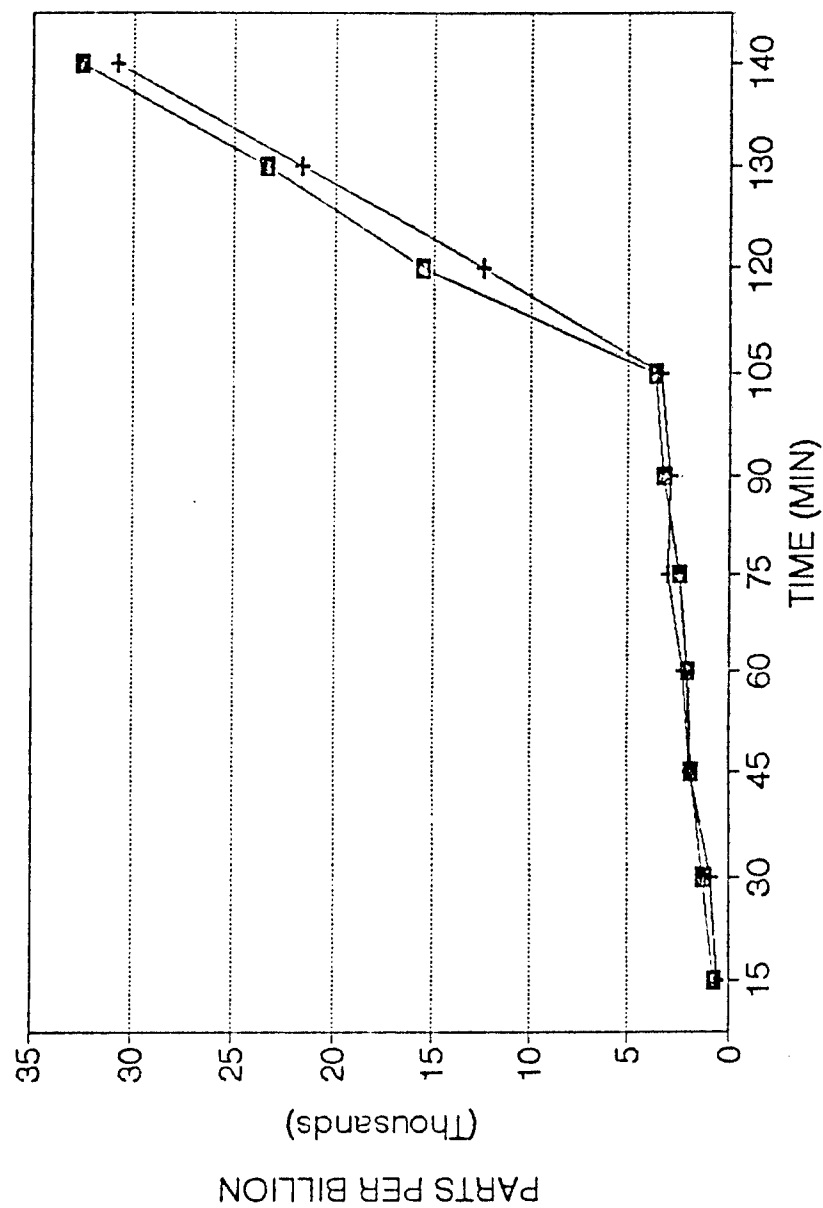


FIGURE 68. GRAPH OF TCE ACCUMULATION OVER TIME.

that the observed accumulation of TCA and TCE may be from volatilization of each compound.

TABLE 6. DATA USED FOR GRAPHS IN FIGURES 67 AND 68.

TIME (MIN)	TCE CONC PLANTS	TCE CONC PLANTS CUT	TCA CONC PLANTS	TCA CONC PLANTS CUT
15	745 PPB	525 PPB	146 PPB	156 PPB
30	1313 PPB	871 PPB	194 PPB	219 PPB
45	1871 PPB	1907 PPB	215 PPB	269 PPB
60	2063 PPB	2243 PPB	213 PPB	324 PPB
75	2467 PPB	3020 PPB	288 PPB	384 PPB
90	3194 PPB	2908 PPB	245 PPB	428 PPB
105	3637 PPB	3349 PPB	312 PPB	393 PPB
120	15636 PPB	12520 PPB	6110 PPB	6432 PPB
130	23409 PPB	21630 PPB	12122 PPB	12021 PPB
140	32556 PPB	30802 PPB	16686 PPB	16715 PPB

In an effort to corroborate this view, we set out to show that the biomass (plant material) did not contain the volatile organic compounds. Plant material was harvested and immediately placed in an air tight container. The air tight container used was a glass jar with a top configured to allow the extraction of accumulated head space gas. This analysis also was accomplished using a FT-IR spectrometer in the following manner. The head space gas from the harvested plants was extracted through a septum into the 50 cm cell (figure 58), which was under vacuum. The introduced sample was then backfilled with N_2 bringing the cell pressure to atmospheric. The single beam spectrum collected was then ratioed against a single beam of pure N_2 at atmospheric pressure to generate our spectrum to be analyzed. An example of this spectrum is presented in figure 69 and shows that we detect no TCA or TCE in the sample. Similar trials involving harvested plant material yielded the same results.

The results of atmospheric monitoring of the chamber with and without plants and analysis of the plant material head space gas only accounted for a small percentage of the total volume of introduced volatile organic compounds. Also, GC analysis of water samples taken from the chamber inlet, well 1, well 2, well 3, well 4, and the chamber outlet repeatedly identified a decline in the TCA and TCE concentrations greater than the amount credited to volatilization. In an effort to investigate this further and to determine the potential utility of the FT-IR spectrometry for water sample analysis, we

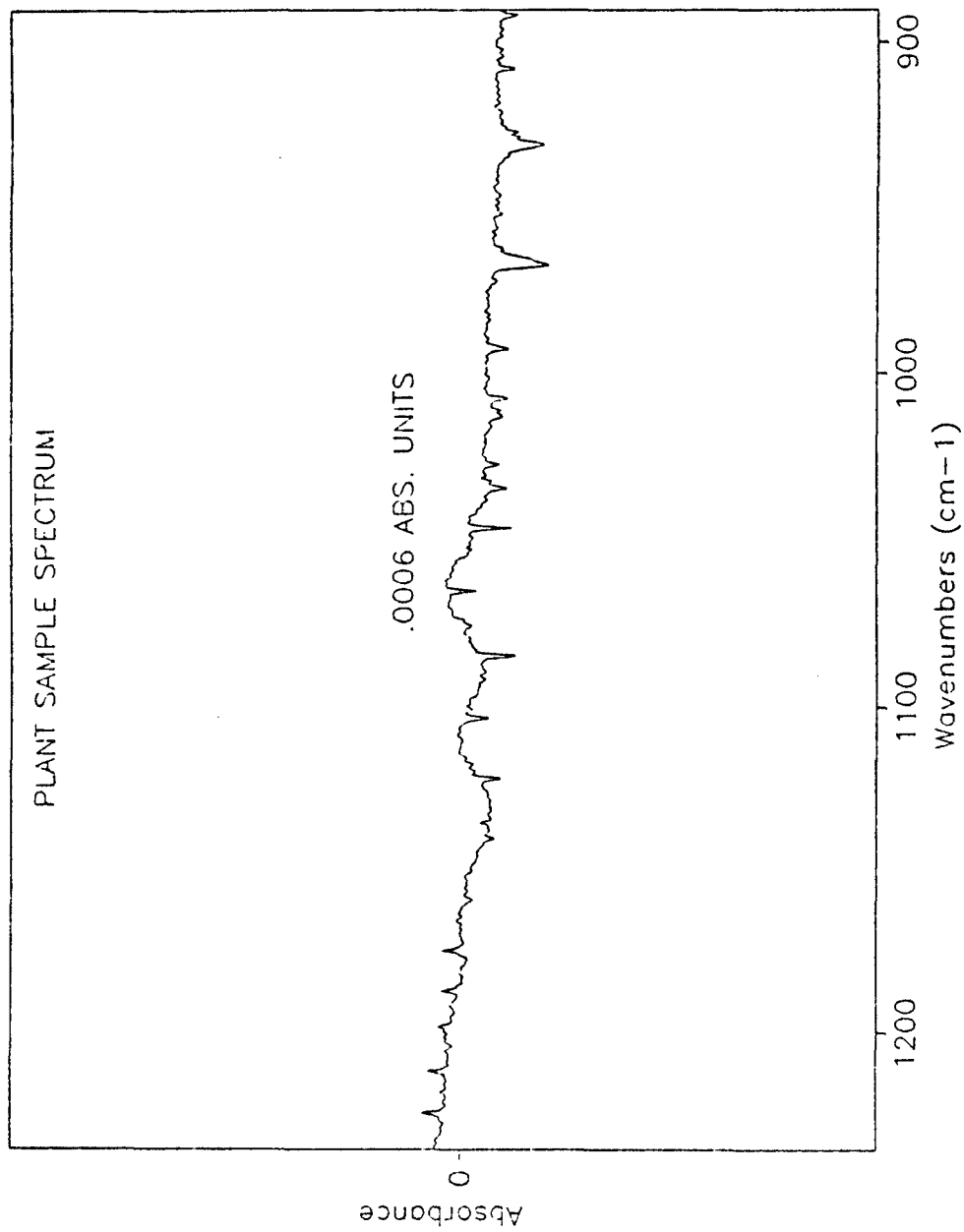


FIGURE 69. SPECTRUM OF PLANT SAMPLE HEAD SPACE GAS.

initiated a novel group of experiments.

The results obtained from studying the head space gas of the collected water samples quickly disclosed some immediate benefits of using FT-IR spectrometry for water sample analysis. Not only was FT-IR spectrometry capable of monitoring the changes in concentration of ground water contaminant compounds in the chamber, it also provided us a means of identifying many other compounds that may be present in the ground water sample. This capability has immediate implication, because it potentially could capture information necessary to determine specific intermediates and/or byproducts of the degradation process. The identification of specific intermediates is critical for determining the specific pathways and mechanisms nature follows in the biodegradation of specific compounds.

Each sample analyzed was the head space gas of a 3 ml water sample. The procedure is identical to the plant head space gas analysis. The spectra shown in figure 70 portrays a progressive decline in the concentration of both TCA (1087 cm^{-1}) and TCE (944 cm^{-1}) from the inlet to the outlet of the chamber. We also discovered an increase in methane present in the ground water samples from well 3, well 4 and the outlet, depicted in figure 71 which supports a methanogenic process. Specific calculated TCA, TCE and methane relative concentrations for the spectra in figures 70 and 71 are provided in table 7. The water sample analysis results described are graphically depicted in figure 72 (TCA), figure 73 (TCE) and figure 74 (Methane). Although methane

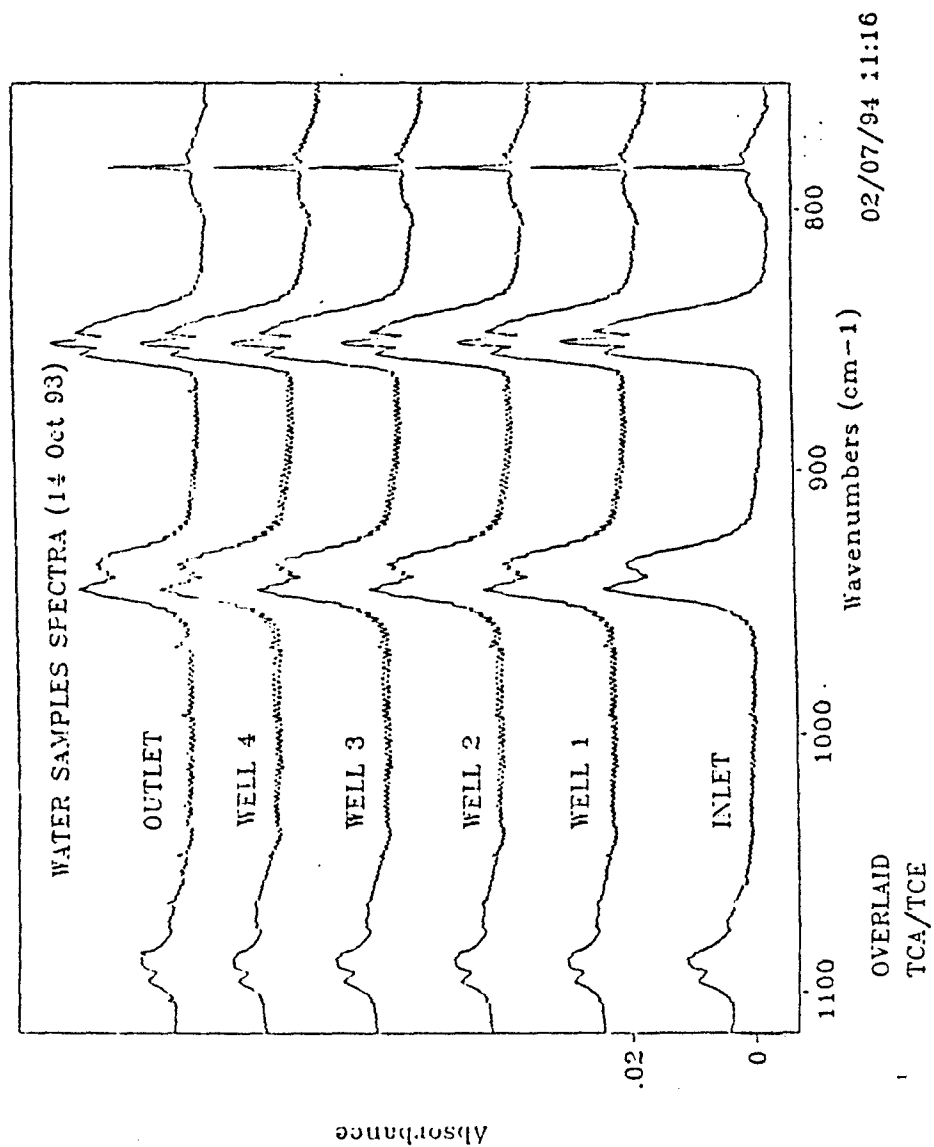


FIGURE 70. SPECTRA OF GROUNDWATER SAMPLES
(TCA AND TCE).

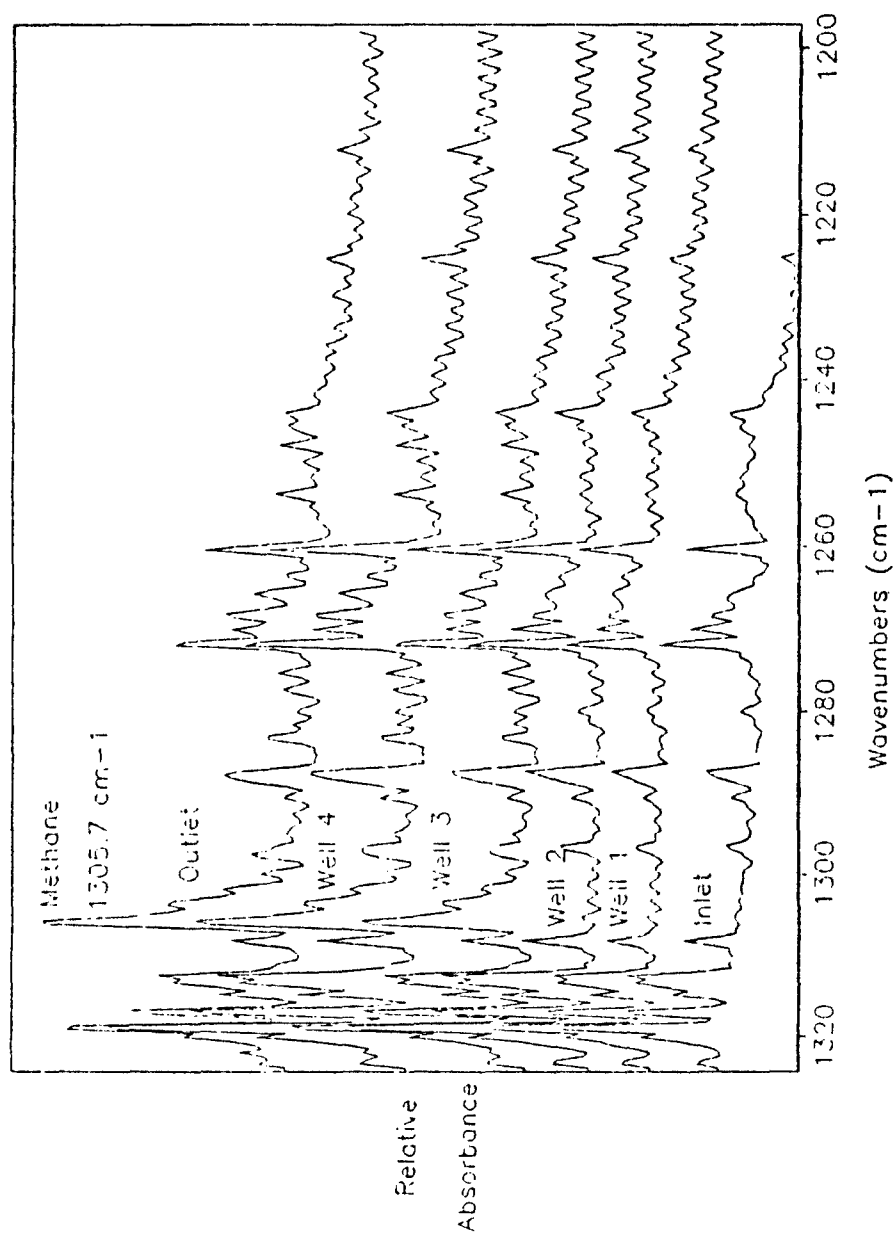


FIGURE 71. SPECTRA OF GROUNDWATER SAMPLES (METHANE).

WATER SAMPLES TCA

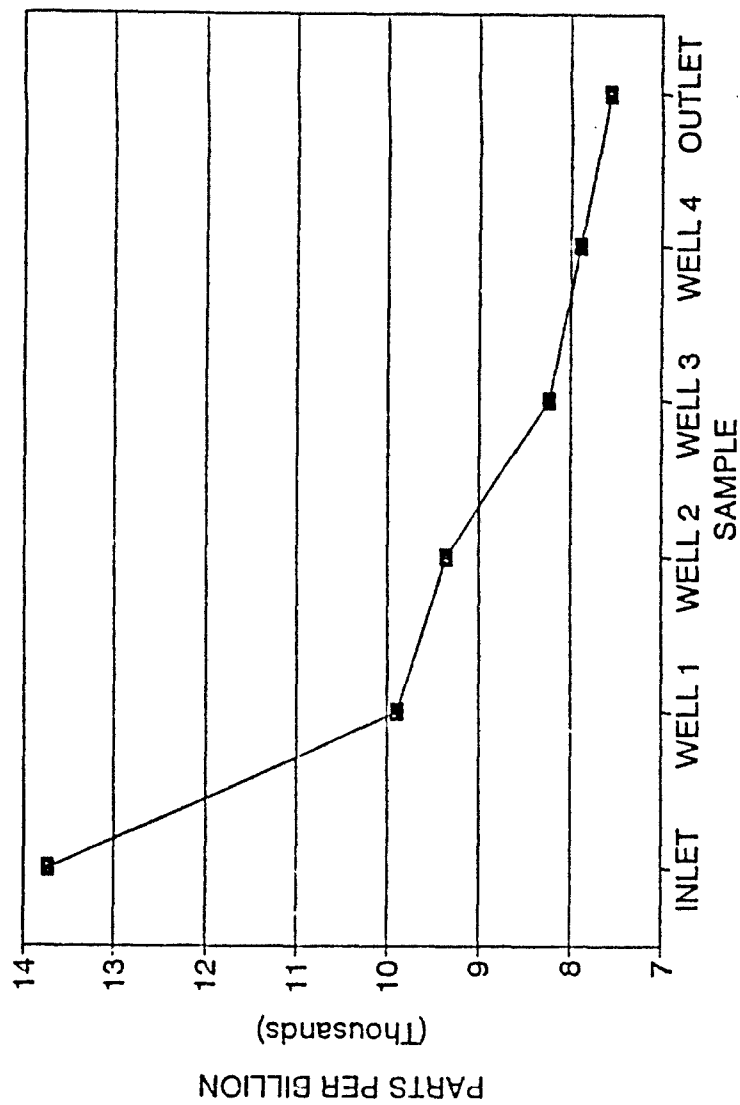


FIGURE 72. GRAPH OF TCA CONCENTRATION IN
GROUNDWATER SAMPLES.

WATER SAMPLES TCE

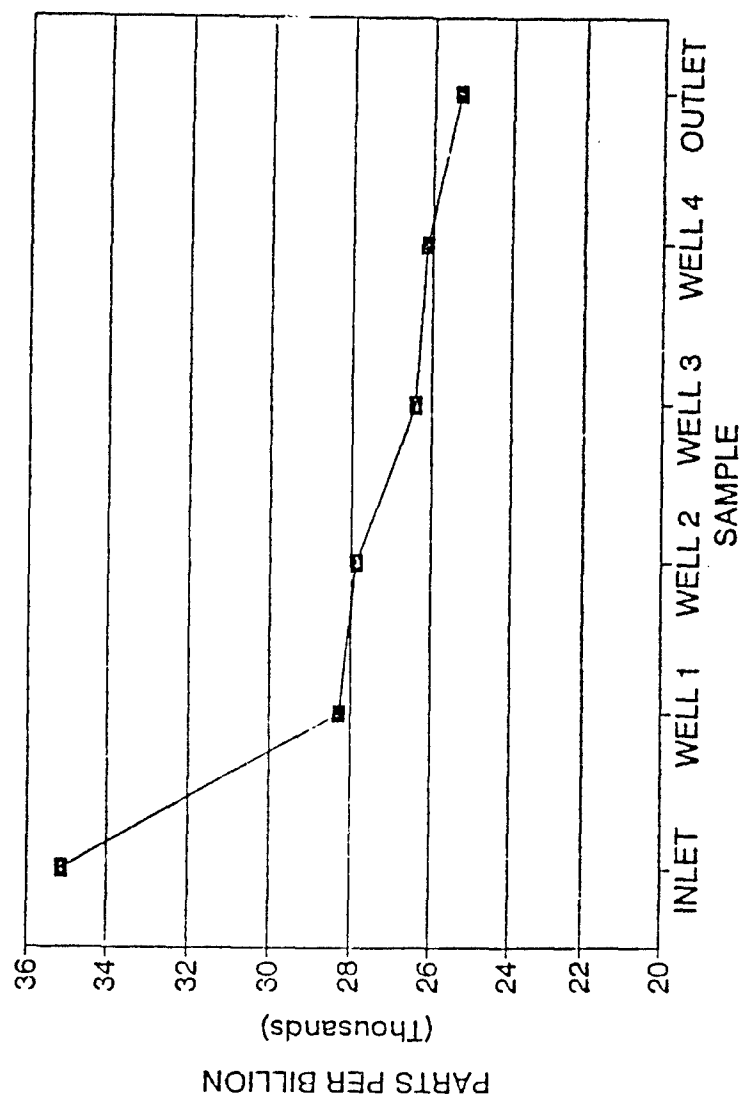


FIGURE 73. GRAPH OF TCE CONCENTRATION IN
GROUNDWATER SAMPLES.

WATER SAMPLES METHANE

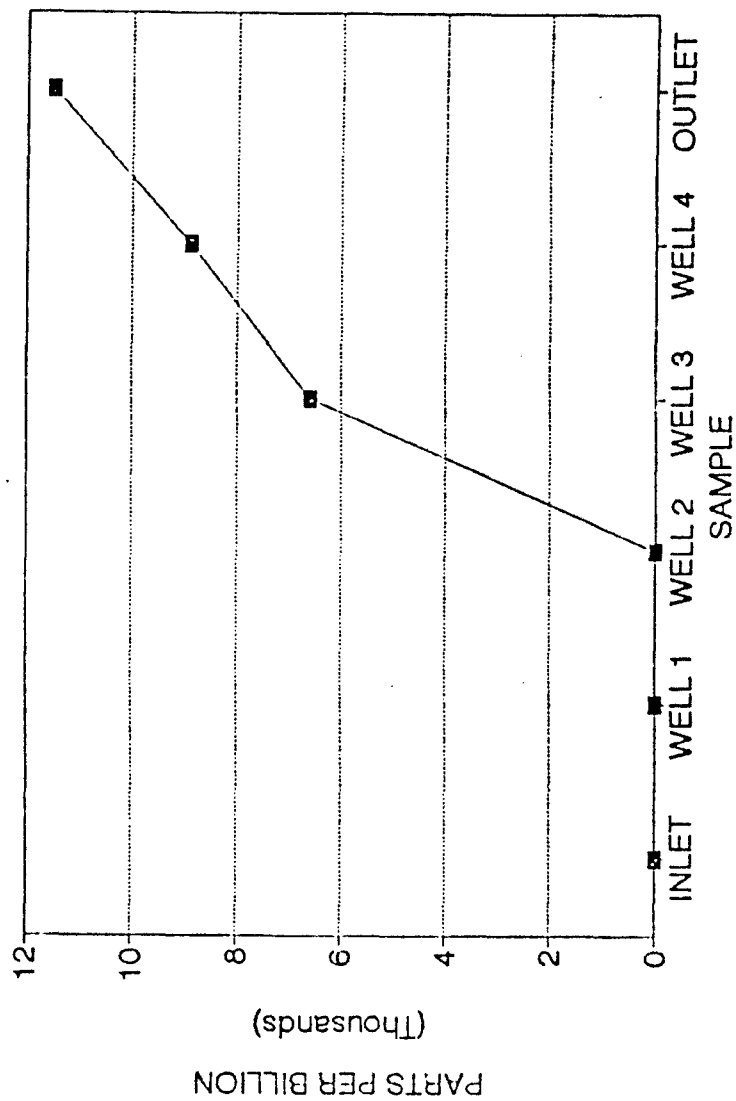


FIGURE 74. GRAPH OF METHANE CONCENTRATION IN
GROUNDWATER SAMPLES.

TABLE 7. TCA, TCE AND METHANE CONCENTRATION (PPM)
PRESENT IN GROUNDWATER SAMPLE.

SAMPLE LOCATION	TCA CONC (PPM)	TCE CONC (PPM)	METHANE CONC(PPM)
INLET	14	35	0
WELL 1	10	28	0
WELL 2	9	28	0
WELL 3	8	26	7
WELL 4	8	26	9
OUTLET	8	25	11

was the only compound in addition to TCA and TCE clearly identified, each spectrum was also examined for the presence of many of the calibrated compounds presented in chapter 5.

The information found in table 8 provides a comparison of the detection limits encountered for these compounds when working in the 50 cm cell pathlength (plant and groundwater samples) and in the 2.44 m pathlength of the plant treatment chamber (atmospheric). These detection limits are mathematically determined using the calibration files as discussed earlier in chapter 5 and summarized here for general reference.

TABLE 8. LIMITS OF DETECTION (LOD) .5 m AND 2.44 m
PATHLENGTHS.

COMPOUND	LOD .5 m	LOD 2.44 m
CARBON DIOXIDE	1135 ppb	444 ppb
CHLOROFORM	625 ppb	245 ppb
1,1-DICHLOROETHANE	565 ppb	221 ppb
1,2-DICHLOROETHANE	1287 ppb	503 ppb
1,1-DICHLOROETHYLENE	3681 ppb	1440 ppb
cis-1,2-DICHLOROETHYLENE	5332 ppb	2086 ppb
trans-1,2-DICHLOROETHYLENE	2545 ppb	996 ppb
METHANE	1677 ppb	656 ppb
PHENOL	1673 ppb	654 ppb
TOLUENE	2500 ppb	978 ppb
1,1,1-TRICHLOROETHANE	2580 ppb	1009 ppb
1,1,2-TRICHLOROETHANE	4114 ppb	1609 ppb
TRICHLOROETHYLENE	7420 ppb	2903 ppb
VINYL CHLORIDE	3192 ppb	1249 ppb

These LODs, although for previous experiments, may assist in future research. Present research involves more analysis of groundwater samples from the plant treatment chamber. The groundwater contaminants have been altered and the system is adapting to the new compounds present in the groundwater and rhizosphere.

CHAPTER 7

CONCLUSION

THE CURTAIN CLOSES

In conclusion, this project has successfully applied Fourier transform infrared (FT-IR) spectrometry to monitoring plant bioremediation of volatile organic compounds (VOCs). FT-IR spectrometry was used in the determination of contaminant levels in the gas phase, groundwater, and plant tissue. Clearly, FT-IR provides a means for rapid analysis of very small amounts of material and detects both the contaminant and its volatile products (if produced as a sufficient fraction of the input material). Finally, the spectrometer system provides mobility and may be easily transported to field sites such as locations where remediation efforts are underway.

In summary, the work presented here pioneers a new practical application of FT-IR spectrometry. Additionally, it readily demonstrates the benefits of interdisciplinary and cooperative research. Bioremediation research will continue and FT-IR spectrometry may provide analytical capability required to find the missing link.

Future work will focus on the development and construction of a improved plant treatment system. Ultimately, a longterm study using open path FT-IR monitoring of an active remediation site is necessary to conclusively prove its practical value in this regard.

ADDITIONAL REFERENCES

1. Levine, Ira N., Molecular Spectroscopy, New York: John Wiley & Sons, 1975.
2. Gibson, David T., ed., Microbial Degradation of Organic Compounds, New York: Marcel Dekker, Inc., 1984.
3. Kamely, Daphne; Chakrabarty, Ananda; and Omenn, Gilbert S., eds., Biotechnology and Biodegradation, (Advances in Applied Biotechnology Series vol 4), Woodlands, Texas: Portfolio Publishing Co, 1990.
4. Hollas, J. Michael, Modern Spectroscopy, 2d ed, New York: John Wiley & Sons, 1992.
5. Nyer, Evan K., Practical Techniques for Groundwater and Soil Remediation, Boca Raton, Florida: Lewis Publishers, 1993.
6. Gibaldi, Joseph and Achtert, Walter S., MLA Handbook for Writers of Research Papers, 2d ed, New York: The Modern Language Association of America, 1984.
7. Van Sciver, Charles and Fowler, Robert, "Increasing the Sensitivity of Field Headspace Analysis for VOCs", in American Environmental Laboratory, February, 1994, pp. 1-10.
8. Bedell, Glenn W., "Higher Plant Bioremediation" in The World and I, December 1992, pp. 260-267.

9. Walton, Barbara T. and Anderson, Todd A., "Microbial Degradation of Trichloroethylene in the Rhizosphere: Potential Application to Biological Remediation in Waste Sites" in Applied and Environmental Microbiology, Vol 56, No. 4, April 1990, pp. 1012-1016.
10. Bowman, John P., Jiménez, Igrid R., Hazen, Terry C., and Sayler, Gary S., "Characterization of the Methanotrophic Bacterial Community Present in a Trichloroethylene-Contaminated Subsurface Groundwater Site", in Applied and Environmental Microbiology, Vol 59, No. 8, Aug 1993, pp. 2380-2387.
11. Ewers, Jens; Freier-Schröder, Doris; and Knackmuss, Hans-Joachim, "Selection of Trichloroethene (TCE) Degrading Bacteria that Resist Inactivation by TCE" in Archives of Microbiology, (1990), 154: pp. 410-413.
12. Kleopfer, Robert D., Easlev, Diane M., Haas Jr., Bernard B., Delhl, Trudy G., Jackson, David E. and Wurrey, Charles J., "Anaerobic Degradation of Trichloroethylene in Soil", in Environmental Science and Technology, (1985), 19, pp. 277-280.
13. Krumme, Mary Lou, Timmis, Kenneth N. and Dwyer, Daryl F., "Degradation of Trichloroethylene by Pseudomonas Cepacia G4 and the Constitutive Mutant Strain G4 5223 PR1 in Aquifier Microcosms" in Applied and Environmental Microbiology, Vol 59, No. 8, Aug 1993, pp. 2746-2749.
14. Sharabi, Nagim El-Din and Bartha, Richard, "Testing of Some Assumptions About Biodegradability in Soil as Measured by Carbon Dioxide Evolution" in Applied and Environmental Microbiology, Vol 59, No. 4, April

1993, pp. 1201-1205.

15. Fan, Shifang and Scow, Kate M., "Biodegradation of Trichloroethylene and Toluene by Indigenous Microbial Populations in Soil" in Applied and Environmental Microbiology, Vol 59, No.6, June 1993, pp. 1911-1918.
16. Gough, T.E. and Wang, Tang-Yu, "The ν_2 Bending Mode Infrared Spectrum of Clustered Carbon Dioxide" in Chemical Physics Letters, Vol 207, No 4,5,6, 28 May 1993, pp. 517-520.
17. Syamsiah, S., Krol, A., Sly, L. and Bell P., "Adsorption and Microbial Degradation of Organic Compounds in Oil Shale Retort Water" in Fuel, 72:6, Jun 1993, pp. 855-861.
18. Korde, V.M., Phelps, T.J., Bienkowski, P.R. and White, D.C., "Biodegradation of Chlorinated Aliphatics and Aromatic Compounds in Total Recycle Expanded-Bed Biofilm Reactors", in Applied Biochemistry and Biotechnology, 39, Spring 1993, pp. 631-641.
19. Kim, B.J. and Gee, C.S., "Hazardous Waste Treatment Technologies" in Water Environment Research, 65:4, Jun 1993, pp. 430-441.
20. Otani, T. and Ae, N., "Ethylene and Carbon Dioxide Concentrations of Soils as Influenced by Rhizosphere of Crops Under Field and Pot Conditions", in Plant and Soil, 150:2, Mar 1993, pp. 255-262.
21. Fennell, D.E., Nelson, Y.M., Underhill, S.E., White, T.E., and Jewell, W.J., "TCE Degradation in a Methanotrophic Attached-Film Bioreactor" in Biotechnology and Bioengineering, 42:7, 20 Sep 1993, pp. 589-572.

22. Bouwer, E.J. and Zehnder, A.J. B., "Bioremediation of Organic Compounds - Putting Microbial Metabolism to Work" in Trends in Microtechnology, 11:8, Aug 1993, pp. 360-367.
23. Nelson, Y.M. and Jewell, W.J., "Vinyl Chloride Biodegradation with Methanotrophic Attached Films", in Journal of Environmental Engineering, ASCE 119:5, Sep-Oct 1993, pp. 890-907.
24. Shannon, M.J. and Unterman, R., "Evaluating Bioremediation - Distinguishing Fact from Fiction" in Annual Review of Microbiology, 47: 1993, pp. 715-738.
25. Hopkins, G.D., Munakata, J., Semprini, L. and Mccarty, P.L., "Trichloroethylene Concentration Effects on Pilot Field-Scale Insitu Groundwater Bioremediation by Phenol-Oxidizing Microorganisms" in Environmental Science & Technology, 27:12, Nov 1993, pp. 2542-2547.
26. Murray, W.D. and Richardson, M., "Progress Toward the Biological Treatment of C(1) and C(2) Halogenated Hydrocarbons" in Critical Reviews in Environmental Science and Technology, 23:1, 1993, pp. 195-217.
27. Smith, J.R., Neuhauser, E.F., Middleton, A.C., Cunningham, J.J., Weightman, R.L. and Linz, D.G., "Treatment of Organically Contaminated Groundwaters in Municipal Activated Sludge Systems" in Water Environment Research, 65:7, Nov-Dec 1993, pp. 804-818.
28. Ensley, B.D. and Kurisko, P.R., "A Gas Lift Bioreactor for Removal of Contaminants from the Vapor Phase" in Applied and Environmental

Microbiology, 60:1, Jan 1994, pp. 285-290.

29. Singleton, I., "Microbial Metabolism of Xenobiotics - Fundamental and Applied Research" in Journal of Chemical Technology and Biotechnology, 59:1, Jan 1994, pp. 9-23.

30. Malachowski, K.J., Phelps, T.J., Teboli, A.B., Minnikin, D.E. and White, D.C., "Aerobic Mineralization of Trichloroethylene, Vinyl Chloride and Aromatic Compounds by Rhodococcus Species" in Applied and Environmental Microbiology, 60:2, Feb 1994, pp. 542-548.

31. Peterson, J.N., Skeen, R.S., Amos, K.M. and Hooker, B.S., "Biological Destruction of CCl₄. 1. Experimental Design and Data" in Biotechnology and Bioengineering, 43:6, 15 Mar 1994, pp. 521-528.